**WEIGHT ANALYSIS OF TWO-STAGE-TO-ORBIT
REUSABLE LAUNCH VEHICLES FOR MILITARY APPLICATIONS**

THESIS

Richard A. Caldwell, 1Lt, USAF

AFIT/GA/ENY/05-M02

**DEPARTMENT OF THE AIR FORCE
AIR UNIVERSITY**

AIR FORCE INSTITUTE OF TECHNOLOGY

Wright-Patterson Air Force Base, Ohio

AFIT/GA/ENY/05-M02

**WEIGHT ANALYSIS OF TWO-STAGE-TO-ORBIT
REUSABLE LAUNCH VEHICLES FOR MILITARY APPLICATIONS**

THESIS

Presented to the Faculty

Department of Aeronautics and Astronautics

Graduate School of Engineering and Management

Air Force Institute of Technology

Air University

Air Education and Training Command

In Partial Fulfillment of the Requirements for the

Degree of Master of Science in Astronautical Engineering

Richard A. Caldwell, BS

First Lieutenant, USAF

March 2005

AFIT/GA/ENY/05-M02

**WEIGHT ANALYSIS OF TWO-STAGE-TO-ORBIT
REUSABLE LAUNCH VEHICLES FOR MILITARY APPLICATIONS**

Richard A. Caldwell, BS
First Lieutenant, USAF

Approved:

/signed/

_____   _____

Milton E. Franke (Chairman)   Date

/signed/

_____   _____

Ralph A. Anthenien (Member)   Date

/signed/

_____   _____

Paul I. King (Member)   Date

AFIT/GA/ENY/05-M02

Abstract

In response to Department of Defense (DoD) requirements for responsive and low-cost space access, this design study provides an objective empty weight analysis of potential reusable launch vehicle (RLV) configurations. Each two-stage-to-orbit (TSTO) RLV has a fixed payload requirement of 20,000 lbf to low Earth orbit. The propulsion systems considered in this study include pure rocket, pure turbine, rocket-based-combined-cycle (RBCC), and turbine-based-combined-cycle (TBCC). The hydrocarbon dual-mode scramjet (DMSJ) engines used in the RBCC and TBCC propulsion systems represent possible applications of the current research being performed in the U.S. Air Force HyTech program. Two sensitivity analyses were then performed on areas of interest directly affecting the propulsion systems in this study, including the effects of orbiter fuel selection, as well as the effects of increasing the turbine installed thrust to weight ratios for the RLVs utilizing afterburning turbine engines. The vertical-takeoff-horizontal-landing (VTHL) RLVs have an empty weight advantage over the horizontal-takeoff-horizontal-landing (HTHL) RLVs. The orbiter propellant switch has either negligible or no empty weight savings for the VTHL RLVs, while it leads to substantial empty weight savings for the HTHL RLVs. For the HTHL RLVs, increasing the turbine installed thrust to weight ratio causes a significant decrease in empty weight.

Acknowledgments

First, I would like to convey my gratitude to my faculty advisor, Dr. Milton Franke, and my sponsor from the Air Force Research Laboratory, Dr. Dean Eklund. Their guidance and support throughout the course of this thesis was certainly appreciated.

Second, I would like express my sincere appreciation to Dr. Ajay Kothari, President of Astrox Corporation. Not only did Dr. Kothari provide HySIDE for this study, he also went out of his way to make sure I understood how to use it and how it works.

Third, I am completely indebted to my wife for her unwavering support during this grueling experience. She provided continual encouragement to me during these last eighteen months, always helping me to focus on what's important in life.

Fourth, and most importantly, I must express my deepest gratitude to the one and only creator of the universe, Jesus Christ. God is enabling me to live life to its fullest, without having to worry about what the future holds. I am still working to view life through God's eternal point of view, but through His grace He has given me peace with the certainty that His ultimate plan will be accomplished.

Richard A. Caldwell

Table of Contents

List of Figures

List of Tables

Nomenclature

Symbol	Description
$\#_{turb}$	number of turbine engines
α	angle of attack (deg)
ϕ	equivalence ratio
ρ	atmospheric density (lbm/ft^3)
A_e	nozzle exit area (ft^2)
AFRL	Air Force Research Laboratory
AFRL/PR	Air Force Research Laboratory Propulsion Directorate
A_{inlet}	geometric inlet capture area (ft^2)
BPR	bypass ratio
C_D	drag coefficient
C_L	lift coefficient
D	drag (lbf)
DMSJ	dual-mode scramjet
DoD	Department of Defense
DP	design point
EELV	evolved expendable launch vehicle
g	standard sea level value of the acceleration due to gravity
G_{loss}	gravity losses (lbf)

GTOW	gross takeoff weight (lbf)
HC	hydrocarbon
HTHL	horizontal-takeoff-horizontal-landing
HySIDE	Hypersonic System Integrated Design Environment
HyTech	Hypersonic Technology
ISP	specific impulse (s)
JP-7	Jet Propellant
$K_{installed}$	HySIDE turbine installation factor
$K_{overall}$	HySIDE overall design uncertainty factor
L	lift (lbf)
LEO	low Earth orbit
LH_2	Liquid Hydrogen
LOX	Liquid Oxygen
M	mass (lbm)
$\dot{m}$	propellant mass flow rate (lbm/s)
$\dot{m}_a$	air mass flow rate (lbm/s)
$\dot{m}_e$	exit (air + fuel) mass flow rate (lbm/s)
$\dot{m}_f$	fuel mass flow rate (lbm/s)
M_{max}	maximum Mach number
NASA	National Aeronautics and Space Administration
NASP	National AeroSpace Plane

OMS	onboard maneuvering system
P_0	ambient atmospheric pressure (psia)
P_e	nozzle exit pressure (psia)
POST	Program to Optimize Simulated Trajectories
RBCC	rocket-based-combined-cycle
RBCC-Rkt	RBCC-powered booster, rocket-powered orbiter
RD-180	liquid hydrocarbon rocket engine
Rkt	pure rocket vehicle
Rkt-Rkt	rocket-powered booster, rocket-powered orbiter
RLV	reusable launch vehicle
RP-1	Rocket Propellant
S	planform area (ft^2)
SEI	SpaceWorks Engineering, Inc.
SSME	Space Shuttle Main Engine
SSTO	single-stage-to-orbit
STS	Space Transportation System
T	thrust (lbf)
T/W	thrust to weight ratio
T/W (Inst)	installed thrust to weight ratio
T/W (Uninst)	uninstalled thrust to weight ratio
$\left(T/W\right)_{TO}$	thrust to weight ratio at rocket ignition

TBCC	turbine-based-combined-cycle
TBCC-Rkt	TBCC-powered booster, rocket-powered orbiter
TJ	pure turbine vehicle
TJ-Rkt	turbine-powered booster, rocket-powered orbiter
TPS	thermal protection system
TSTO	two-stage-to-orbit
T_{TO}	takeoff thrust (lbf)
V	velocity (ft/s)
V_e	propellant exhaust velocity (ft/s)
V_{eq}	equivalent velocity (ft/s)
VTHL	vertical-takeoff-horizontal-landing
W	weight (lbf)

WEIGHT ANALYSIS OF TWO-STAGE-TO-ORBIT

REUSABLE LAUNCH VEHICLES FOR MILITARY APPLICATIONS

1. Introduction

1.1   Motivation

The Department of Defense (DoD) has identified responsive, low-cost space access as vital to sustaining U.S. military dominance [12:2]. Today, all DoD space launch systems are expendable and are completely tailored to launch specific payloads. Current launch systems require months of preparation time. Plus, at about $10,000 per pound to low Earth orbit (LEO), high launch costs substantially limit the number and size of payloads that can be economically launched into space. Although the evolved expendable launch vehicle (EELV) systems being used today are more capable and operable than their predecessors, they are still unable to meet the future requirements set forth by the DoD [45:27-28].

Reusable launch vehicle (RLV) systems, on the other hand, provide the capability to meet both current and future needs of U.S. space launch. RLVs can be designed to be more responsive and operable than their expendable counterparts, providing aircraft-like operations from military installations. And, since they are reusable, they should have significantly reduced operational costs, which in turn reduce the life-cycle costs (a sum of development, acquisition, and operation costs) of a fleet of RLVs [45:27-28].

The National Aeronautics and Space Administration (NASA) also recognizes the benefits provided by RLVs, and there is expected to be some teaming between NASA and the U.S. Air Force. However, this teaming can only go so far. NASA is pursuing a manned scheduled RLV, while the U.S. Air Force, acting on behalf of the DoD, requires an unmanned responsive RLV. This means that NASA is not pursuing some of the critical technologies needed to meet requirements that are unique to the DoD, such as responsiveness and operability. As a result, the U.S. Air Force must carry this burden alone [45:27-28; 15:70-71].

1.2   Research Objectives

The Air Force Research Laboratory (AFRL) Propulsion Directorate sponsored this research effort in order to attain an objective comparison between potential RLV configurations, and then determine which configurations are most promising to meet DoD needs [17]. This will help to highlight where critical advances must be made in RLV technologies, plus provides decision-makers the information needed to choose where to invest for future space access.

The AFRL Propulsion Directorate had three objectives for this study. The first objective was to analyze the total empty weights of four different two-stage-to-orbit (TSTO) RLV configurations, each distinguished by their unique propulsion systems. The second objective was to examine the empty weight sensitivity of these four RLVs to orbiter fuel selection. The third objective was to investigate the RLV empty weight effects of increasing the turbine installed thrust to weight ratios for the RLVs utilizing afterburning turbine engines.

1.3   Research Focus

Each vehicle in this study is completely reusable and unmanned, designed for a roundtrip to a 100 nautical mile circular LEO with a fixed payload requirement of 20,000 lbf. Wherever possible all RLVs were designed with the same group of input values in order to give an "apples to apples" comparison, except when the particular RLV has a unique requirement, such as propulsion method or takeoff thrust to weight ratio. The propulsion systems considered in this study include pure rocket, pure turbine, rocket-based-combined-cycle (RBCC), and turbine-based-combined-cycle (TBCC). The hydrocarbon dual-mode scramjet (DMSJ) engines used in the RBCC and TBCC propulsion systems represent possible applications of the current research being performed in the U.S. Air Force HyTech program [37:1170-1171; 2:1].

1.4   Methodology

Astrox Corporation's HySIDE code has been used as the design tool throughout the study [25]. HySIDE, or Hypersonic System Integrated Design Environment, can be used to study a wide range of airbreathing and rocket RLVs throughout their entire flight regime. It analyzes the vehicles in a completely integrated fashion, which is essential for designing hypersonic vehicles, by combining engine performance, aerodynamic characteristics, heating conditions, mass properties, and volume constraints into a single vehicle model. The propulsion components in HySIDE may include any combination of turbine, DMSJ, or liquid rocket engines operating during user specified trajectory segments. Vehicle propulsion performance, combined with aerodynamic losses, is

3

calculated all the way through the flight trajectory. The RLVs are then finalized, or

closed, by iterating the vehicle dimensions until the available internal volume satisfies

volume requirements [27].

1.5   Thesis Overview

This work is structured into five chapters plus three appendices. Chapter 2

reviews some of the literature related to RLVs, including past U.S. Air Force

involvement with RLV programs, as well as some of the propulsion systems that have

been proposed for future RLVs. Chapter 3 presents the research methodology with an in-

depth discussion of HySIDE, together with the assumptions that went into this study.

Chapter 4 discusses the results of the study, with a thorough analysis of all of the RLV

configurations. Chapter 5 provides the overall conclusions of this study, followed by

recommendations for which configurations are most promising to meet DoD needs.

Throughout the literature review, English units were observed to be the industry

standard for RLV research. Therefore, this work provides all data in English units in

order to be consistent with the U.S. aerospace propulsion community.

2. Literature Review

This chapter starts out with a background discussion on U.S. Air Force involvement with RLVs. The second section then examines the reasons for staging and why a TSTO RLV is the most feasible solution for the near future. Next, the third section reviews some basic rocket and airbreathing propulsion systems that have potential applications in RLVs. The fourth section then gives justifications for incorporating airbreathing propulsion systems in RLVs, even though space launch has traditionally always been performed by rocket engines. Next, the fifth section investigates advanced propulsion systems, and how the best solution for RLV propulsion systems might be to combine airbreathing and rocket systems. The sixth section then discusses the factors involved in fuel selection for RLVs, and how hydrocarbon fuels are potentially more practical and operable for responsive military applications. Lastly, the seventh section describes recent RLV research that is noteworthy and related to this work.

2.1 RLV Background

The U.S. Air Force has a considerable history in the pursuit of RLVs, but three programs come to the forefront in this discussion: Dyna-Soar from the 1950's-1960's, the Space Shuttle from the 1970's-1980's, and the National AeroSpace Plane from the 1980's-1990's. Two other research and development programs, Hyper-X and HyTech, have continued to pursue breakthrough technologies in order to make future RLVs a reality.

The X-20 Dyna-Soar (Dynamic Soaring) was a U.S. Air Force program to develop a reusable spaceplane that could be used for a variety of military missions. As shown in Figure 1, Dyna-Soar was designed to be launched into orbit atop an expendable booster, and would have enabled the Air Force to operate a manned spaceplane during the late 1960s. Dyna-Soar was to be 35 ft long and 20 ft wide, not including the expendable booster. The program was initiated in 1957 and cancelled in 1963 due to political concerns. Much of the research and technology acquired during the Dyna-Soar program went into the Space Shuttle, including ceramic heat-resistant material [43:120-126].
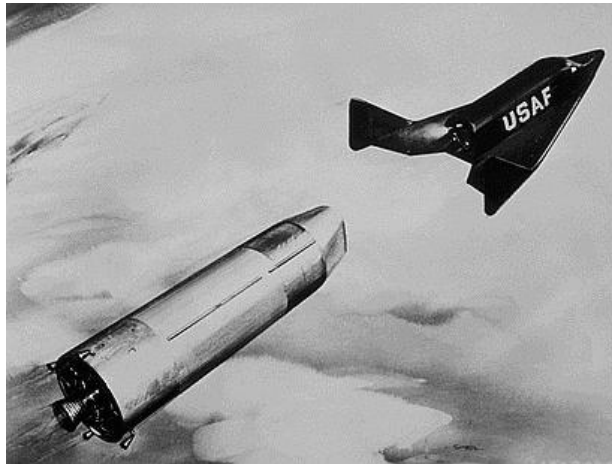
Figure 1. Drawing of Dyna-Soar Separating From Expendable Upper Stage [47]

The Space Shuttle Program, officially known as the Space Transportation System (STS), began in 1972. The Nixon administration advised NASA that there would not be a Space Shuttle if NASA could not get the development cost down and get the U.S. Air Force to participate. Therefore, an agreement was made between NASA and the Air Force that prompted the Air Force to give political support to the threatened Space

Shuttle in turn for military use of the new system. As such, many of the Air Force's requirements had to be met in the Space Shuttle design. Forced to reduce development costs, NASA discarded the concept of reusing anything but the Space Shuttle orbiter. Instead, the shuttle would be boosted by cheap solid fuel boosters as shown in Figure 2, and taking a concept from the Air Force, the liquid propellants would be put in a big expendable drop tank [43:180-184].

The Space Shuttle came up short in two areas. First, the shuttle orbiter ended up almost 20% over its specified weight, resulting in it being unable to boost Air Force payloads into polar orbits from Vandenberg Air Force Base. Second, it failed to reduce the cost of putting payloads into orbit. This was due in large part to the fact that it was a manned vehicle. After the Challenger disaster in 1986, the Air Force withdrew its involvement in the Space Shuttle [43:221-230].
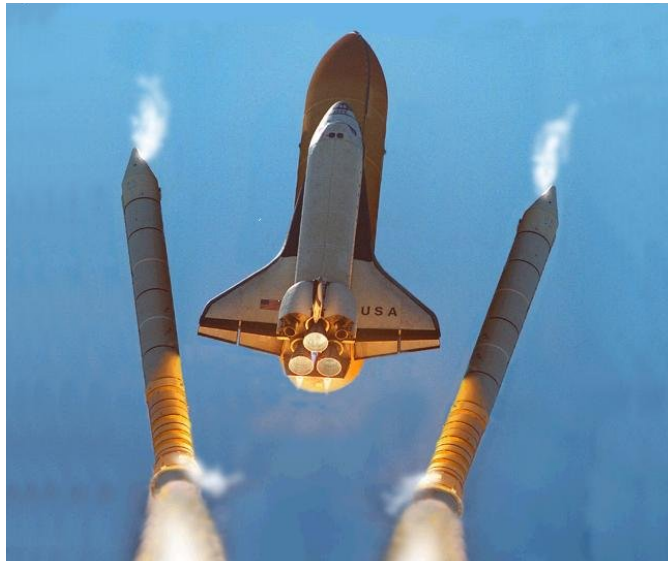
Figure 2. Space Shuttle Orbiter Separating from Solid Rocket Motors [50]

The X-30 National AeroSpace Plane (NASP) was a joint development between NASA and the U.S. Air Force. The objective was to develop a family of hypersonic single-stage-to-orbit aircraft/spacecraft able to take off from and land on conventional runways. As shown in Figure 3, NASP would have utilized a wide, lifting body design, with small wings providing the horizontal control surfaces and dual aft vertical stabilizers. NASP was to employ 3-5 scramjet engines and a single 50,000-70,000 lbf thrust rocket. With a crew of two, NASP was to be 150-200 ft in length, and have a takeoff weight of 250,000-300,000 lbf. The program was initiated in 1986 and cancelled in 1994 due to technical difficulties, budgetary cutbacks, and environmental concerns [39:4-7].
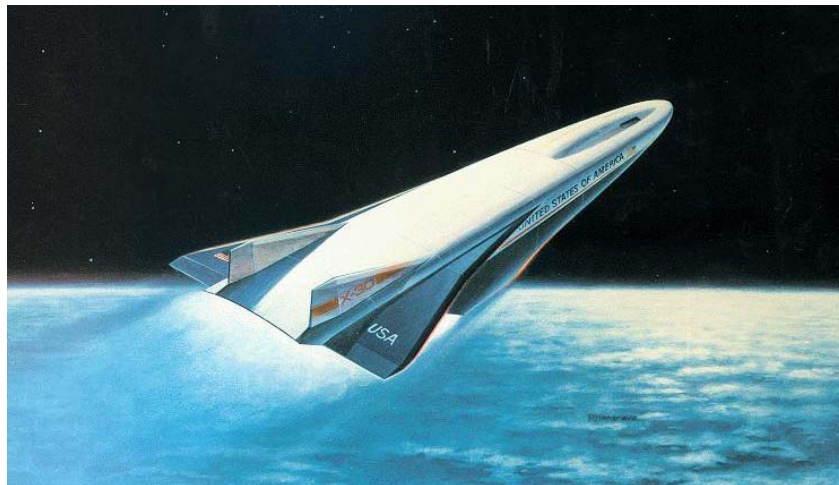
Figure 3. Drawing of National AeroSpace Plane [48]

NASP never came to fruition, but many advanced technologies were still able to be developed, particularly in new resilient lightweight structural materials, propulsion systems, slush hydrogen fuel and thermal protection system techniques. In fact, the

original NASP engine design, significantly modified by NASA, provided the foundation for the scramjet engine used in the X-43A Hyper-X research vehicle program [1:6-7]. The first X-43A flight failed in June 2001 when the booster rocket used to accelerate it to flight speed veered off course and had to be destroyed. However, the second and third flights were successful, with the March 2004 flight reaching Mach 6.8 and the November 2004 flight reaching Mach 9.8 [51].

Although both successful X-43A vehicles were only powered under their own engines for about ten seconds, NASA was able to gather data that has never before been obtained and concluded that the vehicles produced enough thrust to overcome drag. This was a major accomplishment, as the X-43A was the first free-flying demonstration of an airframe-integrated scramjet. However, with NASA now allocating the majority of its resources to restoring the space shuttle fleet to flight, finishing construction of the International Space Station, and developing technology for manned missions to the Moon and Mars, the eight-year Hyper-X program has been canceled with no additional scramjet flights on the drawing board [14].

The U.S. Air Force is now leading the way in scramjet research and development with the Hypersonic Technology (HyTech) program. Headquartered at the AFRL Propulsion Directorate, HyTech was initiated in 1995 to provide a research program on hypersonic technologies following the cancellation of NASP. While most scramjet designs to date have used hydrogen fuel, HyTech runs on conventional hydrocarbon fuels, which have a higher energy density and are much safer and easier to manage than

hydrogen. A full-scale engine is now being built, which will use its own fuel for cooling [37:1170-1171; 2:1].

2.2   RLV Staging Options

Many researchers believe that single-stage-to-orbit (SSTO) is the solution to excessive launch costs; however, staging has many benefits. First, staging can reduce the sensitivity of a vehicle to performance parameter variations. This would require less stringent propellant mass fractions, resulting in lower gross takeoff weight (GTOW) than SSTO vehicles. Second, TSTO vehicles offer greater margin and have higher payload potential than SSTO vehicles. This means that equal performance and lower risk are possible with less advanced technology. Third, if vehicles with airbreathing propulsion are considered, the useful airbreathing corridor for TSTO vehicles is larger than that for SSTO vehicles, and first stages of a TSTO concept have potential for greater atmospheric-cruise capability than SSTO vehicles. Therefore, it is reasoned that TSTO is the most feasible solution for the near future, especially with the lessons learned from the NASP program [39:3-4; 5:2; 20:3-4; 41:1-2].

2.3   RLV Basic Propulsion Options

Space launch vehicles produce thrust by exchanging momentum with a fluid, called a propellant, which is then expelled from the vehicle through the propulsion system. The primary two methods of producing thrust for space launch applications are with either rocket or airbreathing propulsion systems.

2.3.1 Rocket Propulsion Systems

Rockets carry with them all of their propellant, which is a combination of fuel and oxidizer. Thrust is produced by converting the internal energy of the propellant to kinetic energy. This internal energy is released by mixing and burning the stored fuel and oxidizer in the combustion chamber. Momentum is then imparted to the propellant, now in the form of hot gases, as it is expelled through the nozzle. Two types of rocket propulsion are normally considered for space launch vehicles: liquid rocket engines and solid rocket motors [22:469].

For a liquid rocket engine, shown in Figure 4, the fuel and oxidizer are kept in individual tanks. Then they are pumped into the combustion chamber, where they are mixed and combusted at high pressure [24:179-180]. In contrast, a solid rocket motor, shown in Figure 5, is composed of a solid mixture of fuel and oxidizer that is molded to the interior walls of the combustion chamber. This solid mixture then burns at high pressure once it is sufficiently heated [24:295-296].
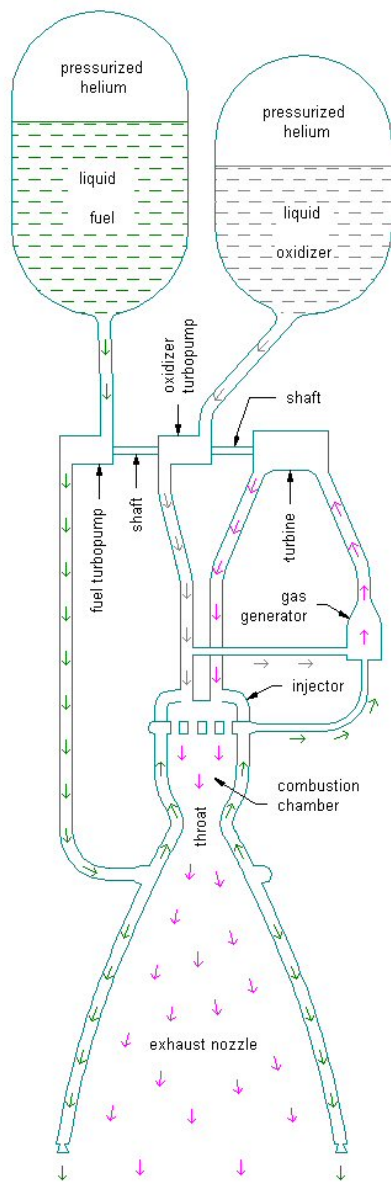
Figure 4. Liquid Rocket Engine [49]
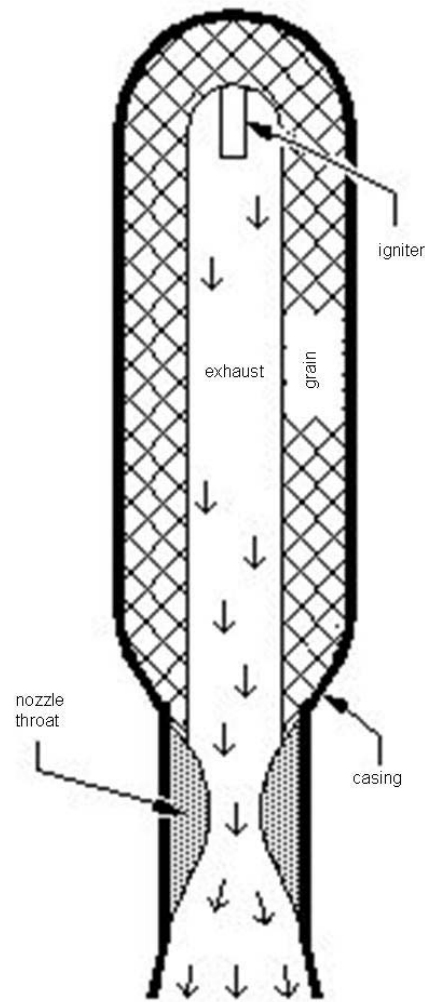
Figure 5. Solid Rocket Motor [49]

Solid rocket motors tend to be simpler than liquid rocket engines due to few moving parts, and they are also able to respond more quickly because the propellant is already loaded in the vehicle. However, liquid rocket engines are able to throttle their thrust levels with the turbine-driven pumps, and they also have the potential to restart.

12

This is not the case in solid rocket motors, where once ignited, it must burn until the propellant supply is exhausted [22:513-514].

An air-augmented rocket is essentially a mixture of rocket propulsion and airbreathing propulsion. When an air-augmented rocket reaches an acceptable speed, such as Mach 2 or Mach 3, it operates fuel-rich, and then augments the oxidation of the fuel with atmospheric air, thereby becoming a quasi-airbreathing engine. It is able to perform like this possibly up to Mach 10, and then convert back to normal rocket function. Air-augmented rockets are placed in a duct that captures air, and are able to boost specific impulse performance by several percentage points over conventional rockets. Both liquid and solid rockets can be made to function as air-augmented rockets [24:631-633].

2.3.2 Airbreathing Propulsion Systems

Airbreathing engines are distinguished from rockets by the fact that they use atmospheric oxygen as the oxidizer for the propulsion system; thus only fuel needs to be carried onboard. The propellant in this case consists of air drawn into the engine through the inlet, plus the fuel that is mixed with the air and burned in the combustion chamber. Three forms of airbreathing propulsion are normally considered for space launch vehicles: turbine, ramjet, and scramjet.

In a turbine engine, shown in Figure 6, thrust is developed by compressing air in the inlet and compressor, injecting fuel into the compressed air and burning in the combustion chamber, and expanding the gas stream through the turbine and nozzle. The expansion of gas through the turbine supplies the power to turn the compressor. The hot

13

gases are then expelled through the nozzle, developing thrust. For additional thrust, an afterburner can be added, in which additional fuel is introduced into the hot exhaust and burned. This gives a resultant increase in engine thrust by way of even higher exit velocity, but at the expense of a lower specific impulse. Turbine engines are most commonly used up to Mach 4 [22:164-165; 45:15].
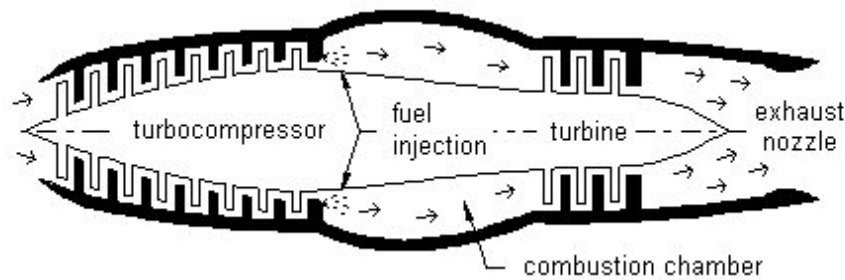
Figure 6. Turbine Engine [49]

A ramjet engine, shown in Figure 7, differs from a turbine engine in that a ramjet has no moving parts. It achieves compression of intake air by the forward velocity of the vehicle. Air enters the inlet where it is decelerated to subsonic conditions and compressed, and then it enters the combustion zone where it is mixed with the fuel and burned. A ramjet is able to operate with no moving parts because the inlet decelerates the incoming air to raise the pressure in the combustion chamber, i.e. the higher the velocity of the incoming air, the greater the pressure rise. It is for this reason that a ramjet can only operate efficiently at high supersonic velocities, so they are typically employed above Mach 3. As the flight velocity reaches approximately Mach 6, the air flow can no longer be efficiently decelerated, because the loss of total pressure and thermal

dissociation degrade the cycle performance. Also, the mechanical loads and thermal stresses on the engine become unbearable at flight velocities approaching Mach 6. Ramjet engines are a proven technology and have found most of their use in missiles, where they are boosted to operating speeds by a rocket motor, or by being attached to a fighter aircraft [22:155-157; 45:15].
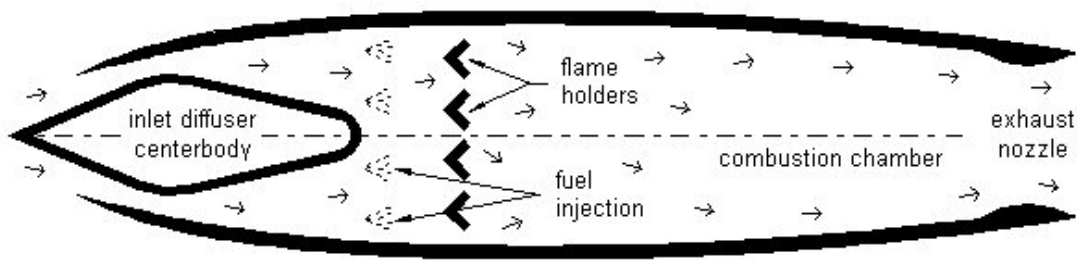
Figure 7. Ramjet Engine [49]

A scramjet engine, shown in Figure 8, is similar to a ramjet, except that the air entering the inlet is not slowed to subsonic speeds in order to keep the temperatures lower. Combustion then takes place at supersonic air velocities through the engine. It is mechanically simple, but vastly more complex aerodynamically than a turbine or ramjet engine. The challenge of making a scramjet engine work is to properly mix the high-speed air with fuel while combusting and expanding that mixture before it exits the tail of the vehicle. This process typically occurs in less than 1 millisecond. Furthermore, the scramjet must burn enough fuel to generate enormous amounts of energy needed to overcome tremendous drag forces experienced when flying at hypersonic speeds [21:23-24].

15
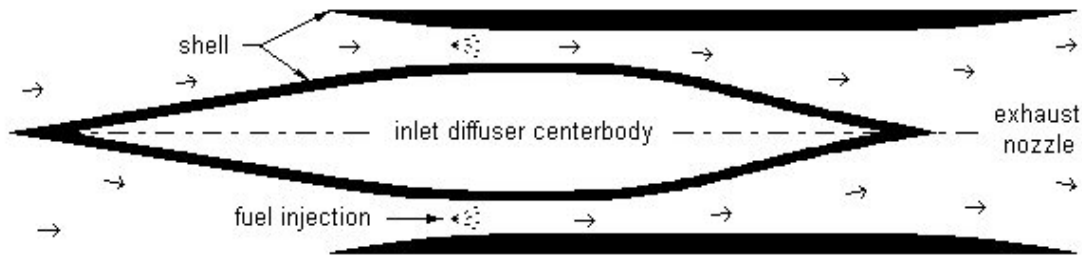
Figure 8. Scramjet Engine [49]

Dual-mode scramjet (DMSJ) engines operate over the entire velocity range of ramjet and scramjet engines. Hydrocarbon-fueled DMSJ engines, such as those researched under the U.S. Air Force HyTech program, are able to efficiently operate up to Mach 8. At that point, the fuel-air equivalence ratio necessary for cooling the vehicle exceeds that which is needed for propulsion. On the other hand, hydrogen-fueled DMSJ engines are theoretically able to operate well beyond Mach 8, since hydrogen has much greater cooling capacity than hydrocarbon fuels [45:15-16]. However, there are many developmental and operational disadvantages to using liquid hydrogen, as discussed in Section 2.6.

2.4   Justification for Airbreathing Propulsion in RLVs

One of the biggest debates among researchers of RLVs is that of rocket versus airbreathing propulsion. Space launch has traditionally always been performed by rocket engines, so why change now?

2.4.1   Airbreathing Propulsion Advantages

There are several key advantages that airbreathing propulsion systems have over conventional rockets. First, airbreathing engines utilize atmospheric oxygen for

16

combustion instead of an onboard supply of oxidant. This is an important advantage over rocket engines because the oxidizer, which makes up a significant portion of the gross weight of a conventional launch vehicle, does not need to be carried aboard the vehicle for the airbreathing engines. For example, as shown in Figure 9, a rocket carries approximately 6 lbm of oxygen for every lbm of hydrogen. In contrast, an airbreathing system processes approximately 34 lbm of air for every lbm of hydrogen (oxygen is still needed for subsonic rocket operation, or for the final push to space). By virtue of this fact, specific impulse of the airbreathing system is greatly increased, as shown in Figure 10. Specific impulse, which is the thrust divided by the weight flow rate of fuel, is essentially a measure of engine fuel efficiency. Another way of thinking about this is that an airbreathing engine, as compared to a rocket engine, operates much more efficiently by using much less propellant carried aboard the vehicle to produce an equivalent amount of thrust [3:2-3; 16].
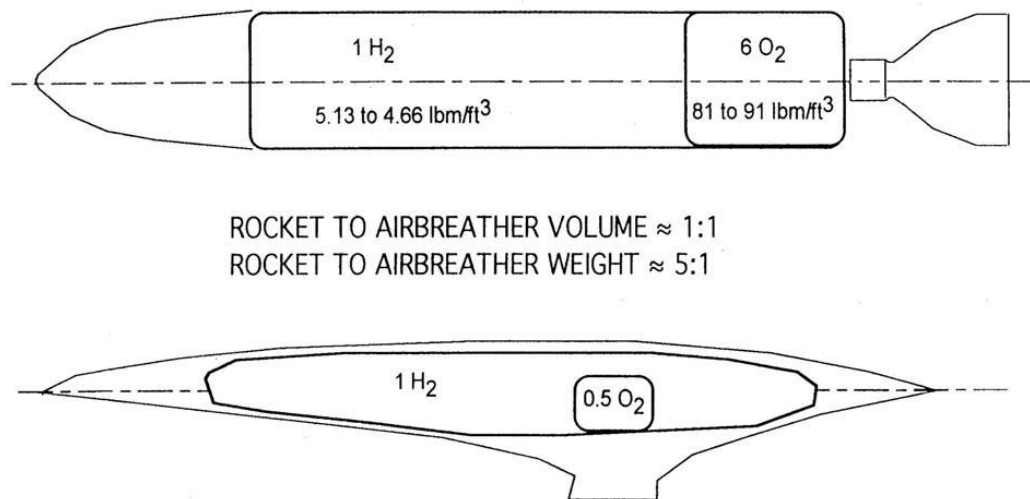
Figure 9. Volume and Weight Comparison of Rocket and Airbreathing Vehicles [16]

17
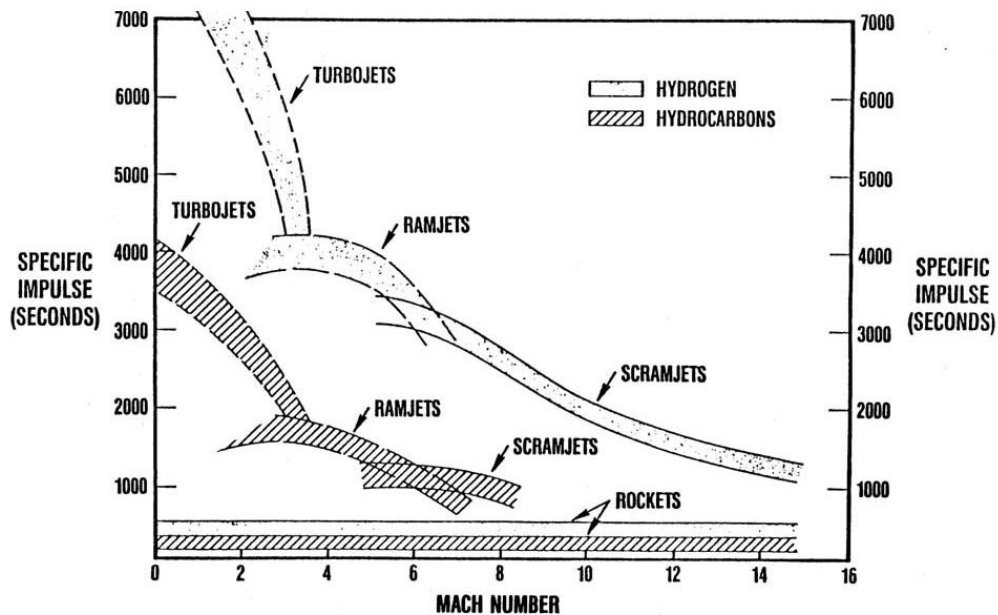
Figure 10. Specific Impulse vs. Mach Number [16]

A second key advantage of airbreathing propulsion systems is the ability to allow for horizontal takeoff, due in large part to the reduced propellant requirements of airbreathing propulsion systems. The horizontal takeoff capability of airbreathing vehicles is extremely attractive, providing many operability benefits including mission abort capability and trajectory flexibility. Horizontal takeoff vehicles also have the potential to utilize existing aircraft ground facilities. The capability to operate from a standard commercial runway eliminates the requirement to rotate the vehicle on a dedicated launch pad. This results in substantial operational cost savings compared to pure rocket systems, which require complex ground support equipment around the launch pad. Furthermore, the range safety is simpler to manage with the airbreathing propulsion system because of its ability to taxi on the runway along with its flyback mission abort

18

capability. These factors result in additional operational cost savings over pure rocket

systems, which require abort scenarios, flight corridors, and safety systems similar to

current processes [3:4-6; 20:3-4; 10:1-2].

A third key advantage of airbreathing engines is that they are less sensitive to

inert mass increases, mainly because of their lower propellant fraction. This allows for

additional safety margin and reduced sensitivity to weight growth as compared to pure

rocket-based systems, and it provides the flexibility to build in reliability, maintainability,

durability, and operability. This is achieved in part because airbreathing propulsion

systems have lower operating pressures than comparable rocket-based systems, which

leads to improved reliability and reusability. This speaks well for airbreathing engines,

because almost half of all space launch failures have been caused by a malfunction in the

propulsion system. Furthermore, the range safety is simpler to manage with the

airbreathing propulsion system because of the flyback mission abort capability [32:1;

42:2-3; 26:1-2].

2.4.2   Airbreathing Propulsion Disadvantages

There are a number of challenges that face airbreathing propulsion systems when

considering application to space launch missions. One disadvantage of airbreathing

engines is that no single engine can cover the same span of Mach numbers as a rocket.

As shown in Figure 11, turbine engines reach their upper limit at Mach 4, ramjets operate

up to Mach 6, and scramjets operate possibly well past Mach 10. From there, rockets are

still needed to reach orbit [33:2].
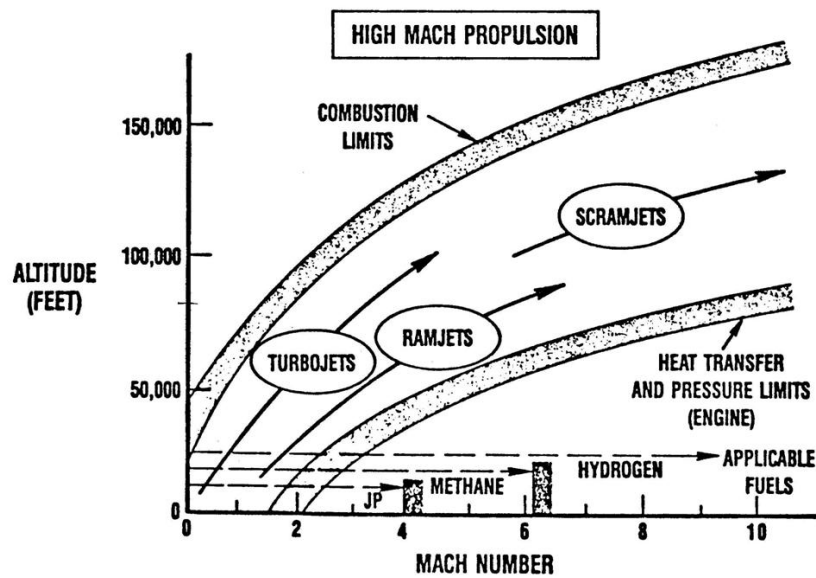
Figure 11. Altitude vs. Mach Number [16]

Another disadvantage of airbreathing propulsion systems is that they have a higher dry weight than a rocket system designed for the same mission. This is due to many factors. First, the thrust to weight ratio of an airbreathing engine is substantially less than that of a rocket engine, which means that airbreathing engines are much larger than rocket engines of the same thrust. Second, a heavier vehicle thermal protection system (TPS) is necessary because of the extreme heating experienced by the vehicle during the high dynamic pressure ascent trajectory. Third, the streamlined configurations required for hypersonic flight create the need for complex internal fuel tanks that conform to the vehicle's aerodynamic shape. These factors combine to increase the dry weight of the propulsion system, which must be traded off against the savings in propellant that the higher specific impulse yields [20:2-3; 30:1-2; 28:1-2].

20

2.5 RLV Advanced Propulsion Options

Now that the advantages and disadvantages of rockets and airbreathing engines have been shown, one might wonder which one is best for space launch applications. Well, the answer might be a combination of some or all of them. If rocket and airbreathing engines were combined into one package, then it might be possible to build and operate a launch system that would cost less, weigh less, and be more reliable than current systems. This is the vision for combined-cycle engines. A notional RLV flight profile utilizing combined-cycle engines is shown in Figure 12.
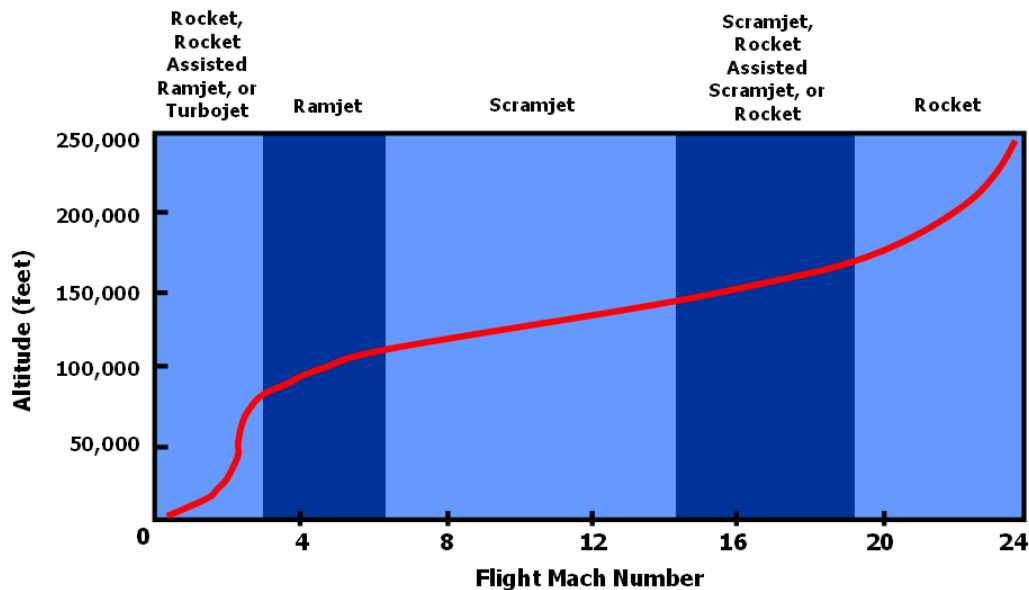
Figure 12. Notional RLV Flight Profile [16]

There are two ways to combine engine cycles, as shown in Figure 13. One way is to integrate the various engine components into a common flowpath. A second way to create a combined-cycle engine is to have two separate flowpaths, with each engine

component only operating during its segment of the flight regime. Either method enables the space launch vehicle to perform multimode operation over a wide speed and altitude range [11:1-3; 18:2-4].
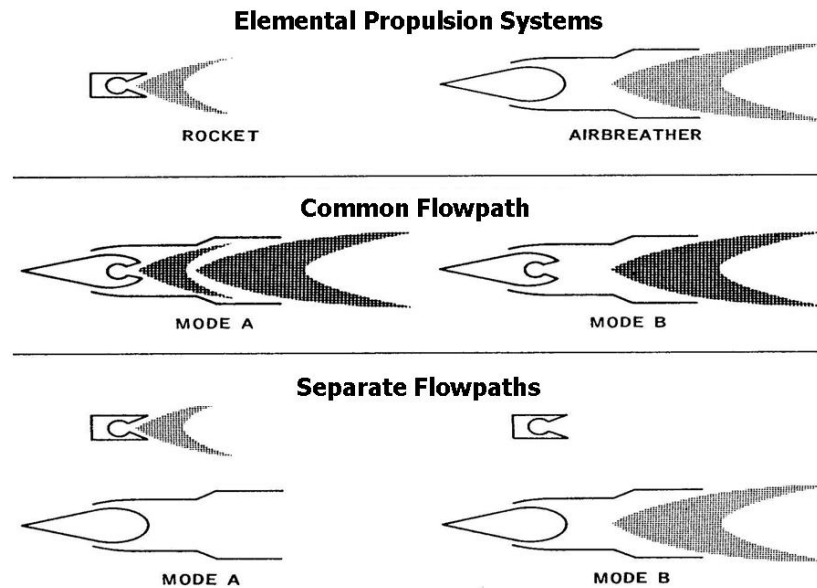
Figure 13. Ways to Combine Engine Cycles [16]

2.5.1 Rocket-Based-Combined-Cycle Propulsion Systems

RBCC propulsion systems consist of integrating rocket, ramjet, and scramjet engines into a single propulsion system [23:2]. An RBCC propulsion system can have up to four primary operating modes, as shown in Figure 14. The first mode consists of either a rocket or an air-augmented rocket, and it operates from takeoff up to ramjet takeover speed. The second mode consists of a ramjet, followed by a scramjet in the third mode.

The fourth mode, if required, is powered by a rocket. An example of a notional RBCC

RLV is shown in Figure 15.
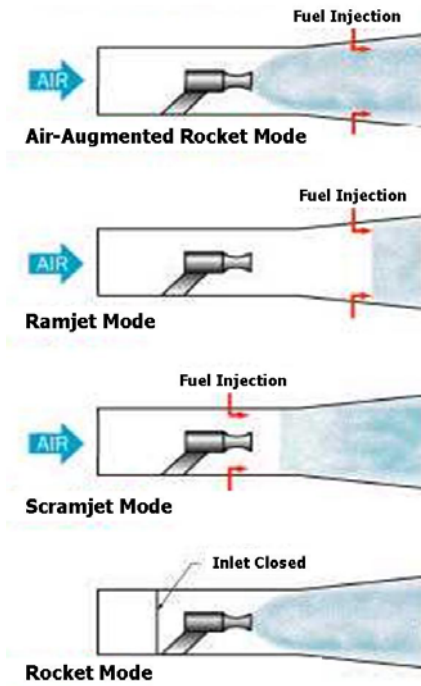
Figure 14. RBCC Operating Modes [16]
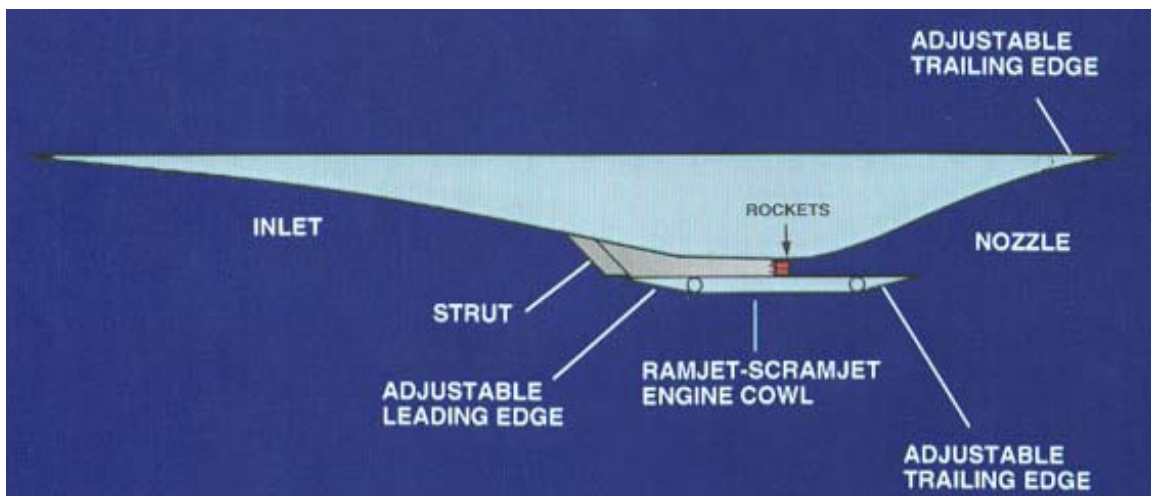
Figure 15. Notional RBCC RLV [46]

2.5.2 Turbine-Based-Combined-Cycle Propulsion Systems

TBCC propulsion systems consist of integrating turbine, ramjet, and scramjet engines into a single propulsion system [9:2]. The TBCC propulsion system has three primary operating modes. The first mode is powered by turbine engines, which operate from takeoff up to ramjet takeover speed. The second mode consists of a ramjet, followed by a scramjet in the third mode. Unless the vehicle also includes rocket engines, TBCC vehicles cannot operate over the entire flight regime and can only be used as the first stage in a TSTO RLV. An example of a notional TBCC RLV is shown in Figure 16.
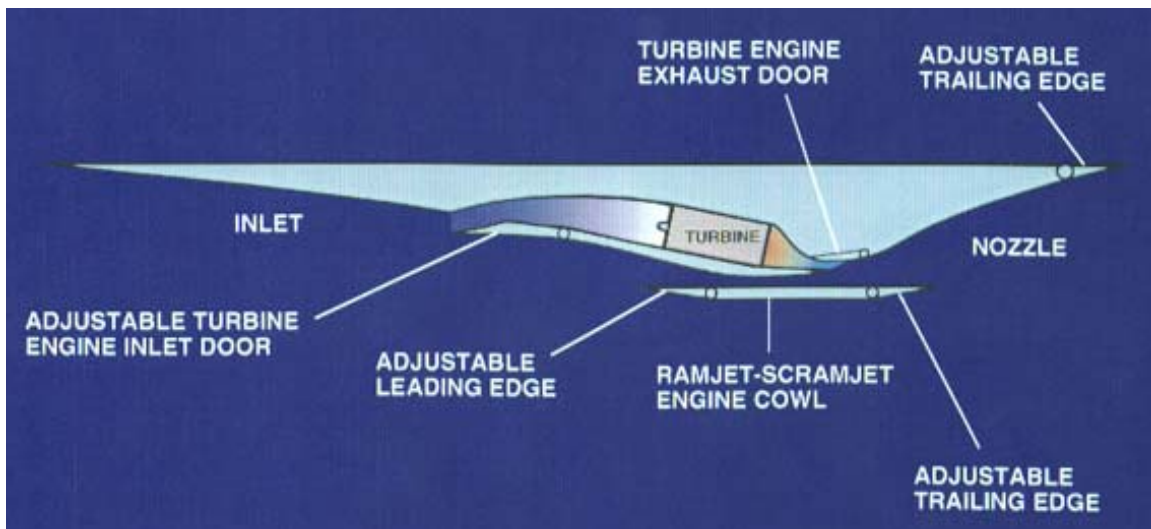
Figure 16. Notional TBCC RLV [46]

2.6 RLV Fuel Options

There are two types of fuels generally used in space launch vehicles: liquid hydrogen and hydrocarbon. Hydrogen has a quicker burning rate and releases a larger

amount of energy per unit weight and than hydrocarbon fuels. However, hydrocarbon

fuels are far denser than liquid hydrogen, meaning that a given volume of hydrocarbon

fuel is significantly more powerful than a similar volume of liquid hydrogen. The tanks

and plumbing of a hydrocarbon-fueled engine are also more compact and lighter than

those of a hydrogen-fueled engine, due to the fact that pressurization and insulation is not

required. All of this equates to smaller fuel tanks for hydrocarbon engines, which helps

to achieve a lower vehicle empty weight [29:1214-1215].

Another advantage of hydrocarbon fuel is the fact that the fuel can be stored at

room temperature, and it is fairly easy to handle as compared to liquid hydrogen.

Hydrocarbon fuel is also relatively inexpensive compared to hydrogen fuels. All of these

factors make hydrocarbon fuels more practical and operable for responsive military

applications [29:1214-1215; 37:1170-1171].

2.7   Recent RLV Research

RLVs are a popular topic for research within industry and academia, and there is a

plethora of RLV designs that have been published. These studies range from a high-level

comparison of several different RLV designs, to an in-depth design study of a single

RLV configuration. This work attempts to incorporate elements of all relevant past RLV

studies and then build upon them. Three studies in particular are noteworthy and related

to this work, and are here called the 2004 AFIT RLV Study, 2004 Astrox RLV Study,

and 2004 SpaceWorks Engineering RLV Study.

2.7.1   2004 AFIT RLV Study

The 2004 AFIT RLV Study investigated the performance of five TSTO RLVs, with stages propelled by rocket engines, turbine engines, and RBCC engines [8]. In this study, a fixed takeoff weight of 1,000,000 lbf was assumed for all five RLVs, and the performance of each RLV was determined by the payload weight delivered to orbit and the total vehicle dry weight. A design method was formulated using a trajectory optimization program, Program to Optimize Simulated Trajectories (POST), to simulate the RLV flight profiles. RLV trajectory constraints, mass fractions, engine performance, and aerodynamics were assumed from literature of similar RLVs or data provided by AFRL. The 2004 AFIT RLV Study concluded that the RLV with both stages propelled by rocket engines lifted the most payload weight into orbit (17,560 lbf) with the lowest vehicle dry weight (98,244 lbf).

2.7.2   2004 Astrox RLV Study

The 2004 Astrox RLV Study compared TSTO RLVs powered by rocket engines with SSTO RLVs powered by RBCC engines [13]. The TSTO RLVs powered by rocket engines were analyzed in hydrocarbon-fuel, hydrogen-fuel, and duel-fuel configurations. The SSTO RLVs powered by RBCC engines were analyzed in hydrogen-fuel and duel-fuel configurations. Each RLV had a fixed payload requirement of 20,000 lbf to orbit, and they were compared on the basis of lowest empty weight. In this study, Astrox Corporation's HySIDE code was used as the vehicle design tool, which can be used to study a wide range of rocket and airbreathing RLVs throughout their entire flight regime.

26

The 2004 Astrox RLV Study concluded that VTHL SSTO RLVs have an empty weight advantage over HTHL SSTO RLVs, with the lowest empty weight in this study coming from the duel-fuel VTHL SSTO RLV using an inward turning inlet (109,311 lbf). The lowest empty weight of the TSTO RLVs powered by rocket engines was achieved with the duel-fuel configuration (174,683 lbf).

2.7.3   2004 SpaceWorks Engineering RLV Study

In the 2004 SpaceWorks Engineering RLV Study, a single HTHL TSTO launch vehicle called Quicksat was designed, capable of launching a payload of 10,020 lbf to orbit [6]. The Quicksat vehicle consists of a completely reusable first stage booster with an expendable second stage orbiter. Quicksat was designed and analyzed using ModelCenter, which is a collaborative, distributed framework containing several industry standard analysis tools. The HTHL Quicksat booster uses a TBCC propulsion system with non-cryogenic hydrocarbon propellants for improved operability in support of military operations. The DMSJ engines used in the TBCC propulsion system represent possible applications of the current research being performed in the U.S. Air Force HyTech program. In addition to the DMSJ engines, the TBCC propulsion system includes six turbine engines, each producing 65,660 lbf of thrust, which results in a turbine installed thrust to weight ratio of 9.96. The booster also has four tail rockets to provide additional thrust through the transonic flight regime. The empty weight of the booster is 167,840 lbf, and the gross takeoff weight of the entire vehicle (reusable booster + expendable orbiter) is 741,760 lbf.

3. Methodology

This chapter discusses the methodology used to determine the empty weight of several distinct TSTO RLV configurations. Turbine, dual-mode scramjet (DMSJ), and liquid rocket engines were all considered as possible elements for the RLV propulsion systems. Astrox Corporation's HySIDE code was an integral tool in this study, which was used to analyze the vehicles in a completely integrated fashion. HySIDE combines engine performance, aerodynamic characteristics, heating conditions, mass properties, and volume constraints into a single vehicle model, which is essential for designing hypersonic vehicles.

Two sensitivity analyses were then performed on areas of interest directly affecting the propulsion systems in this study. The first sensitivity analysis investigated the effect orbiter fuel selection had on the empty weight of the RLV. The second sensitivity analysis investigated the effects of increasing the turbine installed thrust to weight ratios for the RLVs utilizing turbine engines during the ascent phase of their trajectory.

This chapter also discusses the methodology used to verify the results generated with HySIDE by utilizing the Program to Optimize Simulated Trajectories (POST). Additional sections include a discussion of the flight fundamentals employed in this study, as well as the assumptions that were made regarding engine performance and flight trajectories.

3.1   TSTO RLV Configurations

This study considers four unique TSTO RLV configurations, each dictated by the propulsion system chosen for each stage. Vehicle empty weight was the primary figure of merit in this study. According to many researchers, a launch system's acquisition and operational cost is directly related to the system's empty weight, which must therefore be minimized [5:1; 20:4; 13:9; 31:2]. This is based on the assumption that cost vs. weight trends for commercial and military aircraft, which have a nearly linear relationship for empty weight, can be extrapolated to space launch systems.

The booster propulsion systems considered in this study include pure rocket (Rkt), pure turbine (TJ), rocket-based-combined-cycle (RBCC), and turbine-based-combined-cycle (TBCC). The orbiters all have a pure rocket propulsion system. The RBCC propulsion systems were modeled as rocket engines combined with DMSJ engines, while the TBCC propulsion systems were modeled as turbine engines combined with DMSJ engines. Four baseline RLV configurations were analyzed, with two of them vertical-takeoff-horizontal-landing (VTHL) and the other two horizontal-takeoff-horizontal-landing (HTHL). The VTHL configurations include the Rkt-Rkt and RBCC-Rkt. The HTHL configurations include the TBCC-Rkt and TJ-Rkt.

Each vehicle in this study is completely reusable and unmanned, and is designed for a roundtrip to a 100 nautical mile circular LEO. The RLVs all have a payload requirement of 20,000 lbf in a 12 ft diameter by 25 ft length payload bay, plus reserve propellants. The RLVs are serial burn, meaning that the engines for the second stage orbiter are not in operations until after stage separations. All baseline RLV

29

configurations exclusively use hydrocarbon (HC) fuels, either JP-7 or RP-1, combined with air as the oxidizer for airbreathing engines and liquid oxygen as the oxidizer for rocket engines. After staging, all of the boosters use turbine engines to fly back to base, while the orbiters fly to a 50x100 nautical mile parking orbit. The orbiters then utilize onboard maneuvering system (OMS) engines to circularize the orbit to 100 nautical miles.

3.2   Flight Fundamentals

The motion of a reusable launch vehicle is defined by the interaction of the aerodynamic and body forces acting upon it. The body force, caused by gravity, is weight (W). Weight is given by

$$W = M \cdot g \tag{1}$$

where M is mass and g is the standard sea level value of the acceleration due to gravity. Weight decreases throughout the flight profile because of fuel expenditure and staging.

The aerodynamic forces acting upon the vehicle are lift (L), drag (D), and thrust (T). In reality, there is a single, integrated aerodynamic force caused by the pressure variations acting through the center of pressure and by the shear forces along the vehicle surface. However, for analytical purposes, it is often convenient to break these forces into components.

By definition, the component of the aerodynamic force perpendicular to the flight path direction is called lift; the component of the aerodynamic force opposing the flight path direction is called drag. Lift and drag are given by

$$L = C_L \cdot \frac{1}{2} \cdot \rho \cdot V^2 \cdot S \tag{2}$$

$$D = C_D \cdot \frac{1}{2} \cdot \rho \cdot V^2 \cdot S \tag{3}$$

where ρ is the atmospheric density, V is the velocity of the vehicle, and S is the planform area [34:557]. C_L and C_D are the lift coefficient and drag coefficient, respectively, which are dimensionless quantities dependent upon vehicle shape, aerodynamic properties, and angle of attack (α).

Thrust is a force that must be created by the RLV in order to accelerate the vehicle to orbital velocity. In addition to providing vehicle acceleration, thrust must also be able to overcome drag, plus a portion of the vehicle weight when not in straight and level flight. This is shown in Figure 17, where the flight path direction is aligned with the thrust vector, and opposite in direction to the drag vector. For a rocket engine, thrust is given by

$$T = \dot{m} \cdot V_e + (P_e - P_0) \cdot A_e \tag{4}$$

where $\dot{m}$ is the propellant mass flow rate, V_e is the propellant exhaust velocity, P_e is the nozzle exit pressure, P_0 is the ambient atmospheric pressure, and A_e is the nozzle exit area [24:110].
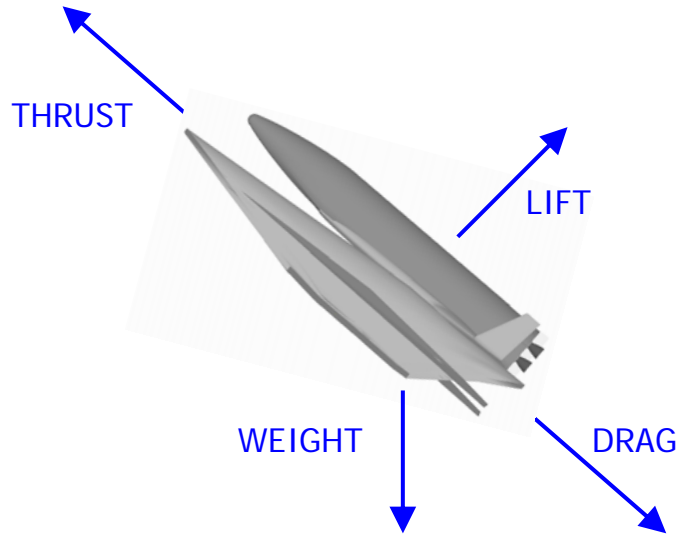
Figure 17. Vehicle Forces

A common measure of performance used for evaluating and comparing propulsion systems is specific impulse (*ISP*), which is basically a measure of fuel efficiency [22:472]. For a rocket engine, specific impulse is given by

$$ISP = \frac{T}{\dot{m} \cdot g} = \frac{V_{eq}}{g} \tag{5}$$

where V_{eq} is the equivalent exhaust velocity, given by

$$V_{eq} = V_e + \frac{(P_e - P_0) \cdot A_e}{\dot{m}} \tag{6}$$

Thrust is a little more complicated to calculate for airbreathing engines, because the propellant in this case consists of air drawn into the engine through the inlet, plus the fuel that is mixed with the air and burned in the combustion chamber. For an airbreathing engine, thrust is given by

$$T = \dot{m}_e \cdot V_e - \dot{m}_a \cdot V + (P_e - P_0) \cdot A_e \tag{7}$$

32

where $\dot{m}_a$ is the air mass flow rate, and $\dot{m}_e$ is the exit (air + fuel) mass flow rate from the nozzle [22:148]. Specific impulse for an airbreathing engine is given by

$$ISP = \frac{T}{\dot{m}_f \cdot g} \tag{8}$$

where $\dot{m}_f$ is the fuel mass flow rate [21:111]. The specific impulse for airbreathing engines are much greater than for rocket engines because captured air, which does not have to be carried aboard the vehicle, is used as the oxidizer.

3.3   RLV Design Methodology

Astrox Corporation's HySIDE code was used as the design tool throughout the study [25], and Reference 27 was consulted for this entire RLV Design Methodology Section. HySIDE, or Hypersonic System Integrated Design Environment, can be used to study a wide range of airbreathing and rocket RLVs throughout their entire flight regime. It analyzes the vehicles in a completely integrated fashion, which is essential for designing hypersonic vehicles, by combining engine performance, aerodynamic characteristics, heating conditions, mass properties, and volume constraints into a single vehicle model. The propulsion components may include any combination of turbine, DMSJ, or liquid rocket engines operating during user specified trajectory segments. Vehicle propulsion performance, combined with aerodynamic losses, is calculated all the way through the flight trajectory. The RLVs are then finalized, or closed, by iterating the vehicle dimensions until the available internal volume satisfies volume requirements.

Two generic vehicle models were employed in HySIDE for this study, which are here called airbreathers and rockets. Examples of HySIDE-generated three-dimensional

33

drawings of these vehicle models are shown in Figure 18. Both vehicle models can be used as either a first stage (booster) or second stage (orbiter) in a TSTO RLV. Each vehicle model can have up to three trajectory segments that are dictated by the velocity range and propulsion method used in the segment. In a SSTO RLV, all three trajectory segments could be used. However, in a TSTO RLV, only two trajectory segments are required for the airbreathers and only one trajectory segment is required for the rockets. The trajectory segments are further described in Sections 3.3.1 and 3.3.2.

ROCKET

AIRBREATHER
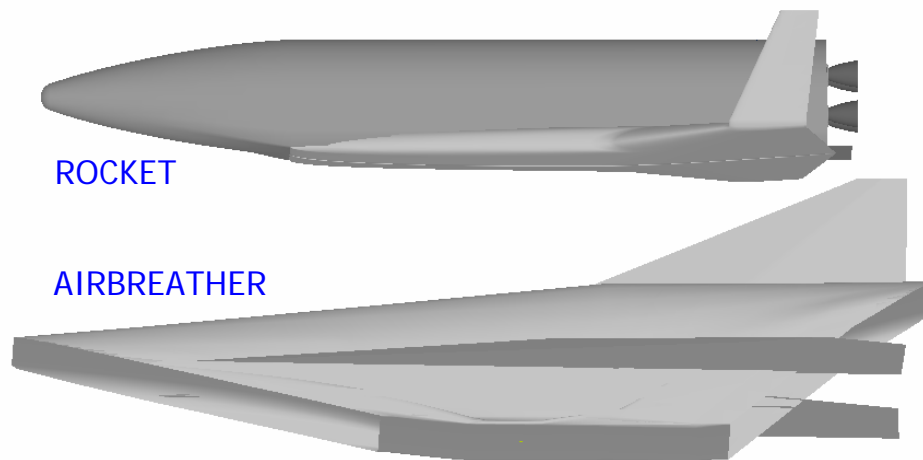
Figure 18. HySIDE Vehicle Drawings

The design point for each vehicle is set at a user specified Mach number and altitude. This is input in the "FreeStream" component of HySIDE, as shown in Figure 19, which shows the inputs on the left and the outputs on the right. The design point for a pure rocket vehicle is not as critical as for an airbreathing vehicle because of the way the rocket vehicle is modeled in HySIDE, as explained in Section 3.3.1. For simplicity, staging conditions are an appropriate choice for a rocket's design point. However,

picking the design point for an airbreathing vehicle is more of an iterative process. For example, if the design Mach number is chosen at the extreme high end of the DMSJ performance spectrum, the vehicle heating will be more manageable at the upper limit, but the vehicle drag will be excessive at the lower limits. This is because the airbreathing vehicle's aerodynamic characteristics are optimized for the design point. Therefore, it is usually best to choose the airbreather's design point one or two Mach numbers below maximum DMSJ engine operation. Airbreathing vehicles fly along a constant dynamic pressure path during DMSJ operation, so the design point altitude should be chosen to match the desired dynamic pressure with the design point Mach number.
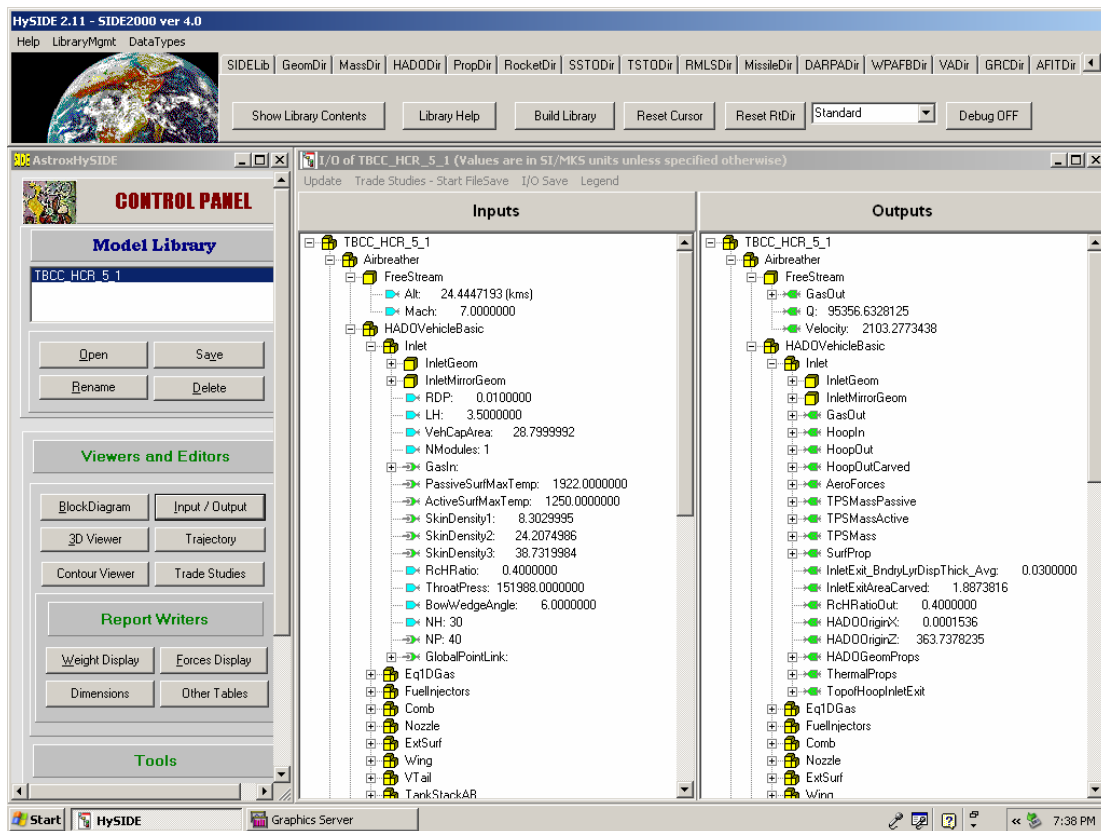
Figure 19. HySIDE Screenshot showing "FreeStream" Component

Lift is calculated throughout the flight trajectory using Equation (2), with the lift coefficients calculated by Missile Datcom [4; 36:2-3]. Missile Datcom is an industry-standard code for predicting missile and launch vehicle aerodynamic characteristics at speeds ranging from subsonic to hypersonic. Missile Datcom provides prediction of six-degree-of-freedom aerodynamic coefficients based upon the airframe model. In HySIDE, angle of attack is iterated upon until the lift required is equal to the lift available. For horizontal takeoff boosters, the design lifting requirements are based on takeoff conditions, while for vertical takeoff boosters or for orbiters, the design lifting requirements are based on landing conditions. The wing planform area is sized based on user inputs in HySIDE such as structural weight per unit area, design Mach number, design lift coefficient, aspect ratio, thickness to chord ratio, leading edge sweep, and taper. The wing is then positioned to meet stability requirements.

3.3.1   Rocket Vehicle Design Methodology

A rocket vehicle model uses either the first or third trajectory segment, as described in Section 3.3, depending on whether it is the booster or orbiter. If the rocket is used as the booster, the first trajectory segment is rocket-powered from takeoff to vehicle staging, and the other trajectory segments are not used. If the rocket is used as the orbiter, only the third trajectory segment is used, which is rocket-powered from vehicle staging to orbit.

Rocket engine sizing is dictated by takeoff thrust requirements, which either occurs at the beginning of the first stage engine operation, in the case of a booster, or the

beginning of the second stage engine operation, in the case of an orbiter. The takeoff

thrust is given by

$$T_{TO} = \left(T/_W\right)_{TO} \cdot GTOW \tag{9}$$

where $\left(T/_W\right)_{TO}$ is the vehicle thrust to weight ratio at rocket ignition, a user input, and

GTOW is the remaining vehicle gross weight, which is an output variable from HySIDE.

The propellant mass flow rate is then calculated by

$$\dot{m} = \frac{T_{TO}}{ISP \cdot g} \tag{10}$$

where ISP is a user input in the "Velocity vs. ISP" table, which can either be directly

input by the user or chosen from a drop-down list in HySIDE. The "Velocity vs. ISP"

table assumes a nominal rocket trajectory and takes into account atmospheric density

effects. Propellant mass flow rate is held constant for the duration of the rocket

sequence. Engine thrust is then calculated throughout the rocket trajectory by

$$T = \dot{m} \cdot ISP \cdot g \tag{11}$$

Drag (D) is calculated over the vehicle using Equation (3) with the drag

coefficients calculated by Missile Datcom, as described in Section 3.3. Gravity loss,

which is the thrust required to overcome the force of gravity, is calculated in HySIDE by

$$G_{loss} = M \cdot g \cdot \frac{\Delta H / \Delta t}{V} \tag{12}$$

where $\Delta H / \Delta t$ is the vertical velocity. After the vehicle drag and gravity loss are

accounted for, these forces are converted into specific impulse equivalents to provide a

net specific impulse, given by

$$ISP_{net} = ISP - \frac{D}{\dot{m} \cdot g} - \frac{G_{loss}}{\dot{m} \cdot g} \tag{13}$$

A net vehicle thrust can now be calculated by

$$T_{net} = \dot{m} \cdot ISP_{net} \cdot g \tag{14}$$

3.3.2   Airbreathing Vehicle Design Methodology

Airbreather vehicle models always have the DMSJ operation as the second trajectory segment, as described in Section 3.3, which uses air as the oxidizer and flies along a constant dynamic pressure path. In the case of an airbreather booster, the third trajectory segment is not used and the vehicle stages at the end of DMSJ operation. The first trajectory segment can be either turbine-powered or rocket-powered, and can be either horizontal takeoff or vertical takeoff. In the case of an airbreather orbiter, the first trajectory segment is not used and the third trajectory segment is rocket-powered, taking the vehicle from DMSJ cutoff to orbit.

The design point for an airbreather is chosen at a Mach number and altitude during the DMSJ operation. Then the individual components of the airbreather are created for optimal operation at the design point. These components include the inlet, isolator, combustor, nozzle, and upper surface, as shown in Figure 20.
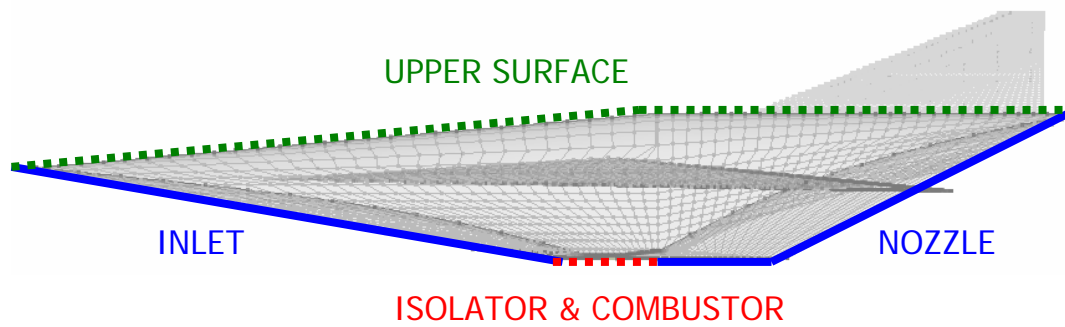
Figure 20. Airbreather Components

First, the inlet flow field is generated through an axisymmetric method of characteristics solution based on several user inputs in HySIDE, such as the inlet width/height ratio, geometric capture area, throat pressure, bow shock angle, maximum passively-cooled surface temperature, maximum actively-cooled surface temperature, and skin density. The method of characteristics is a method of solving partial differential equations by finding curves in the plane, called characteristic curves, which reduce the equations to a set of ordinary differential equations that are much easier to solve. The inlet surface is designed by tracing the streamlines from the cross section of the captured streamtube projection onto the inlet flow field. Once the streamline trace is complete, the inviscid forces on the inlet surface and the flow conditions at the inlet exit are calculated. A reference temperature method is then used for the boundary layer calculations, thus modifying the inlet geometry to account for the displacement thickness. Using oblique shock theory, the result is that at the design point, the vehicle "rides" the bow shock on the underside of the inlet, as shown in Figure 21.
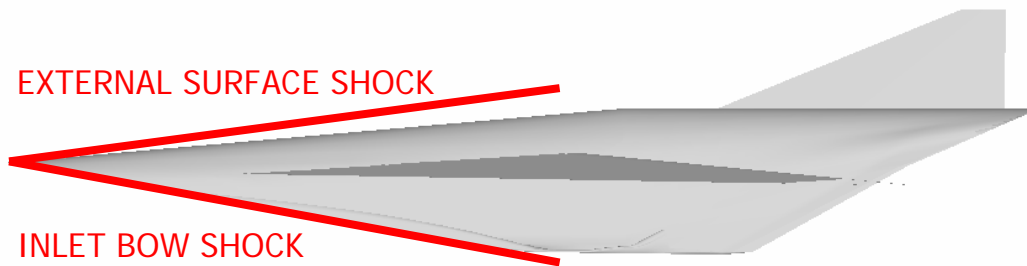
Figure 21. Airbreather Design Point Shocks

Next, the isolator and combustor are evaluated with a quasi one-dimensional combustor model based on several user inputs in HySIDE, such as fuel type, maximum fuel temperature, fuel total pressure, mixing fraction, mixing length, minimum equivalence ratio, maximum inlet ram Mach number, average combustor entrance boundary layer displacement thickness, and combustion efficiency. This combustor model analyzes the mixing and burning of the fuel by assuming equilibrium chemistry. The code calculates the heat release in 10 delta-x (length) steps, and based on the new temperatures at each step, it calculates new values of the specific heat at constant pressure and the new compositions. Once the composition at the end of the combustor is calculated, HySIDE then designs the isolator and combustor surfaces.

The nozzle flow field is then created by using the same method of characteristics solution as for the inlet flow field based on several user inputs in HySIDE, such as the flow path area ratio, truncation factor, maximum passively-cooled surface temperature, maximum actively-cooled surface temperature, and skin density. Using similar logic as for the inlet, including the reference temperature method to account for the viscous forces, HySIDE then designs the nozzle surface.

Finally, the upper surface of the vehicle is defined joining the inlet and exit areas, producing a specified external surface shock along the leading edge.

Now that the DMSJ engine has been designed, the net thrust applied to the vehicle throughout the engine flowpath is calculated at the design point by integrating the map of pressure forces and viscous forces at every point in the flowpath. By having the design point net thrust, an actual value for the design point specific impulse can be calculated for this vehicle by

$$ISP_{DP} = \frac{T_{DP}}{\dot{m}_f \cdot g} \tag{15}$$

where the subscript *DP* refers to the design point. The fuel mass flow rate is given by

$$\dot{m}_f = \dot{m}_a \cdot \phi \cdot FuelStoicRatio \tag{16}$$

where ϕ is the equivalence ratio, a user input in the "Phi vs. ISP" table, *FuelStoicRatio* is the fuel stoichiometric mass ratio, also a user input, and $\dot{m}_a$ is the air mass flow rate. The air mass flow rate is given by

$$\dot{m}_a = \rho \cdot V \cdot A_{inlet} \cdot AirRatio \tag{17}$$

where A_{inlet} is the geometric inlet capture area, a user input, and *AirRatio* is the actual area of captured air divided by the design area of captured air. *AirRatio* is calculated with a power series equation, which is only a function of Mach number [44].

The DMSJ specific impulse values input by the user in the "Velocity vs. ISP" table are used as a trend to calculate thrust at off-design conditions. An ISP difference is calculated by

$$\Delta ISP = ISP_{DP} - ISP_{table.DP} \tag{18}$$

41

where $ISP_{table.DP}$ is the specific impulse table value at the design point. The DMSJ off-design specific impulse is then given by

$$ISP = ISP_{table} + \Delta ISP \tag{19}$$

where ISP_{table} is the specific impulse table value at each particular off-design point. Now, thrust can be calculated at every point in the DMSJ trajectory by

$$T = \dot{m}_f \cdot ISP \cdot g \tag{20}$$

Aerodynamic losses are calculated for off-design conditions in the same manner as they were for the rocket vehicles. These losses are converted into specific impulse equivalents to give a net specific impulse, given by

$$ISP_{net} = ISP - \frac{D}{\dot{m}_f \cdot g} - \frac{G_{loss}}{\dot{m}_f \cdot g} \tag{21}$$

Net thrust at all off-design points can now be calculated by

$$T_{net} = \dot{m}_f \cdot ISP_{net} \cdot g \tag{22}$$

Rocket engines on airbreathers, which are embedded in the DMSJ nozzle, are analyzed in the same way as for rocket vehicles. Turbine engine performance is handled in the same manner as for rocket engines, based on takeoff thrust requirements given by Equation (9). The user input "Velocity vs. ISP" table is also used directly for thrust calculations as it is for rocket vehicles. However, the fuel mass flow rate is calculated as it is for DMSJ engines, given by Equation (16). Net specific impulse and thrust are then given by Equations (21) and (22), respectively.

3.4 Assumptions

Assumptions were made regarding the performance, weights, and sizes of the different types of engines. Rocket and turbine engines were modeled as rubberized engines, meaning that the engine performance and dimensional data were scaled from a nominal engine by whatever scale factor was required to provide the desired thrust. In the case of rocket engines, the nominal engines are engines that currently exist. In the case of turbine engines, there isn't a nominal engine per se, but rather a set of historical data that has been statistically compiled into a set of equations. Assumptions were also made regarding the flight trajectories, which are discussed in Section 3.4.4. A complete list of HySIDE inputs used in this study is given in Appendix B.

3.4.1 Rocket Engines

Hydrocarbon rocket engines were modeled as rubberized RD-180 engines, which are used on the Atlas III and Atlas V launch vehicles, while hydrogen rocket engines were modeled as rubberized Space Shuttle Main Engines (SSMEs). Table 1 shows the nominal rocket engine performance and dimensional data used in HySIDE during this analysis. This RD-180 rocket engine data was also used in the 2004 AFIT RLV Study as described in section 2.7.1 [8], and this RD-180 and SSME rocket engine data was used in the 2004 Astrox RLV Study as described in Section 2.7.2 [13].

Table 1. Rocket Engine Performance and Dimensional Data [17]

	RD-180	SSME
Fuel	Rocket Propellant (RP-1)	Liquid Hydrogen (LH2)
Oxidizer	Liquid Oxygen (LOX)	Liquid Oxygen (LOX)
Mixture Ratio	2.6 / 1	6.0 / 1
Thrust / Weight Ratio	80.0	73.3
Nozzle Area Ratio	36.4	77.5
Chamber Pressure (psia)	3,722	3,260
Characteristic Velocity (ft/s)	5,914	7,684
ISP - Sea Level (s)	311.0	370.8
ISP - Vacuum (s)	337.0	454.4
Average Thrust - Sea Level (lbf)	860,000	418,130
Average Thrust - Vacuum (lbf)	933,000	512,410
Weight (lbf)	11,675	6,990
Length (ft)	13.0	14.0
Diameter (ft)	9.8	8.0

The installed weight of the rocket engines for each vehicle is given by

$$W_{Rkt} = \frac{T_{TO}}{\left(T/W\right)_{Rkt}} \cdot K_{overall} \qquad (23)$$

where T_{TO} is the required takeoff thrust, an output from HySIDE, $\left(T/W\right)_{Rkt}$ is the rocket

engine thrust to weight ratio, a user input, and $K_{overall}$ is the overall design uncertainty

factor, also a user input. In order to provide growth margin without being overly

conservative, an overall design uncertainty factor of 1.1 was used for all vehicles

throughout the analysis.

3.4.2   Turbine Engines

Turbine engines were modeled using performance data from the Air Force

Research Laboratory Propulsion Directorate (AFRL/PR). Performance data for this

hydrocarbon afterburning turbine engine comes from AFRL's conceptual Mach 4.4

turbine accelerator design, which is the same turbine engine data used in the 2004 AFIT RLV Study as described in Section 2.7.1 [8]. Table 2 shows the turbine "ISP vs. Velocity" table used in HySIDE during this analysis, while the entire set of AFRL Turbine Accelerator engine performance data is shown in Appendix A.

Table 2. AFRL Turbine Accelerator Engine ISP vs. Velocity [17]

V, ft/sec	ISP (sec)
0.000	2122.000
500.000	1963.000
800.000	1776.000
1000.000	1745.000
1500.000	1787.000
2000.000	1780.000
2500.000	1735.000
3000.000	1676.000
3250.000	1630.000
3750.000	1535.000
4000.000	1501.000
4400.000	1453.000
4500.000	0.000
10000.000	0.000
27000.000	0.000

A parametric statistical approach was used to size the afterburning turbine engines based upon historical data [40:235]. The uninstalled weight ($W_{uninstalled}$), length ($L_{uninstalled}$), and diameter ($D_{uninstalled}$) of each turbine engine are given by

$$W_{uninstalled} = 0.063 \cdot \left(\frac{T_{TO}}{\#_{turb}} \right)^{1.1} \cdot M_{max}^{\,0.25} \cdot e^{-0.81 \cdot BPR} \cdot (0.8) \ \text{lbf} \qquad (24)$$

$$L_{uninstalled} = 0.255 \cdot \left(\frac{T_{TO}}{\#_{turb}}\right)^{0.4} \cdot M_{max}^{0.2} \cdot (0.8) \ \text{ft} \qquad (25)$$

$$D_{uninstalled} = 0.024 \cdot \left(\frac{T_{TO}}{\#_{turb}}\right)^{0.5} \cdot e^{0.04 \cdot BPR} \cdot (0.9) \ \text{ft} \qquad (26)$$

where T_{TO} is the required takeoff thrust, an output from HySIDE, $\#_{turb}$ is the number of turbine engines, a user input, M_{max} is the maximum Mach number, a user input, and *BPR* is the bypass ratio, a user input [40:235]. A bypass ratio of 0.95 was assumed for all turbine engines in order to be comparable to the turbine engines in the 2004 SpaceWorks Engineering RLV Study, as described in Section 2.7.3 [6]. These user inputs are entered in the "TurbineCluster" component of HySIDE, as shown in Figure 22.
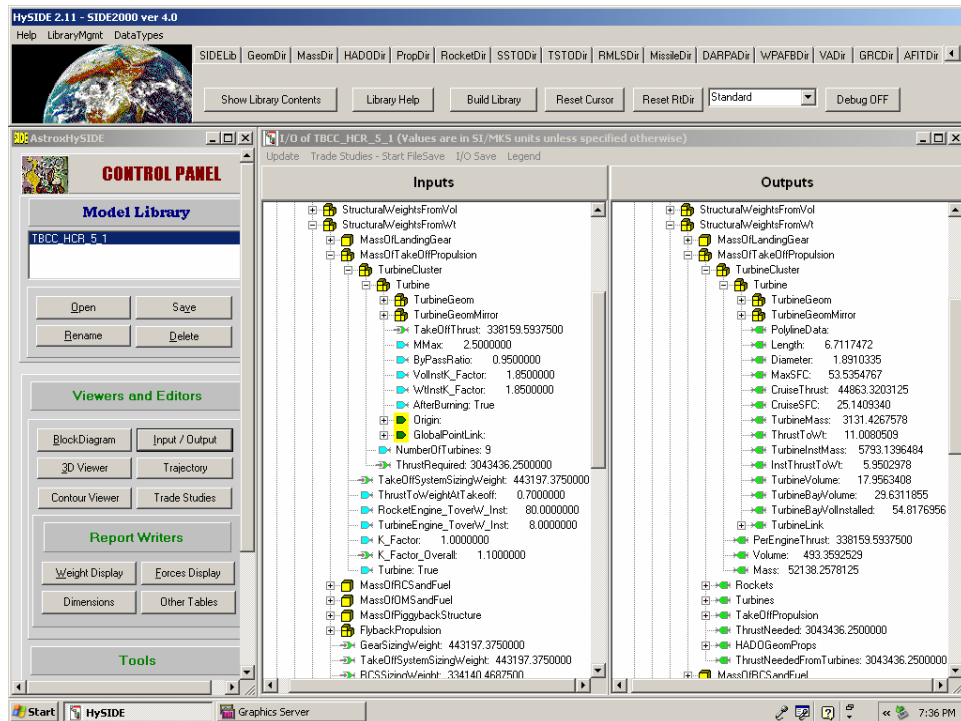
Figure 22. HySIDE Screenshot showing "TurbineCluster" Component

46

Equations (24)-(26) are intended for use with Mach numbers below 2.5. For Mach numbers above 2.5, errors will be introduced into the solution because $M_{max} = 2.5$ must be used in the equations. The basic form of these equations represent historical trends, so for a next-generation engine, HySIDE added improvement factors to each equation, which are shown in parenthesis, in order to account for technology advances.

In HySIDE, the turbine uninstalled weight refers only to the turbine engine, while the turbine installed weight refers to the turbine engine plus all of the required additional interfaces to the vehicle, including the inlet and nozzle. The installed weight of each turbine engine is then given by

$$W_{installed} = W_{uninstalled} \cdot K_{installed} \cdot K_{overall} \tag{27}$$

where $K_{installed}$ is the turbine installation factor, a user input. The turbine installation factor can be used to control the turbine installed thrust to weight ratio. A turbine installation factor of 1.85 resulted in the baseline turbine installed thrust to weight ratio of 6, which represents today's state of the art for a turbine accelerator engine [17].

3.4.3 Dual-Mode Scramjet Engines

DMSJ engines were modeled using performance data from AFRL/PR, which was acquired from SpaceWorks Engineering, Inc. (SEI) in support of the U.S. Air Force HyTech program. SEI used SRGULL, a performance prediction code for airframe-integrated scramjet engines, to obtain the engine performance data for this hydrocarbon DMSJ engine in a 2-D NASP-derived lifting-body vehicle configuration. This is the same DMSJ engine performance data that was used in the 2004 SpaceWorks Engineering RLV Study, as described in Section 2.7.3 [6]. Table 3 shows the DMSJ "ISP vs.

Velocity" table used in HySIDE during this analysis, while the entire set of AFRL

HyTech DMSJ engine performance data is shown in Appendix A.

Table 3. AFRL HyTech DMSJ Engine ISP vs. Velocity [17]

V, ft/sec	ISP (sec)
0.000	0.000
3500.000	0.000
3750.000	1765.000
4000.000	1628.000
4500.000	1645.000
5000.000	1412.000
6000.000	975.000
7000.000	859.000
8000.000	771.000
8250.000	747.000
8500.000	0.000
15000.000	0.000
19000.000	0.000
23000.000	0.000
27000.000	0.000

The weight of the DMSJ engine is not individually calculated, because so much of

the entire vehicle is designed around the DMSJ engine operation. In other words, the

airbreathing vehicles are essentially flying engines, so it isn't meaningful to differentiate

the weight of the DMSJ engine from the rest of the vehicle.

3.4.4   Flight Trajectory Assumptions

Based upon the literature review, several flight trajectory assumptions were made,

including takeoff velocity, vehicle thrust to weight at takeoff, staging velocity, and

landing velocity [41:2; 13:4; 31:3; 19:2-3]. A takeoff velocity of 225 knots (380 ft/s) was

chosen for all HTHL RLVs, while a landing velocity of 180 knots (305 ft/s) was chosen for all RLVs. The launch site was chosen to be Cape Canaveral Air Force Station, with a latitude of 28.5 degrees north. The vehicle thrust to weight at takeoff was chosen to be 1.4 for VTHL RLVs and 0.7 for HTHL RLVs based upon the literature review.

The staging velocities were chosen for the airbreathing vehicles to maximize the operating envelopes of the airbreathing engines, as shown in Tables 2 and 3, with a slight amount of performance margin. Therefore, the staging velocity for the TJ-Rkt was 4,000 ft/s, and the staging velocity for the RBCC-Rkt and TBCC-Rkt was 8,000 ft/s. The staging velocity for the Rkt-Rkt was chosen to be 7,000 ft/s based upon the literature review. Orbital velocity was set at 25,500 ft/s, and orbital altitude was set at 50 nautical miles (303,800 ft) for the 50x100 nautical mile parking orbit.

3.5   Sensitivity Analyses

Two sensitivity analyses were performed on areas of interest directly affecting the propulsion systems in this study. The first sensitivity analysis investigated the effects of selecting a different fuel for the second stage orbiter. For this part of the study, all four RLVs were analyzed using hydrogen as the fuel for the orbiter, while still utilizing hydrocarbon fuel for the booster. The high density of hydrocarbon fuel makes it a sensible choice for RLV boosters, where high density equates to smaller vehicles and thus less drag. However, hydrogen provides much more energy for a given fuel mass, which makes it a reasonable choice for RLV orbiters, where drag is much less of a factor.

The second sensitivity analysis researched the effect of the turbine installed thrust to weight ratio for the RLVs utilizing turbine engines during the ascent phase of their

trajectory. The baseline turbine installed thrust to weight ratio for this study was 6, representing today's state of the art turbine accelerator engine, and so the effect of increasing this ratio through technology advances 10 and 20 years from now was investigated. A turbine installed thrust to weight ratio of 8 is expected to be feasible in 5-10 years, and a turbine installed thrust to weight ratio of 10 is expected to be feasible in 15-20 years [17]. From Equation (27), a turbine installation factor of 1.38 resulted in a turbine installed thrust to weight ratio of 8, while a turbine installation factor of 1.11 resulted in a turbine installed thrust to weight ratio of 10.

Table 4 lists all RLVs studied, both for the baseline configurations and for the two sensitivity analyses, along with their identifiers, propulsion and fuel types, trajectories, and comments. This nomenclature is used for the remainder of the study.

Table 4. Summary of Vehicle Configurations Investigated in TSTO RLV Weight Analysis

RLV Identifier	Booster		Orbiter		Trajectory	Comments
	Propulsion	Fuel	Propulsion	Fuel		
Rkt-Rkt	Rocket	HC	Rocket	HC	VTHL	Baseline Configuration
RBCC-Rkt	RBCC	HC	Rocket	HC	VTHL	Baseline Configuration
TBCC-Rkt	TBCC	HC	Rocket	HC	HTHL	Baseline Configuration
TJ-Rkt	Turbine	HC	Rocket	HC	HTHL	Baseline Configuration
Rkt-Rkt (H_2)	Rocket	HC	Rocket	H_2	VTHL	Hydrogen Orbiter
RBCC-Rkt (H_2)	RBCC	HC	Rocket	H_2	VTHL	Hydrogen Orbiter
TBCC-Rkt (H_2)	TBCC	HC	Rocket	H_2	HTHL	Hydrogen Orbiter
TJ-Rkt (H_2)	Turbine	HC	Rocket	H_2	HTHL	Hydrogen Orbiter
TBCC-Rkt (T/W=8)	TBCC	HC	Rocket	HC	HTHL	Turbine Installed T/W = 8
TBCC-Rkt (T/W=10)	TBCC	HC	Rocket	HC	HTHL	Turbine Installed T/W = 10
TJ-Rkt (T/W=8)	Turbine	HC	Rocket	HC	HTHL	Turbine Installed T/W = 8
TJ-Rkt (T/W=10)	Turbine	HC	Rocket	HC	HTHL	Turbine Installed T/W = 10

3.6   Verification Methodology

A second computer program was used to verify the accuracy of the results generated with HySIDE. The Program to Optimize Simulated Trajectories (POST) was utilized on two of the RLV configurations to validate that they are capable of reaching the desired orbit with the given amount of empty weight, propellant, and engine performance. The Rkt-Rkt configuration was chosen to represent the VTHL RLVs, and the TBCC-Rkt was chosen to represent the HTHL RLVs.

Created by NASA and Lockheed-Martin, POST is an industry standard tool for optimizing RLV trajectories [38; 35]. It is a generalized event-oriented Fortran 77 computer code that can be used to optimize a user-specified performance function, given certain user-specified constraints. Within an input file, the user structures the trajectory by a sequential series of steps, and also models the RLV by specifying vehicle weights and propulsion system performance parameters. This three-degrees-of-freedom program then numerically integrates the equations of motion by iterating control variables in order to converge upon a solution. The optimization performance function used in this study was propellant consumption minimization, while the control variables used were vehicle pitch angles.

4. Analysis and Results

This chapter presents the results of the TSTO RLV empty weight analysis. Each RLV in this study was created and analyzed using Astrox Corporation's HySIDE code, designed for a roundtrip to a 100 nautical mile circular LEO with a fixed payload requirement of 20,000 lbf. The hydrocarbon DMSJ engines used in the RBCC-Rkt and TBCC-Rkt configurations represent possible applications of the current research being performed in the HyTech program by the U.S. Air Force [37:1170-1171; 2:1]. Wherever possible all RLVs were designed with the same group of input values in order to accurately compare, except when the particular RLV has a unique requirement, such as propulsion method or takeoff thrust to weight ratio. Because of these unique requirements, each RLV has a distinct ascent trajectory profile, as shown in Figure 23. The staging point for each RLV is also given in Figure 23. These differences in ascent trajectories and staging conditions affect things such as vehicle heating and booster flyback fuel, which are detailed in the following sections. Other ascent trajectory information for the baseline configurations, including vehicle weight, thrust, drag, and dynamic pressure versus velocity are given in Appendix C.

Staging Points

	Altitude (ft)	Downrange (nm)
Rkt-Rkt	133,718	36
RBCC-Rkt	86,305	411
TBCC-Rkt	86,305	417
TJ-Rkt	58,000	67
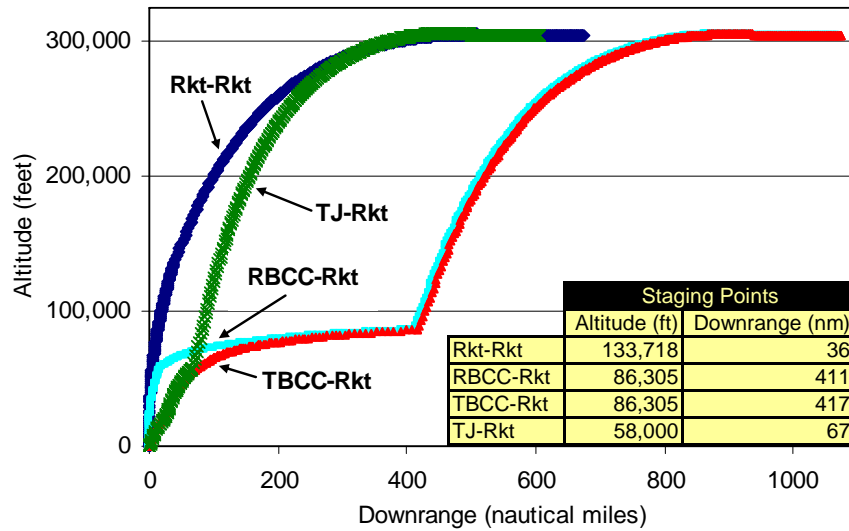
Figure 23. Baseline RLV Ascent Trajectories with Staging Points

The first section in this chapter discusses the empty weight results for the baseline configurations, as well as gives further details about the vehicle gross weights and dimensions. The second section discusses the results from the propellant sensitivity analysis, explaining how the vehicles changed by using hydrogen as the orbiter fuel instead of hydrocarbon. The third section discusses the results from the turbine installed thrust to weight ratio sensitivity analysis, with details on vehicle empty weights, gross weights, overall vehicle dimensions, and turbine engine weights and dimensions. The fourth section compares all of the RLVs from the baseline configurations as well as both sensitivity analyses, and gives discussion on which RLVs are the most feasible and economical. The fifth section discusses the results from the two validation cases with POST and compares them to the results generated with HySIDE.

4.1   Baseline RLV Results

RLV empty weight is the primary figure of merit in this study. Table 5 lists the

empty weights of the baseline RLVs in ascending order, along with their corresponding

gross weights. These results show that the Rkt-Rkt has the lowest empty weight at

161,000 lbf, even though it has the highest gross weight at almost 1.5 million lbf. The

empty weight of the RBCC-Rkt follows closely behind at 168,000 lbf, which is only 4%

heavier than the Rkt-Rkt. The TBCC-Rkt comes in third in empty weight at 311,000 lbf,

a 93% increase from the Rkt-Rkt. The heaviest empty RLV is the TJ-Rkt at 426,000 lbf,

which is 165% more massive than the Rkt-Rkt.

Table 5. Baseline RLV Empty and Gross Weights

	Empty Weight (lbf)			Gross Weight (lbf)			
	Booster	Orbiter	Total	Booster	Orbiter	Payload	Total
Rkt-Rkt	108,793	52,274	**161,067**	1,037,651	426,583	20,000	**1,484,234**
RBCC-Rkt	118,543	49,562	**168,105**	919,157	375,061	20,000	**1,314,218**
TBCC-Rkt	261,299	49,562	**310,861**	603,324	375,061	20,000	**998,384**
TJ-Rkt	347,906	78,560	**426,466**	583,940	860,600	20,000	**1,464,540**

4.1.1   Baseline RLV Dimensions

Figure 24 lists the dimensions of the baseline RLVs, along with vehicle

schematics showing the size comparisons. As these drawings show, the Rkt-Rkt is not

only the lightest empty RLV, but it is also the smallest RLV. As for the three

airbreathing RLVs, the RBCC-Rkt has the smallest wings and narrowest fuselage, and the

54

TJ-Rkt has the largest wings and widest fuselage. The reasons behind these differences are discussed in subsequent sections.

Rkt-Rkt Dimensions (ft)		RBCC-Rkt Dimensions (ft)		TBCC-Rkt Dimensions (ft)		TJ-Rkt Dimensions (ft)	
Length	93	Length	101	Length	106	Length	104
Width	66	Width	59	Width	85	Width	103
Height	36	Height	31	Height	31	Height	36
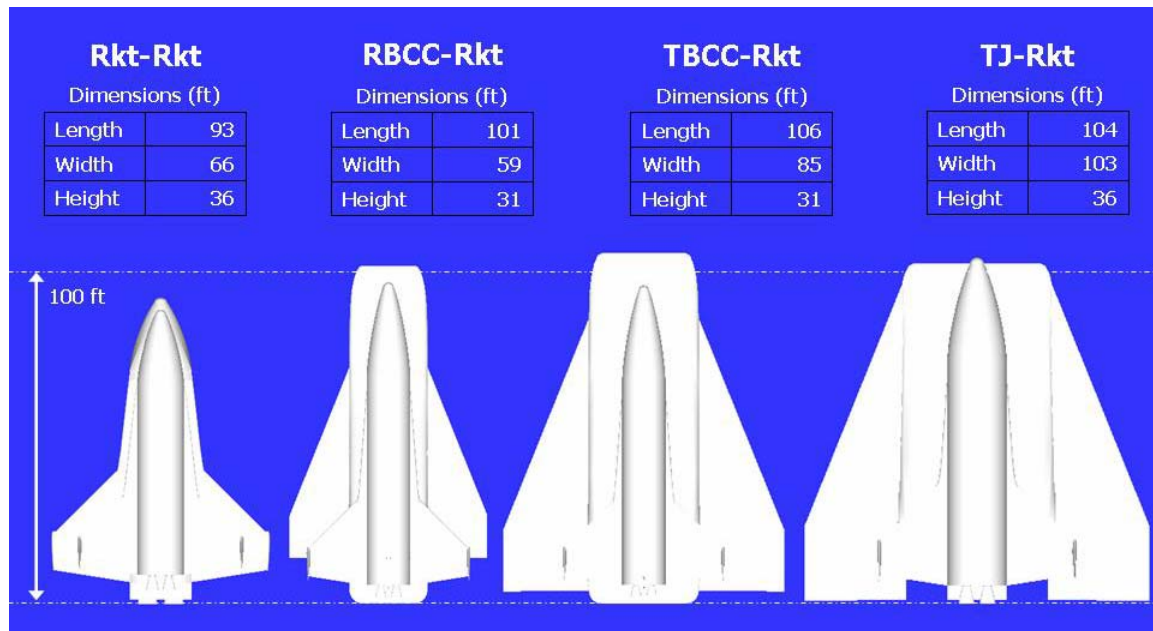
Figure 24. Baseline RLV Dimensions

4.1.2   Baseline RLV Afterburning Turbine Engines

The fuselage width of the three airbreathing RLVs depends on the size and number of afterburning turbine engines required for the ascent trajectory. In order to have reasonably sized afterburning turbine engines that provide the required takeoff thrust, an odd number of turbine engines was chosen to fit the engines within the fuselage and also provide for maximum packing efficiency. A tradeoff was reached between engine thrust, size, and number of engines, resulting in 9 afterburning turbine engines for the TBCC-Rkt and 13 afterburning turbine engines for the TJ-Rkt, as shown in Figure 25.

55

The RBCC-Rkt does not require any turbine engines for the ascent trajectory, so it can have a narrow fuselage.
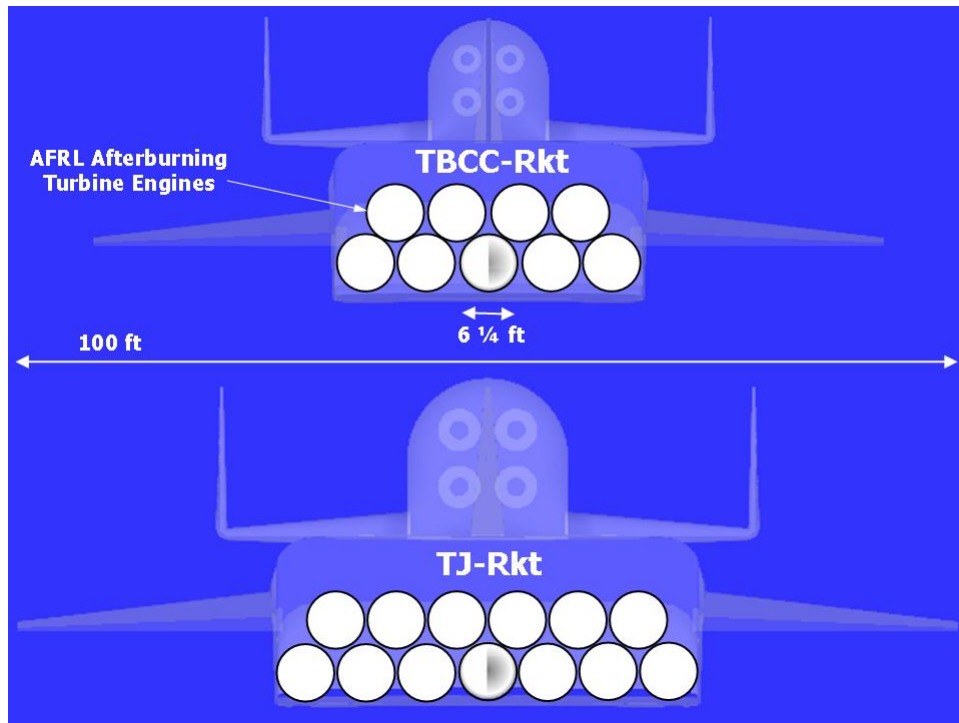
Figure 25. Baseline RLVs Using Afterburning Turbine Engines

Table 6 lists the dimensions, weights, thrust levels, and thrust to weight ratios, both uninstalled and installed, for the baseline TBCC-Rkt and TJ-Rkt. In HySIDE, the turbine uninstalled weight refers only to the turbine engine, while the turbine installed weight refers to the turbine plus all of the required additional interfaces to the vehicle, including the inlet and nozzle. The average length of each turbine engine is slightly over 22 ft, the average diameter is 6 ¼ ft, the average uninstalled weight is approximately 7,000 lbf, and the average thrust is approximately 77,000 lbf. This results in an uninstalled thrust to weight ratio of 11, and an installed thrust to weight ratio of 6.

56

Table 6. Afterburning Turbine Engine Performance and Dimensional Data for Baseline RLVs Using Afterburning Turbine Engines

			TBCC-Rkt	TJ-Rkt
Per Turbine	Length	ft	22.0	22.3
	Diameter	ft	6.2	6.3
	Weight (Uninstalled)	lbf	6,904	7,135
	Weight (Installed)	lbf	12,772	13,058
	Thrust	lbf	76,021	78,337
Total	Turbines	#	9	13
	Weight (Uninstalled)	lbf	62,133	92,759
	Weight (Installed)	lbf	114,945	169,749
	Thrust	lbf	684,189	1,018,383
	T/W (Uninstalled)		11.0	11.0
	T/W (Installed)		6.0	6.0

4.1.3   Detailed Baseline RLV Empty Weight Breakdown

Figure 26 displays a detailed listing of the baseline RLV empty weights, broken down by booster propulsion, booster structure, booster thermal protection system (TPS), booster systems, and orbiter. The booster systems category includes avionics, landing gear, and everything else not included in the other categories. Figure 27 then displays a detailed listing of the baseline RLV gross weights, broken down by booster empty, booster propellant, orbiter empty, orbiter propellant, and payload. The propellant categories include the propellant required for the ascent trajectory, as well as startup propellant, flyback propellant (booster only), OMS propellant (orbiter only), reserve propellant, and trapped unusable propellant. These divisions highlight where the weight differences are between the baseline configurations.
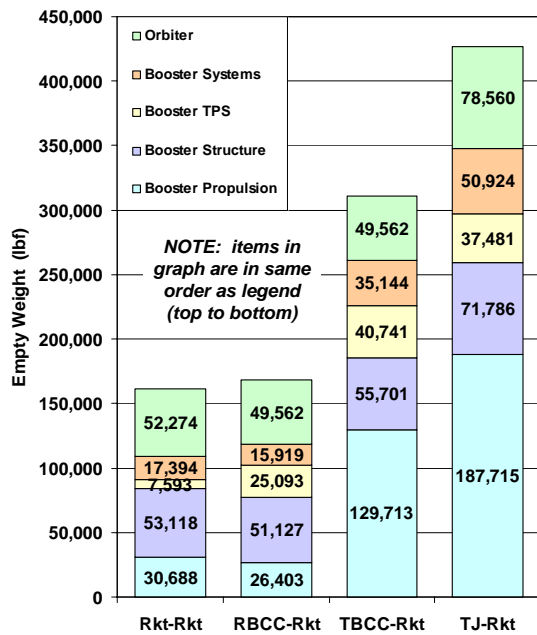
Figure 26. Baseline RLV Empty Weights
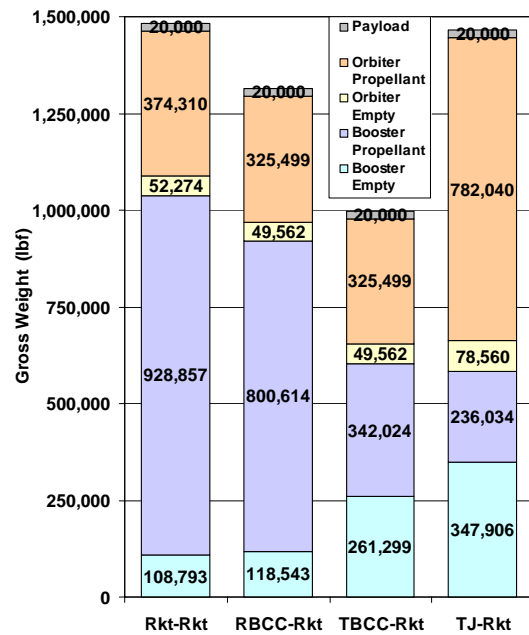
Figure 27. Baseline RLV Gross Weights

In comparing the two lowest empty weight baseline RLVs, the biggest difference in empty weight comes from the booster TPS, where the RBCC-Rkt requires 17,500 lbf more TPS than the Rkt-Rkt in order to keep the RBCC-Rkt within its temperature range during the high dynamic pressure ascent required during the DMSJ operation. The RBCC-Rkt is lighter than the Rkt-Rkt in the other four empty weight categories, but overall the large TPS requirement for the RBCC-Rkt makes it a heavier RLV. The largest difference in the other empty weight categories is between the booster propulsion systems, which is 4,300 lbf lighter for the RBCC-Rkt due to its lower gross weight. The gross weight of the RBCC-Rkt is 170,000 lbf lighter than the Rkt-Rkt, which is mainly due to the booster propellant savings achieved by using airbreathing engines for part of the ascent trajectory. For VTHL RLVs, the size of the booster propulsion system is

based on a takeoff thrust to weight ratio of 1.4, so a lower gross weight results in a smaller booster propulsion system empty weight.

The reason for the 2,700 lbf difference in orbiter dry weight between the Rkt-Rkt and RBCC-Rkt comes from the difference in staging velocity, which is 1,000 ft/s lower for the Rkt-Rkt than for the RBCC-Rkt. Since the orbiter for the Rkt-Rkt has a larger delta velocity to achieve, it requires more propellant and therefore has a higher gross weight. The size of the orbiter propulsion system is based on a light-off thrust to weight ratio of 1.0, and since the orbiter for the RBCC-Rkt has a smaller gross weight, it also has a smaller empty weight. After everything is accounted for, the empty weight saving that was achieved by using airbreathing engines in the RBCC-Rkt is not enough to make up for the added TPS weight required for the DMSJ operation. Therefore, even though the Rkt-Rkt is 170,000 lbf heavier at takeoff than the RBCC-Rkt, the Rkt-Rkt has the lowest empty weight of all the baseline RLVs. In fact, the gross weight of either VTHL RLV is essentially a non-issue, because neither RLV depends on a runway for takeoff, and because propellant is cheap in comparison to RLV hardware [31:3].

In comparing the empty weight of the baseline TBCC-Rkt to those of the two baseline VTHL RLVs, the biggest difference in empty weight comes from the booster propulsions systems. In fact, the booster propulsion system for the TBCC-Rkt makes up 42% of its empty weight, while for either VTHL RLV, the booster propulsion system makes up less than 20%. In order to achieve a takeoff thrust to weight ratio of 0.7, and still have reasonably sized afterburning turbine engines that fit within the fuselage, 9 turbine engines were required by the TBCC-Rkt. The weight of its booster propulsion

system, which mostly consists of these turbine engines, is almost 130,000 lbf, which is more than four times heavier than the booster propulsion system of either VTHL RLV due to the lower weight of rocket engines as compared to turbine engines. To put this in perspective, the booster propulsion system of the TBCC-Rkt weighs 80% as much as the entire Rkt-Rkt.

All of the other empty weight categories for the TBCC-Rkt booster are also heavier, since it is a HTHL RLV. The size of the booster structure, which consists in large part on the wing size, and of the booster systems, which depend in large part on the landing gear size, are based on the takeoff weight for HTHL RLVs, whereas they are based on the landing weight for VTHL RLVs. Therefore, even though the TBCC-Rkt has the lowest gross weight of any of the baseline RLVs, the wings and landing gear are still larger than for either VTHL RLV. The reason for the large difference in booster TPS weights between the TBCC-Rkt and RBCC-Rkt, which both employ DMSJ engines from 4,000 ft/s to 8,000 ft/s, is twofold. First, the TBCC-Rkt spends more of its ascent trajectory in high-heating conditions caused by the high dynamic pressure requirement of the turbine engines. Second, the TBCC-Rkt has more surface area as a result of its greater wing size, which requires more surface area to be covered in TPS.

Even though the empty weight of the TBCC-Rkt is 93% heavier than the Rkt-Rkt, the horizontal takeoff capability of the TBCC-Rkt has the potential to reduce operational costs over the vertical takeoff RLVs [3:4-6; 33:20; 7:3; 20:3-4; 10:1-2]. The gross takeoff weight of the TBCC-Rkt is low enough to enable operation from most commercial runways, which are able to handle approximately 1.3 million lbf of gross

takeoff weight. In fact, with a gross weight of just under 1 million lbf, the TBCC-Rkt is

lighter than either the Airbus 380 at 1.2 million lbf or the Antonov 225 at 1.3 million lbf,

and is just slightly heavier than a Boeing 747 freighter at 900,000 lbf. The ability of the

TBCC-Rkt to utilize existing aircraft ground facilities eliminates the requirement to rotate

the vehicle on a dedicated launch pad. This can potentially lead to substantial operational

cost savings compared to vertical takeoff RLVs, which require complex ground support

equipment around the launch pad. The horizontal takeoff capability of the TBCC-Rkt

also provides many other operability benefits, including mission abort capability and

trajectory flexibility.

In comparing the empty weight of the baseline TJ-Rkt to the other three baseline

RLVs, the biggest difference in empty weight again comes from the booster propulsion

systems. The 13 turbine engines required by the TJ-Rkt weigh almost 188,000 lbf, which

is more than six times heavier than the booster propulsion system of either one of the

VTHL RLVs, and more than 40% heavier than the booster propulsion system of the

TBCC-Rkt. In fact, the booster propulsion system of the TJ-Rkt weighs over 10% more

than either one of the VTHL RLVs.

With the exception of booster TPS, all of the other empty weight categories for

the TJ-Rkt booster are also heavier than for any of the other baseline RLVs. This comes

from the fact that the TJ-Rkt is a HTHL RLV, meaning that the wing and landing gear are

sized for takeoff conditions, which makes the booster structure and booster systems very

heavy. On the other hand, the booster TPS is a little lighter for the TJ-Rkt than for the

TBCC-Rkt, which is because the vehicle only has to operate in high dynamic pressure

conditions up to a velocity of 4,000 ft/s, as opposed to 8,000 ft/s for the TBCC-Rkt. However, there isn't a large reduction in booster TPS weight because the surface area of the TJ-Rkt is much larger than for the TBCC-Rkt. The reason for the larger orbiter empty weight for the TJ-Rkt is due to the lower staging velocity, which is similar to the difference in orbiter empty weights between the RBCC-Rkt and Rkt-Rkt.

An additional thing to note with the TJ-Rkt is that its gross takeoff weight, at almost 1.5 million lbf, will prevent it from flying out of most commercial runways. Therefore, it would require new infrastructure to be built for its operation. This, combined with the fact that the empty weight of the TJ-Rkt is 37% heavier than the TBCC-Rkt and 165% heavier than the Rkt-Rkt, makes the TJ-Rkt the least viable or economical of the baseline configurations.

4.2   Propellant Sensitivity Analysis Results

Table 7 lists the empty weights of the alternate propellant RLVs in ascending order, along with the corresponding gross weights. In all of the RLVs except the RBCC-Rkt, changing the orbiter fuel from hydrocarbon to hydrogen reduces the RLV empty weight over that of the baseline configuration. In all cases, the gross weight is reduced by at least 13%. These weight reductions are highlighted in Figure 28, which shows that the empty weight is reduced by 0.3% for the Rkt-Rkt, 7.7% for the TBCC-Rkt, and 12.6% for the TJ-Rkt. However, for the RBCC-Rkt, the empty weight actually increases by 2.7% with the orbiter fuel switch from hydrocarbon to hydrogen. The reasons behind these differences are discussed in subsequent sections.

Table 7. Alternate Propellant RLV Empty and Gross Weights

	Empty Weight (lbf)			Gross Weight (lbf)			
	Booster	Orbiter	Total	Booster	Orbiter	Payload	Total
Rkt-Rkt (H$_2$)	92,943	67,634	**160,577**	851,243	336,453	20,000	**1,207,696**
RBCC-Rkt (H$_2$)	108,202	64,400	**172,602**	809,092	302,771	20,000	**1,131,863**
TBCC-Rkt (H$_2$)	222,470	64,400	**286,870**	536,951	302,774	20,000	**859,725**
TJ-Rkt (H$_2$)	269,907	102,956	**372,863**	477,082	647,019	20,000	**1,144,101**
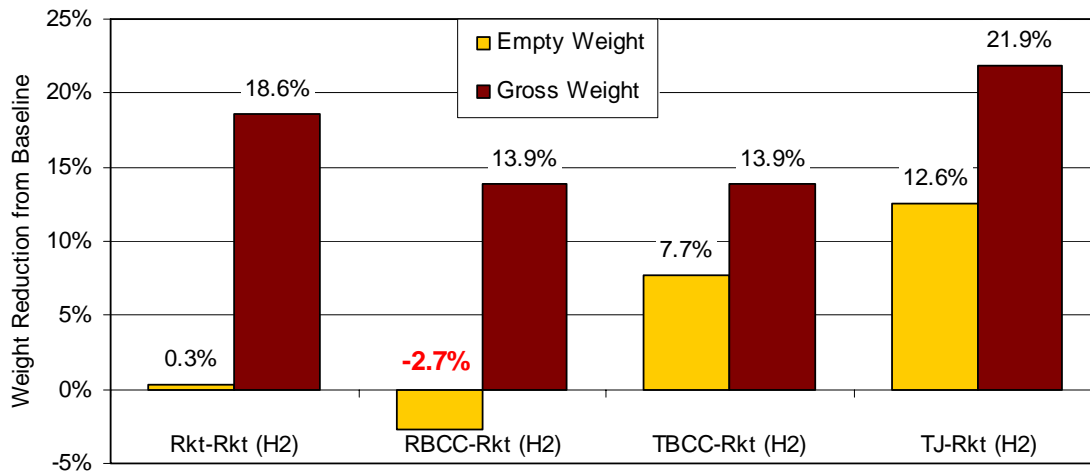
Figure 28. Weight Reduction in RLV Empty and Gross Weight by Changing the Orbiter Fuel from Hydrocarbon to Hydrogen

4.2.1 Propellant Sensitivity Analysis Dimensions

Figures 29-32 list the dimensions of the baseline RLVs compared to the alternate propellant RLVs, along with vehicle schematics showing the size comparisons. As would be expected, all of the hydrogen-fueled orbiters are much larger than their equivalent hydrocarbon-fueled orbiters because of the much lower density of hydrogen. However, before this sensitivity analysis, it was not known what the result would be on the boosters. As these graphics illustrate, and as the detailed weight breakdowns illustrate in the next section, the boosters all decrease in size with the orbiter fuel switch.
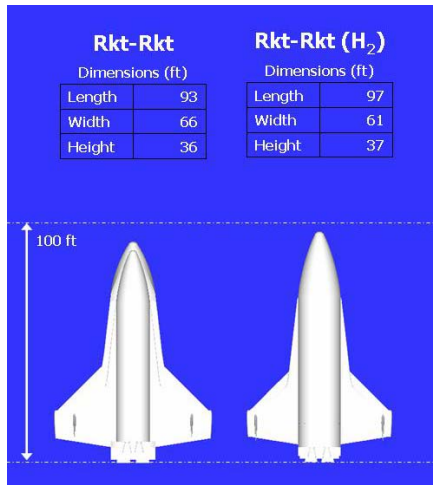
Figure 29. Rkt-Rkt Propellant Sensitivity Analysis Dimensions

Rkt-Rkt			Rkt-Rkt (H$_2$)		
Dimensions (ft)			Dimensions (ft)		
Length		93	Length		97
Width		66	Width		61
Height		36	Height		37
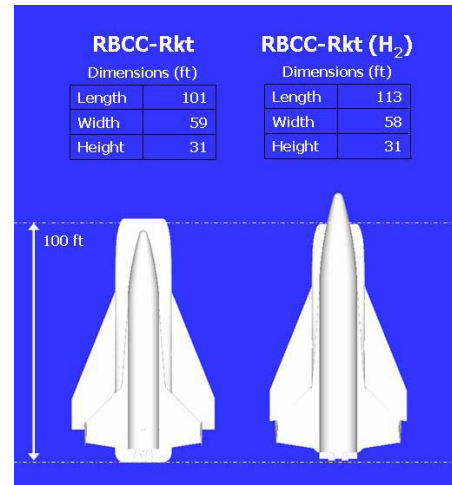
Figure 30. RBCC-Rkt Propellant Sensitivity Analysis Dimensions

RBCC-Rkt			RBCC-Rkt (H$_2$)		
Dimensions (ft)			Dimensions (ft)		
Length		101	Length		113
Width		59	Width		58
Height		31	Height		31
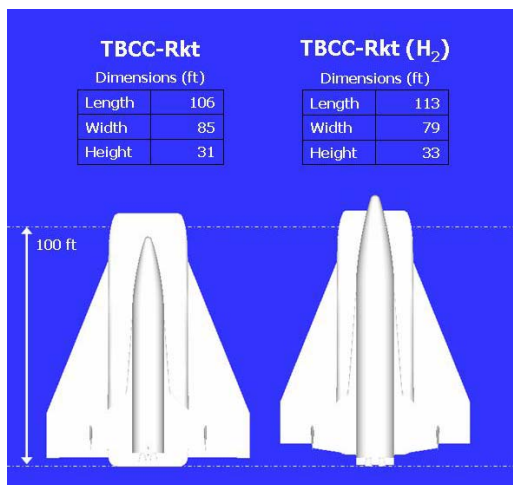
Figure 31. TBCC-Rkt Propellant Sensitivity Analysis Dimensions

TBCC-Rkt			TBCC-Rkt (H$_2$)		
Dimensions (ft)			Dimensions (ft)		
Length		106	Length		113
Width		85	Width		79
Height		31	Height		33
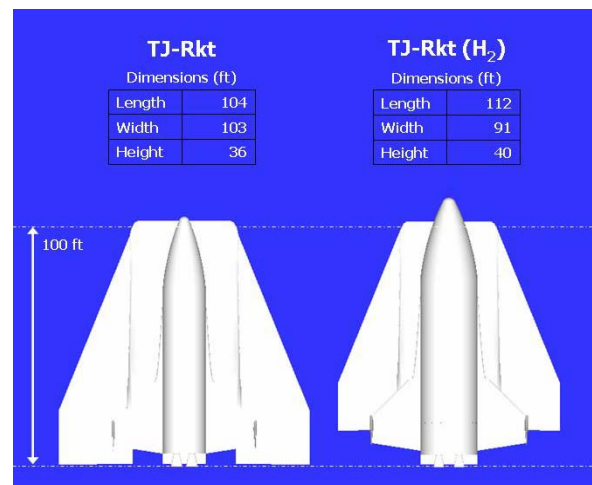
Figure 32. TJ-Rkt Propellant Sensitivity Analysis Dimensions

TJ-Rkt			TJ-Rkt (H$_2$)		
Dimensions (ft)			Dimensions (ft)		
Length		104	Length		112
Width		103	Width		91
Height		36	Height		40

4.2.2 Detailed Propellant Sensitivity Analysis Empty Weight Breakdown

Figures 33 and 35 display the VTHL and HTHL RLV detailed empty weights, respectively, from the propellant sensitivity analysis. These figures are broken down by booster propulsion, booster structure, booster TPS, booster systems, and orbiter. Figures

64

34 and 36 then display the VTHL and HTHL RLV detailed gross weights, respectively, from the propellant sensitivity analysis. These figures are broken down by booster empty, booster propellant, orbiter empty, orbiter propellant, and payload. These divisions highlight where the weight differences are between the baseline RLVs and alternate propellant RLVs.
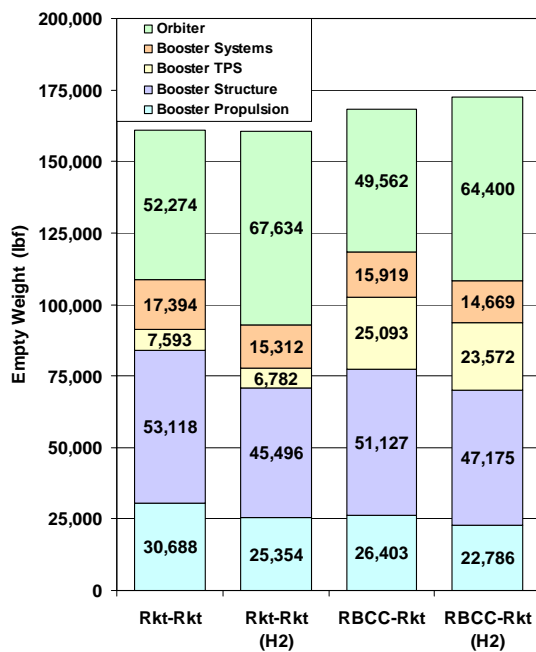
Figure 33. VTHL Propellant Sensitivity Analysis RLV Empty Weights
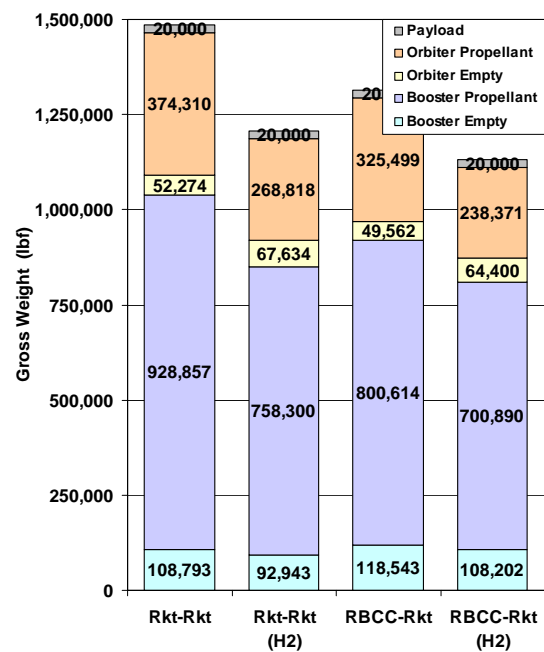
Figure 34. VTHL Propellant Sensitivity Analysis RLV Gross Weights
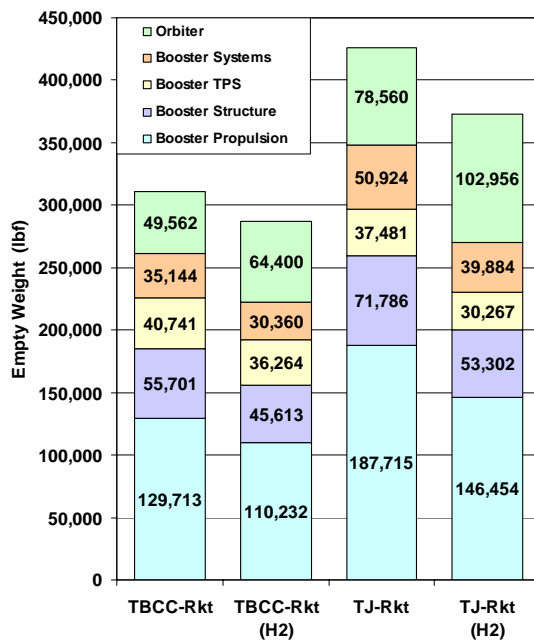
Figure 35. HTHL Propellant Sensitivity Analysis RLV Empty Weights
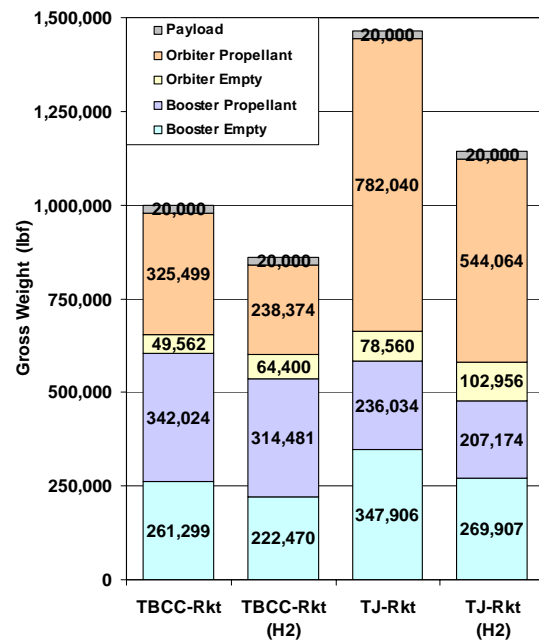
Figure 36. HTHL Propellant Sensitivity Analysis RLV Gross Weights

In comparing the baseline RLVs to the alternate propellant RLVs, all of the empty weight booster categories are lighter for the alternate propellant configurations, while the empty weight of the orbiter is heavier for the alternate propellant configurations. There are several reasons for the booster empty weight decrease for the alternate propellant configurations. First, the booster propulsion system is lighter for each alternate propellant RLV because of its lower gross weight, which is what drives the sizing of the booster propulsion system. This lower gross weight is achieved by orbiter propellant weight savings from the use of hydrogen fuel, which then leads to much less propellant required from the booster to reach staging velocity. Second, the booster structure is lighter because of the reduction in booster propellant, which requires less volume and

66

leads to smaller fuel tanks and an overall smaller booster. Third, the booster TPS is lighter because, with a smaller booster, there is less surface area to cover in TPS. Fourth, the booster systems are lighter in large part because of the reduction in landing gear weight. For VTHL RLVs, this comes from the reductions in empty weight of the other categories, which for VTHL vehicles is what drives the sizing of the wings and landing gear. For HTHL RLVs, this comes from the reductions in gross weight.

The reason for the increase in orbiter empty weight for each alternate propellant RLV is due to the physical properties of the liquid hydrogen propellant. Even though a hydrogen-fueled vehicle requires less fuel to achieve the same delta velocity, the lower density of hydrogen fuel requires much more volume than hydrocarbon fuel. This means the orbiter must be larger with more surface area, causing an increase in the amount of TPS required. Hydrogen fuel tanks are also heavier than hydrocarbon fuel tanks, because hydrogen tanks must be more highly pressurized and insulated [29:1214-1215]. In addition, all of this makes the wings and landing gear grow in size to account for the increase in landing weight for the orbiter.

After everything is accounted for, the booster empty weight savings achieved with the alternate propellant VTHL RLVs are essentially nullified by the growth in orbiter empty weight. For the RBCC-Rkt, the baseline configuration is easily the better choice, because the empty weight of the baseline configuration is lighter than that of the alternate propellant configuration. For the Rkt-Rkt, there are minimal empty weight savings with the alternate propellant configuration, but the baseline configuration is again the better choice for two reasons. First, the baseline Rkt-Rkt uses the same set of engines on each

67

stage. This will greatly decrease the developmental costs, because the engines are the costliest component of technology development [20:3]. Second, the benefit of having an all hydrocarbon fueled vehicle with the same set of engines on each stage provides for simpler vehicle maintenance and safer vehicle operations, which will in turn reduce the operational costs [37:1170; 2:1].

However, for the HTHL RLVs, the booster empty weight savings achieved with the alternate propellant configurations are much greater than the growth in orbiter empty weight. This is because the booster makes up a much larger percentage of the total empty weight for HTHL RLVs, as shown in Figure 37. For the HTHL RLVs, including both the baseline and alternate propellant configurations, the booster makes up between 72% to 84% of the total RLV empty weight. In contrast, for the VTHL RLVs, the booster makes up between 58% to 71% of the total RLV empty weight. This means that a booster empty weight savings does not affect the total empty weight of the VTHL RLVs nearly as much as it does the HTHL RLVs.
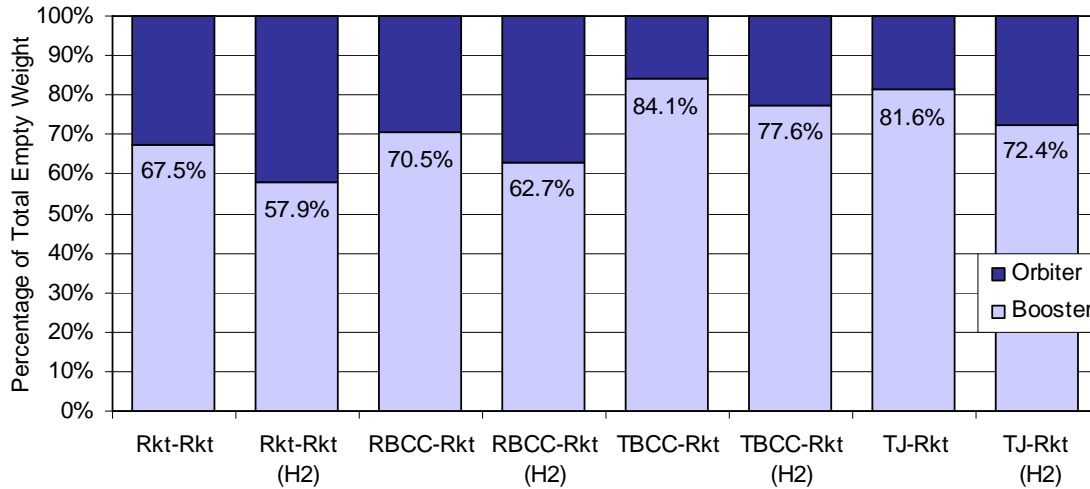
Figure 37. Percentage of Total RLV Empty Weights for Boosters and Orbiters in Propellant Sensitivity Analysis

For the TBCC-Rkt, the empty weight of the alternate propellant configuration is 24,000 lbf lighter than the baseline configuration, which is a reduction of 8%. For the TJ-Rkt, the empty weight of the alternate propellant configuration is 54,000 lbf lighter than the baseline configuration, which is a reduction of 13%. Moreover, the gross takeoff weight of the alternate propellant TJ-Rkt, unlike that of its baseline counterpart, is low enough to enable operation from most commercial runways. Choosing empty weight as the primary figure of merit, the alternate propellant configurations of both HTHL RLVs are better choices than the baseline configurations. However, in a more thorough economic analysis, the operational complexities and hazards of using liquid hydrogen in the orbiters would have to be taken into account and evaluated against the savings in total RLV empty weight.

4.3   Turbine Installed Thrust to Weight Ratio Sensitivity Analysis Results

Table 8 lists the empty weights of the RLVs from the turbine installed thrust to weight ratio sensitivity analysis, along with the corresponding gross weights. As would be expected, increasing the turbine installed thrust to weight ratio for each configuration reduces the RLV total empty weight and gross weight. As shown in Figure 38, increasing the turbine installed thrust to weight ratio from 6 to 8 reduces the total empty weight of the TBCC-Rkt by 17%, and reduces the total empty weight of the TJ-Rkt by 15%. A further increase of the turbine installed thrust to weight ratio to 10 reduces the total empty weight of the TBCC-Rkt by 24% over that of the baseline TBCC-Rkt, and reduces the total empty weight of the TJ-Rkt by 22% over that of the baseline TJ-Rkt. The reasons for these changes are discussed in subsequent sections.

**Table 8. RLV Empty and Gross Weights from the Turbine
Installed Thrust to Weight Ratio Sensitivity Analysis**

	Empty Weight (lbf)			Gross Weight (lbf)			
	Booster	Orbiter	Total	Booster	Orbiter	Payload	Total
TBCC-Rkt (Baseline)	261,299	49,562	**310,861**	603,324	375,061	20,000	**998,384**
TBCC-Rkt (T/W=8)	207,604	49,563	**257,167**	534,638	375,073	20,000	**929,711**
TBCC-Rkt (T/W=10)	188,200	49,562	**237,762**	518,346	375,061	20,000	**913,407**
TJ-Rkt (Baseline)	347,906	78,560	**426,466**	583,940	860,600	20,000	**1,464,540**
TJ-Rkt (T/W=8)	285,951	78,560	**364,511**	522,094	860,599	20,000	**1,402,693**
TJ-Rkt (T/W=10)	252,452	78,560	**331,012**	493,793	860,600	20,000	**1,374,393**
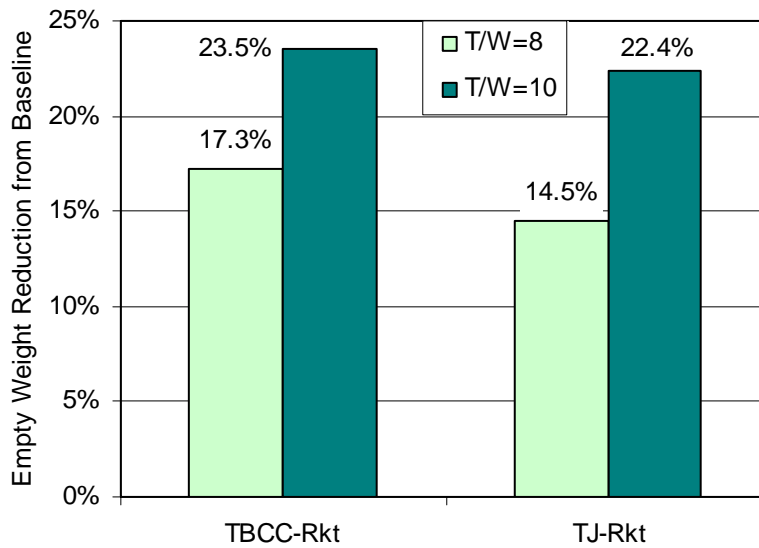
**Figure 38. Reduction in RLV Empty Weight from Baseline Configuration
by Increasing the Turbine Installed Thrust to Weight Ratio**

4.3.1 Turbine Installed Thrust to Weight Ratio Sensitivity Analysis Dimensions

Figures 39 and 40 list the dimensions of the baseline TBCC-Rkt and TJ-Rkt compared to the RLVs with an increased turbine installed thrust to weight ratio, along with vehicle schematics showing the size comparisons. As would be expected, increasing the turbine installed thrust to weight ratio for each configuration reduces the size of each RLV. However, before this sensitivity analysis was undertaken, the magnitude of these changes was unknown. As these graphics illustrate, the boosters all decrease in size with an increased turbine installed thrust to weight ratio, while the orbiters remain unchanged since the staging conditions have not changed. For the TBCC-Rkt, the booster size reduction is fairly large for the jump in turbine installed thrust to weight ratio from 6 to 8,

71

but is barely noticeable from 8 to 10. For the TJ-Rkt, the booster size reduction is very

slight with an increase in turbine installed thrust to weight ratio.

**Figure 39. TBCC-Rkt Turbine Installed Thrust to Weight Ratio
Sensitivity Analysis Dimensions**

**Figure 40. TJ-Rkt Turbine Installed Thrust to Weight Ratio
Sensitivity Analysis Dimensions**

4.3.2 Turbine Installed Thrust to Weight Ratio Sensitivity Analysis Afterburning Turbine Engines

The fuselage width of each TBCC-Rkt and TJ-Rkt depends on the size and number of afterburning turbine engines required for the ascent trajectory. The number of turbine engines was held at 9 for the TBCC-Rkt and 13 for the TJ-Rkt, while the sizes of the turbine engines were determined by Equations (24)-(26). In order to meet the requirement that the fuselage width be large enough to fit all of the afterburning turbine engines, the width to height ratio of the inlet had to be increased in HySIDE for each configuration to correspond to the increase in the turbine installed thrust to weight ratio, which is expanded upon in the next section. Table 9 lists the dimensions, weights, thrust levels, and thrust to weight ratios, both uninstalled and installed, for all of the RLVs in the turbine installed thrust to weight ratio sensitivity analysis. As shown in Figure 41, increasing the turbine installed thrust to weight ratio from 6 to 8 reduced the installed turbine weight by 30% for the TBCC-Rkt, and by 28% for the TJ-Rkt. Increasing the turbine installed thrust to weight ratio from 6 to 10 reduced the installed turbine weight by 45% for the TBCC-Rkt, and by 43% for the TJ-Rkt.

Table 9. Afterburning Turbine Engine Performance and Dimensional Data for RLVs in Turbine Installed Thrust to Weight Ratio Sensitivity Analysis

			TBCC-Rkt			TJ-Rkt		
			Baseline	T/W=8	T/W=10	Baseline	T/W=8	T/W=10
Per Turbine	Length	ft	22.0	21.5	21.3	22.3	21.9	21.7
	Diameter	ft	6.2	6.0	6.0	6.3	6.2	6.1
	Weight (Uninst)	lbf	6,904	6,468	6,338	7,135	6,808	6,657
	Weight (Inst)	lbf	12,772	8,926	7,035	13,058	9,395	7,389
	Thrust	lbf	76,021	71,647	70,339	78,337	75,061	73,548
Total	Turbines	#	9	9	9	13	13	13
	Weight (Uninst)	lbf	62,133	58,211	57,044	92,759	88,501	86,541
	Weight (Inst)	lbf	114,945	80,332	63,319	169,749	122,131	96,061
	Thrust	lbf	684,189	644,821	633,051	1,018,383	975,790	956,129
	T/W (Uninst)		11.0	11.1	11.1	11.0	11.0	11.0
	T/W (Inst)		6.0	8.0	10.0	6.0	8.0	10.0
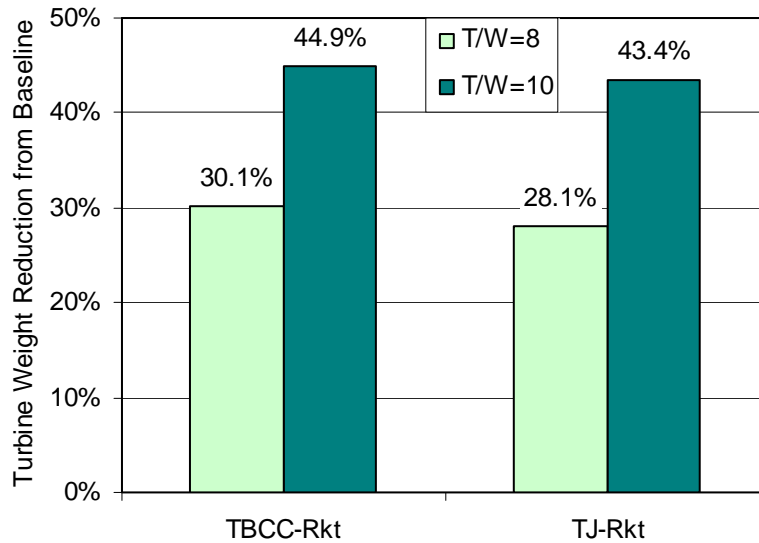
Figure 41. Reduction in Turbine Installed Weight from Baseline Configuration by Increasing the Turbine Installed Thrust to Weight Ratio

4.3.3 Detailed Turbine Installed Thrust to Weight Ratio Sensitivity Analysis Empty Weight Breakdown

Figures 42 and 44 display the TBCC-Rkt and TJ-Rkt detailed empty weights, respectively, from the turbine installed thrust to weight ratio sensitivity analysis. These figures are broken down by booster propulsion, booster structure, booster TPS, booster systems, and orbiter. Figures 43 and 45 then display the TBCC-Rkt and TJ-Rkt detailed gross weights, respectively, from the turbine installed thrust to weight ratio sensitivity analysis. These figures are broken down by booster empty, booster propellant, orbiter empty, orbiter propellant, and payload. These divisions highlight where the weight differences are between the RLVs in the turbine installed thrust to weight ratio sensitivity analysis.
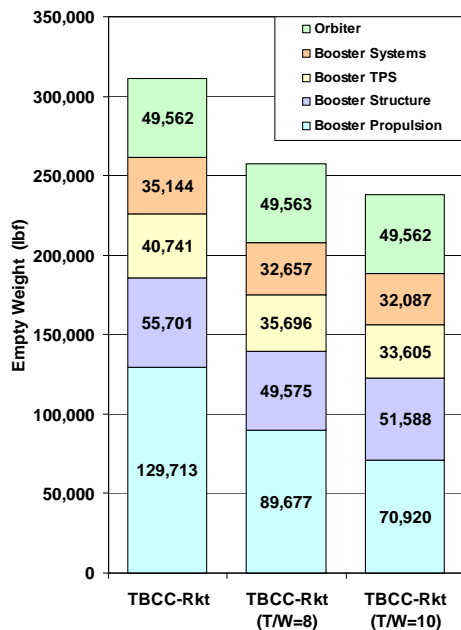
Figure 42. TBCC-Rkt Turbine Installed Thrust to Weight Ratio Sensitivity Analysis Empty Weights
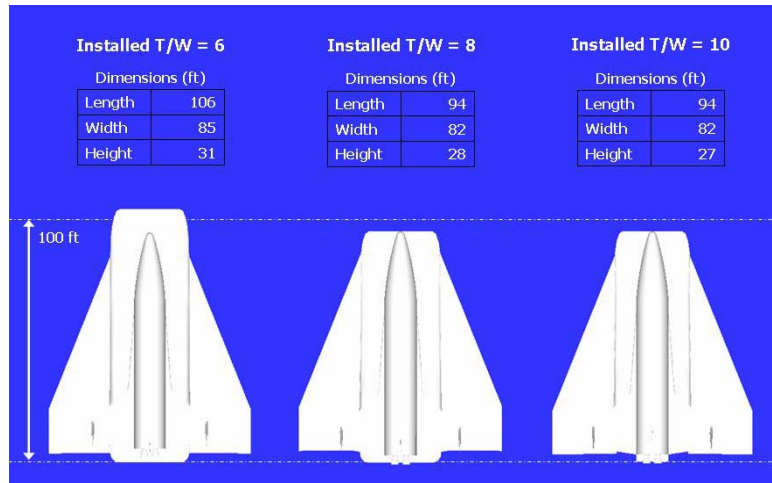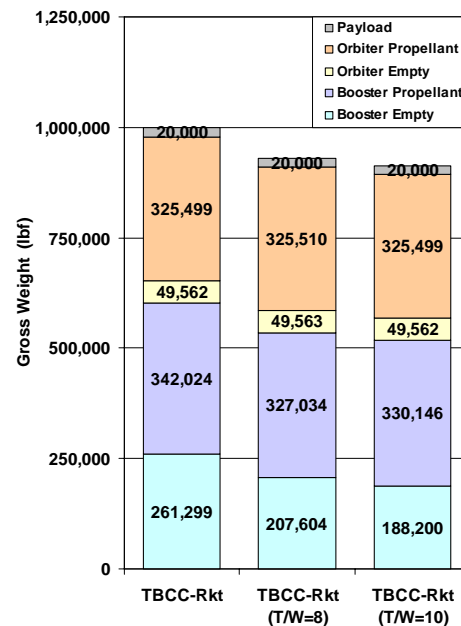

Figure 43. TBCC-Rkt Turbine Installed Thrust to Weight Ratio Sensitivity Analysis Gross Weights
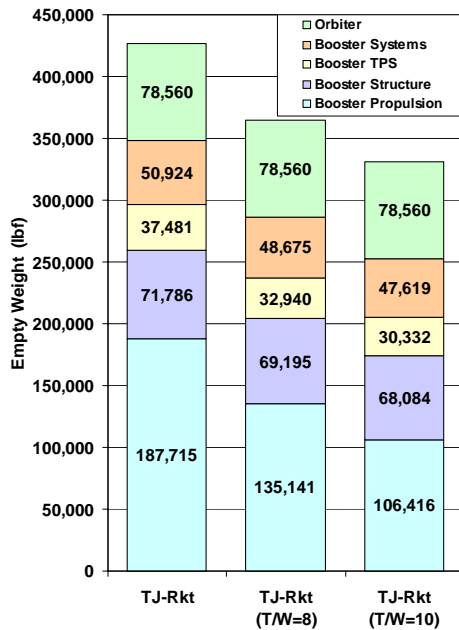
Figure 44. TJ-Rkt Turbine Installed Thrust to Weight Ratio Sensitivity Analysis Empty Weights
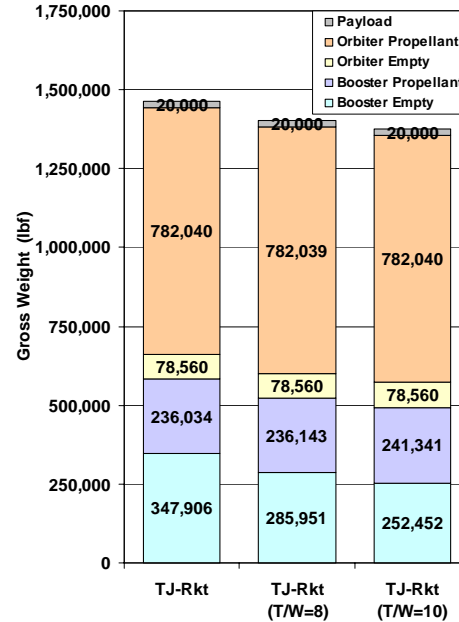
Figure 45. TJ-Rkt Turbine Installed Thrust to Weight Ratio Sensitivity Analysis Gross Weights

In comparing the RLVs in the turbine installed thrust to weight ratio sensitivity analysis, the biggest changes in empty weight are with the booster propulsion system, which are a direct result of the change in turbine installed thrust to weight ratios. For the TBCC-Rkt, increasing the turbine installed thrust to weight ratio from 6 to 8 reduces the empty weight of the booster propulsion system by 40,000 lbf. Increasing this ratio from 8 to 10 reduces the empty weight of the booster propulsion system by another 19,000 lbf. For the TJ-Rkt, increasing the turbine installed thrust to weight ratio from 6 to 8 reduces the empty weight of the booster propulsion system by 53,000 lbf. Increasing this ratio from 8 to 10 reduces the empty weight of the booster propulsion system by another 29,000 lbf.

All of the other empty weight booster categories decrease in value with an increase in the turbine installed thrust to weight ratio, with the exception of the change in booster structure empty weight going from a turbine installed thrust to weight ratio of 8 to 10 for the TBCC-Rkt. The weight of the orbiters do not change, because the staging conditions have not changed. With the noted exception from the TBCC-Rkt, all of these changes are expected, because most categories directly scale with either the RLV empty weight or gross weight. The reason for the increase in the TBCC-Rkt booster structure empty weight going from a turbine installed thrust to weight ratio of 8 to 10 is due to the requirement that the fuselage width be large enough to fit all of the afterburning turbine engines. As stated earlier, this is accomplished by increasing the width to height ratio of the inlet in each configuration to correspond with the increase in the turbine installed thrust to weight ratio. For the TBCC-Rkt, this turbine packing requirement led to an increase in booster structure weight when the turbine installed thrust to weight ratio was increased from 8 to 10.

For all of the RLVs in the turbine installed thrust to weight sensitivity analysis, it is clear that increasing the turbine installed thrust to weight ratio causes a decrease in the RLV empty weight. Utilizing empty weight as the primary figure of merit, the best choices in this sensitivity analysis are the configurations with the most aggressive turbine installed thrust to weight ratios. However, in a more thorough economic analysis, the technological complexities and risks of developing afterburning turbine engines with high installed thrust to weight ratios would have to be taken into account and evaluated against the savings in total RLV empty weight.

4.4   Overall RLV Results

Figure 46 lists the empty weights of all the RLVs considered in this study, including the baseline configurations as well as the configurations from each sensitivity analysis. The RLV empty weights are shown in ascending order, with the alternate propellant Rkt-Rkt at the low end and the baseline TJ-Rkt at the high end.
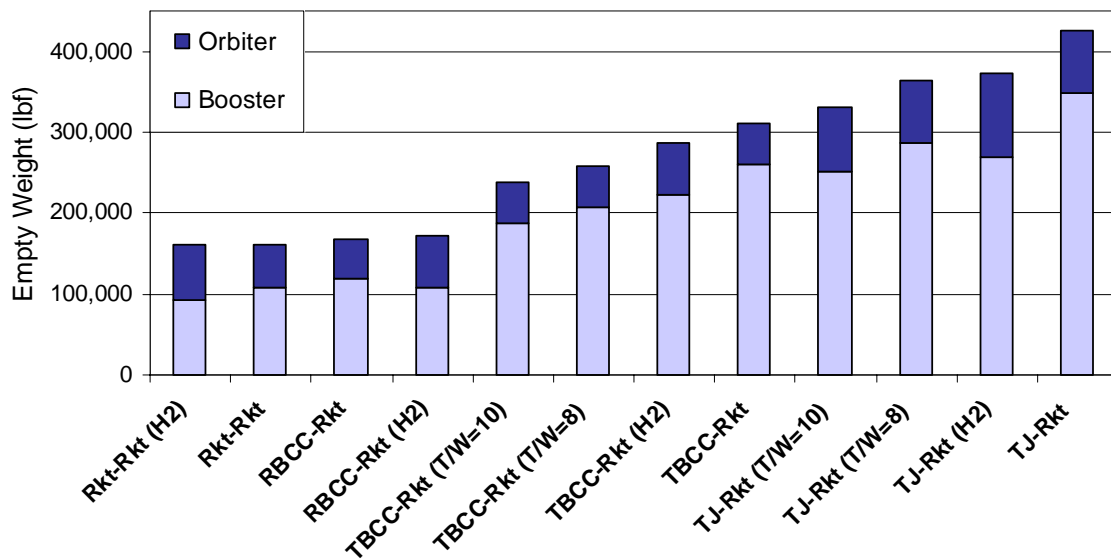
Figure 46. Overall RLV Empty Weight Comparisons

Three findings stand out in this figure. First, the empty weights of the VTHL RLVs are all under 175,000 lbf, while the lowest empty weight of the HTHL RLVs is close to 240,000 lbf. These results show that vertical takeoff RLVs clearly have an empty weight advantage over horizontal takeoff RLVs, although there are some operational benefits associated with horizontal takeoff, as discussed in Section 4.1.3.

The second finding indicates that changing the orbiter fuel from hydrocarbon to hydrogen produces either negligible or no empty weight savings for the VTHL RLVs. On the other hand, the orbiter propellant switch leads to substantial empty weight savings for the HTHL RLVs. However, these empty weight savings must be measured against the associated operational and safety issues, as discussed in Section 4.2.2.

The third finding shows that increasing the turbine installed thrust to weight ratio causes an empty weight decrease in all of the RLVs utilizing afterburning turbine engines. However, these empty weight savings must be measured against the technological complexities and risks associated with developing afterburning turbine engines with high installed thrust to weight ratios, as discussed in Section 4.3.3.

4.5   Validation of Results

In order to validate the results generated with HySIDE, two configurations were selected to be analyzed in POST and then compared to the data obtained with HySIDE. The baseline Rkt-Rkt was chosen to represent the VTHL RLVs, and the baseline TBCC-Rkt was chosen to represent the HTHL RLVs. Table 10 lists the RLV empty weights obtained with POST. This empty weight is obtained by using the gross weight that was output by POST at either the vehicle staging or payload insertion, and then subtracting any leftover weight that was calculated with HySIDE. For the booster, this leftover weight includes the gross weight of the orbiter and payload, flyback propellant, reserve ancillary propellant, and trapped unusable propellant. For the orbiter, this leftover weight includes the gross weight of the payload, reserve ancillary propellant, and trapped unusable propellant.

Table 10. Baseline RLV Empty Weights Obtained with POST

	Rkt-Rkt		TBCC-Rkt	
	Booster	**Orbiter**	**Booster**	**Orbiter**
POST Gross Weight (lbf)	568,952	76,814	734,953	73,239
- (Orbiter + Payload Total)	-446,583	-20,000	-395,061	-20,000
- (Flyback Propellant)	-6,253	-0	-87,392	-0
- (Reserve Propellant)	-8,876	-3,617	-2,481	-3,142
- (Trapped Unusable Propellant)	-4,438	-1,808	-1,241	-1,571
POST Empty Weight (lbf)	**102,803**	**51,389**	**248,778**	**48,527**

Figure 47 shows the empty weight differences between HySIDE and POST. The

total empty weight difference is 4.3% for the Rkt-Rkt, and 4.4% for the TBCC-Rkt. This

excellent correlation is also reflected in the trajectory plots for these RLVs. Figures 48

and 49 show Rkt-Rkt trajectory information from HySIDE and POST, respectively, and

Figures 50 and 51 show TBCC-Rkt trajectory information from HySIDE and POST,

respectively. These plots show vehicle weight, thrust, and drag on the left axis, with

dynamic pressure on the right axis, all versus velocity.
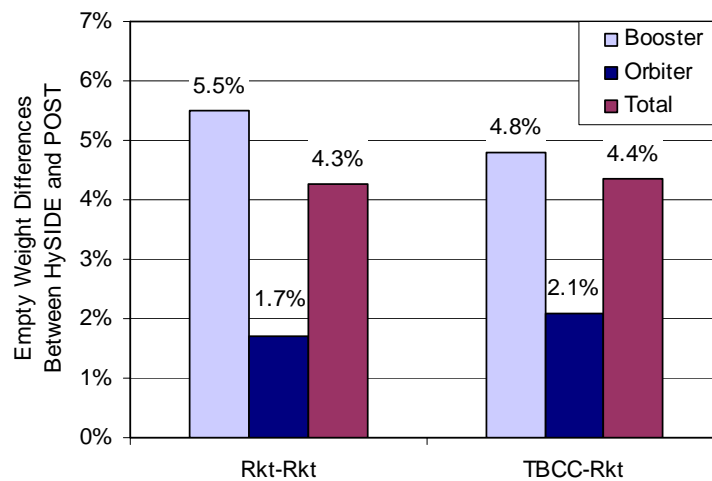
Figure 47. Empty Weight Differences Between HySIDE and POST
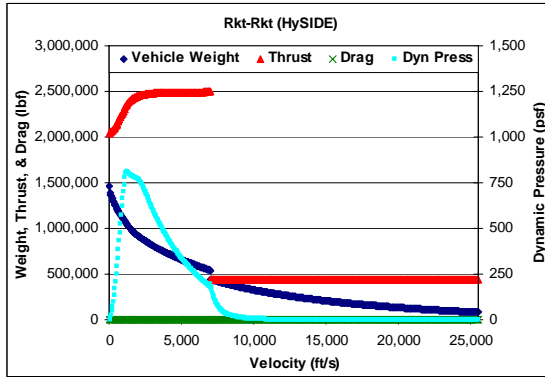
Figure 48. Rkt-Rkt Trajectory with HySIDE
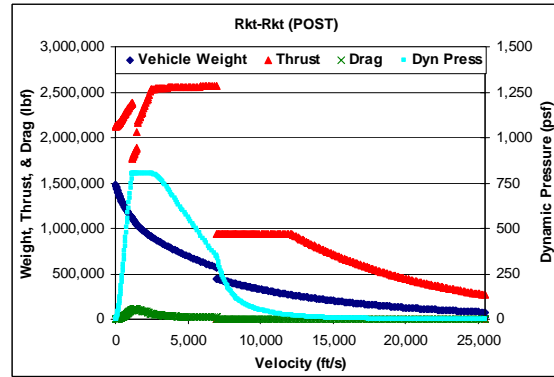
Figure 49. Rkt-Rkt Trajectory with POST
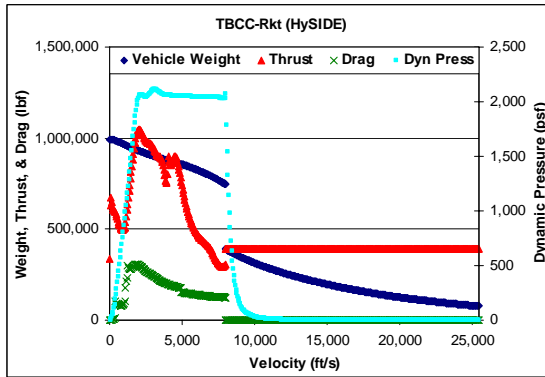
Figure 50. TBCC-Rkt Trajectory with HySIDE
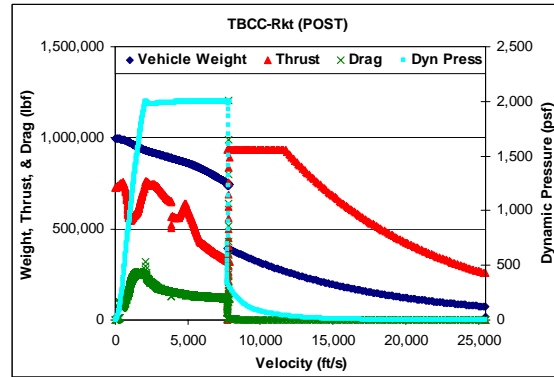
Figure 51. TBCC-Rkt Trajectory with POST

There are a few reasons for the small differences between HySIDE and POST. First, vehicle aerodynamic characteristics have to be assumed for POST, whereas they are calculated in HySIDE. In POST, the X-43 lifting body aerodynamic data set was assumed for both RLVs because of its easy availability [8:80-82]. This data set was then scaled by a constant to make the drag numbers approximate those from HySIDE. For the Rkt-Rkt, this scaling factor is ¼, and for the TBCC-Rkt, this scaling factor is ⅓. As

81

shown in these graphs, the vehicle drag versus velocity is similar in both HySIDE and POST.

Second, rocket engines are not throttled in HySIDE, but they are throttled in POST to control things such as maximum dynamic pressure and maximum acceleration. In the POST graphs, the thrust discontinuities in the first stage of the rocket engine operation for the Rkt-Rkt are due to the rocket engine throttling as previously mentioned. The decaying thrust profile for the second stage orbiters in both POST graphs are also due to the rocket engine throttling. For the Rkt-Rkt in HySIDE, the maximum dynamic pressure is 800 psf, and the maximum acceleration is 5.5 g's, so these were input into POST as the maximum dynamic pressure and acceleration for the Rkt-Rkt. Likewise, for the TBCC-Rkt in HySIDE, the maximum dynamic pressure is 2,000 psf, and the maximum acceleration is 5.0 g's, so these were input into POST as the maximum dynamic pressure and acceleration for the TBCC-Rkt.

Third, airbreathing engines have a different set of input requirements in HySIDE and POST. The airbreathing engine performance data required by HySIDE is ISP versus velocity, which is flown along a constant dynamic pressure profile of 2,000 psf. The airbreathing engine performance data required by POST is thrust coefficient and ISP versus Mach number, angle of attack, and dynamic pressure. Another difference in the HySIDE and POST airbreathing engine simulations is that HySIDE calculates a design point ISP for the airbreathing engine which is used to offset the tabular data that is provided. Because of these differences, the airbreathing thrust profile for the TBCC-Rkt is slightly different for HySIDE and POST.

5. Conclusions and Recommendations

In response to DoD requirements for responsive and low-cost access to space, the AFRL Propulsion Directorate sponsored this research effort in order to attain an objective comparison between potential hydrocarbon-fueled RLV configurations for military operations. Many design studies have been performed with hydrogen-fueled vehicles, but there has been limited research into RLVs utilizing hydrocarbon scramjet engines, which have the potential to be more practical and operable for responsive military operations. To fill this void, this study utilized hydrocarbon Duel-Mode Scramjet (DMSJ) engine performance data from the U.S. Air Force HyTech program in the propulsion systems of the Rocket-Based-Combined-Cycle (RBCC) and Turbine-Based-Combined-Cycle (TBCC) booster configurations. The conclusions and recommendations of this study provide decision-makers some of the information needed in order to choose where to invest for future space access.

5.1   Conclusions of Research

1. Vertical-takeoff-horizontal-landing (VTHL) RLVs have a significant empty weight advantage over horizontal-takeoff-horizontal-landing (HTHL) RLVs, which is mainly due to the extremely heavy booster propulsion systems caused by the HTHL afterburning turbine engines. Additionally, HTHL RLVs have heavier wings and landing gear, since the size of these systems is based on the gross takeoff weight for HTHL RLVs instead of the landing weight, as is the case for VTHL RLVs. HTHL RLVs also have higher TPS weights, which is because of the greater amount of surface area to cover in

TPS as a result of the greater wing size. However, the RLV empty weights do not take into account the operational benefits associated with horizontal takeoff, which could potentially lead to substantial operational cost savings.

2. Changing the orbiter fuel from hydrocarbon to hydrogen produces different overall empty weight effects in VTHL RLVs than it does in HTHL RLVs. This orbiter propellant switch has either negligible or no empty weight savings for the VTHL RLVs, while it leads to substantial empty weight savings for the HTHL RLVs. In comparing the baseline RLVs to the alternate propellant RLVs, all of the empty weight booster categories are lighter for the alternate propellant configurations, while the empty weight of the orbiter is heavier for the alternate propellant configurations. After everything is accounted for, the booster empty weight savings achieved with the alternate propellant VTHL RLVs are essentially nullified by the growth in orbiter empty weight. Conversely, for the HTHL RLVs, the booster empty weight savings achieved with the alternate propellant configurations are much greater than the growth in orbiter empty weight. This is because the booster makes up a much larger percentage of the total empty weight for HTHL RLVs. However, the RLV empty weights do not account for the associated operational and safety issues of using liquid hydrogen in a high-tempo military environment, which will have to be considered in a total vehicle analysis.

3. For the HTHL RLVs, increasing the turbine installed thrust to weight ratio causes a decrease in empty weight. Since the afterburning turbine engines dominate the empty weight of the HTHL RLVs, reductions in turbine weights have tremendous impacts on the overall RLV empty weights. However, a balance must be found between

savings in empty weight, and the technological complexities and risks associated with being overly aggressive in the development of afterburning turbine engines with very high installed thrust to weight ratios.

5.2   Recommended RLV Configurations

1. The first recommended RLV configuration is the baseline Rkt-Rkt, which has the second lowest empty weight of all the configurations in this study. If empty weight was the only figure of merit, then it would appear that the alternate propellant Rkt-Rkt was the best choice, since many researchers correlate a launch system's acquisition and operational cost to the system's empty weight [5:1; 20:4; 13:9; 31:2]. However, even though the empty weight of the baseline Rkt-Rkt is 500 pounds heavier than that of the alternate propellant Rkt-Rkt, the baseline configuration is the better choice for two reasons. First, the baseline Rkt-Rkt uses the same set of engines on each stage. This will greatly decrease the developmental costs, because the engines are the most expensive component of technology development [20:3]. Second, the benefit of having an all hydrocarbon fueled vehicle with the same set of engines on each stage provides for simpler maintenance and safer fueling, which will in turn reduce the operational costs [37:1170; 2:1].

2. The second recommended RLV configuration is the TBCC-Rkt with the highest possible turbine installed thrust to weight ratio, which in this study is 10. Even though the empty weight of this TBCC-Rkt configuration is 48% higher than the baseline Rkt-Rkt, this TBCC-Rkt configuration has the lightest empty weight of all the HTHL RLVs, and the horizontal takeoff capability of the TBCC-Rkt reduces operational costs

over vertical takeoff RLVs. For example, the ability of the TBCC-Rkt to utilize existing aircraft ground facilities eliminates the requirement to rotate the RLV on a dedicated launch pad. This results in substantial operational cost savings compared to vertical takeoff RLVs, which require complex ground support equipment around the launch pad. In addition, the horizontal takeoff capability of the TBCC-Rkt provides many operability benefits, including mission abort capability and trajectory flexibility. This TBCC-Rkt configuration also has the lowest gross takeoff weight of all the configurations, which leads to the easiest fueling and takeoff operations [3:4-6; 33:20; 7:3; 20:3-4; 10:1-2].

5.3   Recommendations for Future Research

1. The TBCC-Rkt should be studied further to find its most optimal configuration. A sensitivity study combining a hydrogen-fueled orbiter with turbine installed thrust to weight ratios of 8 and 10 could yield a solution with the lowest possible empty weight of the HTHL RLVs. Another potential study involving the TBCC-Rkt would be to quantify the operational benefits of the TBCC-Rkt as compared to vertical takeoff RLVs.

2. An empty weight analysis should be accomplished on TSTO RLVs with RBCC orbiters. Two possible configurations include a horizontal takeoff turbine-powered booster with an RBCC orbiter, and a vertical takeoff rocket-powered booster with an RBCC orbiter. This new analysis could then be compared to the results of this study to find out if the Rkt-Rkt and TBCC-Rkt are still the best two configurations.

Appendix A. Airbreathing Engine Performance Data

AFRL Turbine Accelerator Engine Thrust (lbf)

Mach # Altitude (ft)	0	0.5	0.8	1.0	1.5	2.0	2.5	3.0	3.25	3.75	4.0	4.4
0	51,621.0	54,326.0	51,785.0	53,721.0	74,073.0	0	0	0	0	0	0	0
5,000	0	47,598.0	39,940.0	45,774.0	65,959.0	0	0	0	0	0	0	0
10,000	0	0	33,160.0	38,853.0	58,108.0	81,412.0	127,578.0	0	0	0	0	0
20,000	0	0	22,508.0	26,583.0	42,066.0	65,315.0	100,391.0	146,736.0	0	0	0	0
30,000	0	0	14,923.0	17,615.0	29,340.0	48,284.0	71,157.0	100,641.0	0	0	0	0
40,000	0	0	9,584.4	11,293.0	19,106.0	31,506.0	46,397.0	65,463.0	74,388.0	92,791.0	103,912.0	119,178.0
42,000	0	0	0	10,254.0	17,324.0	28,618.0	42,120.0	59,417.0	67,514.0	84,201.0	94,279.0	108,120.0
50,000	0	0	0	6,966.7	11,778.0	19,448.0	28,620.0	40,321.0	45,834.0	57,072.0	63,871.0	73,190.0
60,000	0	0	0	4,295.0	7,270.1	11,984.0	17,650.0	24,826.0	28,208.0	35,084.0	39,236.0	44,908.0
70,000	0	0	0	2,638.8	4,479.5	7,362.4	10,815.0	15,206.0	17,256.0	21,419.0	23,971.0	27,422.0
72,000	0	0	0	2,391.9	4,063.7	6,669.8	9,792.5	13,770.0	15,619.0	19,403.0	21,696.0	24,808.0
80,000	0	0	0	1,620.7	2,748.4	4,502.2	6,610.1	9,293.5	10,525.0	13,053.0	14,604.0	16,683.0
90,000	0	0	0	1,005.0	1,700.8	2,780.2	4,071.7	5,719.5	6,468.0	8,007.4	8,954.3	10,234.0
100,000	0	0	0	627.4	1,058.2	1,727.3	2,526.8	3,548.0	4,003.0	4,945.4	5,535.9	6,309.4

AFRL Turbine Accelerator Engine ISP (sec)

Mach # Altitude (ft)	0	0.5	0.8	1.0	1.5	2.0	2.5	3.0	3.25	3.75	4.0	4.4
0	2122.1	1957.1	1765.5	1719.4	1605.4	0	0	0	0	0	0	0
5,000	0	1963.6	1776.4	1731.2	1640.8	0	0	0	0	0	0	0
10,000	0	0	1759.1	1745.2	1674.3	1558.7	1563.0	0	0	0	0	0
20,000	0	0	1732.6	1731.0	1719.8	1671.2	1652.7	1605.6	0	0	0	0
30,000	0	0	1717.3	1716.2	1765.1	1751.7	1708.5	1649.0	0	0	0	0
40,000	0	0	1721.4	1718.3	1786.9	1780.2	1734.7	1676.4	1630.0	1534.9	1501.1	1453.0
42,000	0	0	0	1717.6	1783.6	1779.4	1733.7	1675.1	1628.0	1533.4	1499.4	1451.1
50,000	0	0	0	1714.2	1780.9	1776.4	1729.8	1669.8	1623.0	1526.7	1492.1	1442.8
60,000	0	0	0	1708.9	1777.6	1769.5	1724.5	1662.6	1615.0	1517.6	1482.3	1431.5
70,000	0	0	0	1702.6	1775.0	1763.2	1714.8	1650.8	1602.0	1502.7	1467.6	1415.5
72,000	0	0	0	1701.0	1773.8	1760.2	1710.8	1647.3	1598.0	1498.9	1463.7	1411.0
80,000	0	0	0	1694.4	1764.8	1747.3	1698.0	1633.3	1582.0	1481.5	1446.8	1393.2
90,000	0	0	0	1688.3	1756.2	1734.4	1681.9	1615.5	1563.0	1459.6	1424.3	1370.6
100,000	0	0	0	1681.8	1745.7	1720.3	1666.4	1598.1	1543.0	1437.9	1402.5	1347.0

AFRL HyTech DMSJ Engine Performance Data

Flight Path Angle = 0 deg				Flight Path Angle = 4 deg			
Mach Number	Q (psf)	Thrust Coefficient	ISP (sec)	Mach Number	Q (psf)	Thrust Coefficient	ISP (sec)
3.5	0	0	0	3.5	0	0	0
	250	0	0		250	0	0
	500	0	0		500	0	0
	1000	0	0		1000	0	0
	2000	0	0		2000	0	0
3.75	0	0	0	3.75	0	0	0
	250	0.546	1310.13		250	0.674	1344.75
	500	0.728	1746.84		500	0.899	1793.00
	1000	0.741	1759.93		1000	0.914	1804.57
	2000	0.745	1765.23		2000	0.914	1800.45
4.0	0	0	0	4.0	0	0	0
	250	0.632	1212.62		250	0.744	1218.96
	500	0.843	1616.82		500	0.992	1625.28
	1000	0.817	1621.24		1000	1.014	1643.38
	2000	0.822	1628.02		2000	1.020	1648.68
4.5	0	0	0	4.5	0	0	0
	250	0.586	1222.44		250	0.722	1225.07
	500	0.782	1629.92		500	0.962	1633.43
	1000	0.794	1639.12		1000	0.977	1642.76
	2000	0.805	1645.86		2000	0.990	1649.38
5.0	0	0	0	5.0	0	0	0
	250	0.666	1051.40		250	0.832	1050.79
	500	0.888	1401.87		500	1.109	1401.05
	1000	0.901	1408.23		1000	1.127	1405.80
	2000	0.909	1412.73		2000	1.144	1409.60
6.0	0	0	0	6.0	0	0	0
	250	0.419	701.00		250	0.545	709.48
	500	0.559	934.66		500	0.727	945.97
	1000	0.578	956.39		1000	0.751	964.88
	2000	0.595	975.34		2000	0.772	981.51
7.0	0	0	0	7.0	0	0	0
	250	0.346	605.15		250	0.460	616.26
	500	0.461	806.87		500	0.613	821.68
	1000	0.489	838.25		1000	0.649	849.72
	2000	0.506	859.19		2000	0.671	868.22
8.0	0	0	0	8.0	0	0	0
	250	0.284	532.38		250	0.401	545.00
	500	0.379	709.84		500	0.534	726.66
	1000	0.409	747.77		1000	0.573	760.93
	2000	0.427	771.15		2000	0.597	782.85
8.25	0	0	0	8.25	0	0	0
	250	0.270	514.30		250	0.385	525.84
	500	0.360	685.73		500	0.513	701.12
	1000	0.390	724.26		1000	0.553	736.59
	2000	0.407	747.43		2000	0.577	758.03

Appendix B. HySIDE Design Inputs

<u>Airbreather</u>

FreeStream
  Alt (km): 24.44472
  Mach: 7.0
    (these values are in the upper HC DMSJ range along constant Q path)
HADOVehicleBasic
  Inlet
    RDP: 0.01 for 2D inlet (leading to wedge-shaped, NASP-type vehicle)
    LH: 3.0 (inlet width/height ratio; may need to increase if
    NumberOfTurbines increases)
    VehCapArea (m^2): ___ (change this value to refine VolRatio_VAoverFVR
    in Outputs {ratio of volume available over fuel volume required})
  Comb
    FuelNumber: 1 for H2; 6 for HC (JP-7)
    FuelTempMax (K): 833 for H2
  Wing
    Origin: change X value to move front of wing forward or backward
    LaunchMachNo: 0.350 (230 knots) for HTO; 0.285 (185 knots) for VTO
    or 2nd stage
    LaunchCL: 0.9 for HTO; 0.6 for VTO or 2nd stage
      (LaunchMachNo and LaunchCL refer to landing for VTO or 2nd
      stage)
  StructuralWeightsFromWt
    MassOfTakeOffPropulsion
      TurbineCluster
        Turbine
          Origin: change to move single turbine shown in 3D
          Viewer
        NumberOfTurbines: 9 (fewer turbines = larger turbines)
      ThrustToWeightAtTakeoff: 0.7 for HTO; 1.4 for VTO; 1.0 for 2nd
      stage
      RocketEngine_ToverW_Inst: 73.5 for H2; 80.0 for HC
      TurbineEngine_ToverW_Inst: 8.0
      Turbine: True for TJ and TBCC; False for RBCC
    FlybackPropulsion
      TurbineToverW: 0.0 for TJ and TBCC; 8.0 for RBCC
      Range (nm): vehicle dependent, get from Trajectory XYPlots
      Viewer
  HeatLoopType: FuelTempLoop
    (only use PhiLoop if FuelTempReached in Outputs exceeds
    FuelTempMax)

EstPhi: 1.0 (unless using PhiLoop, where it will be greater than 1.0)
FixedWeights
    PayloadAndAccomodations (kg): 0.0 for 1st stage; 9070.2949219 for 2nd stage (20k lbm)
    PayloadVolume (m^3): 0.0 for 1st stage; 79.3199997 for 2nd stage (2800 ft^3)
PropellantUsage
    TrajSegment1 (turbine or rocket)
        VelISPMap: choose from drop-down list, or input your own
    TrajSegment2 (ram-scram)
        VelISPMap: choose from drop-down list, or input your own
    TrajSegment3 (rocket)
        VelISPMap: choose from drop-down list, or input your own
    V2 (ft/s): 4000 (transition from Segment 1 to Segment 2)
    V4 (ft/s): StagingVelocity for 1st stage; 25550 for 2nd stage (orbital velocity)
    PropTypeDetails
        Name: JP1 for turbine; JP1 or LH2 for ram-scram; RP1 or LH2 for rocket
        MassRatio: 0.0 for JP1; 2.5 for RP1; 5.9 for LH2
Trajectory
    ThirdSegInitialHeight (ft): 86000 for DMSJ ending at Mach=8.0 and Q=2000 psf
    HeightFinal (ft): 303800 (50 nautical miles)
    ToverWSeg3: 1.0 (thrust/weight ratio for Segment 3)
    VelAltMapSeg1: DefaultHorizontalTakeoff for HTO; RMLS_VerticalRocket for VTO
    FuelStoicRatioSeg1Turbine: 0.0673 for HC
    FuelStoicRatioSeg2RamScram: 0.0673 for HC; 0.0291 for H2
    Latitude: 28.5 for Cape Canaveral FL

<u>Rocket</u>

FreeStream
    Alt (km): 26.14303
    Mach: 8.0
        (example case; these values are at the end of HC DMSJ along constant Q path)
Rocket
    RocketFuselage
        RadiusMax (m): ___ (rocket fuselage radius)
        LengthOgive (m): ___ (conical nose section length)
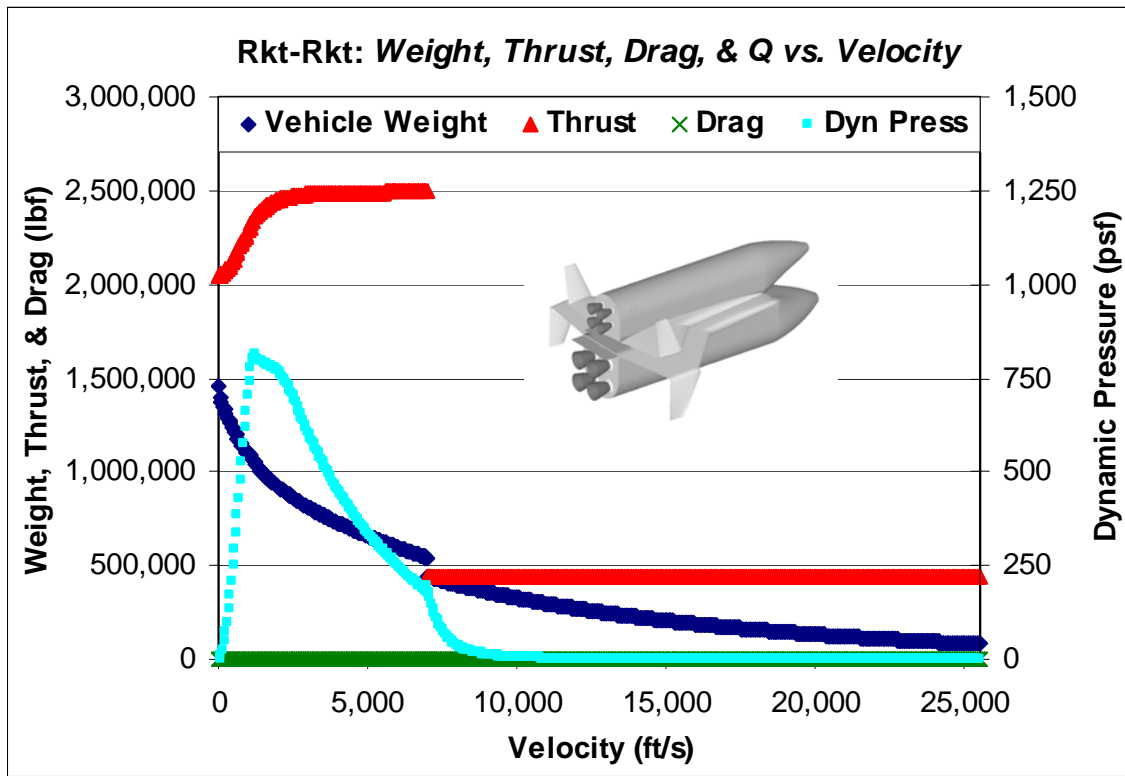   LengthCylinder (m): ___ (length after conical nose section)
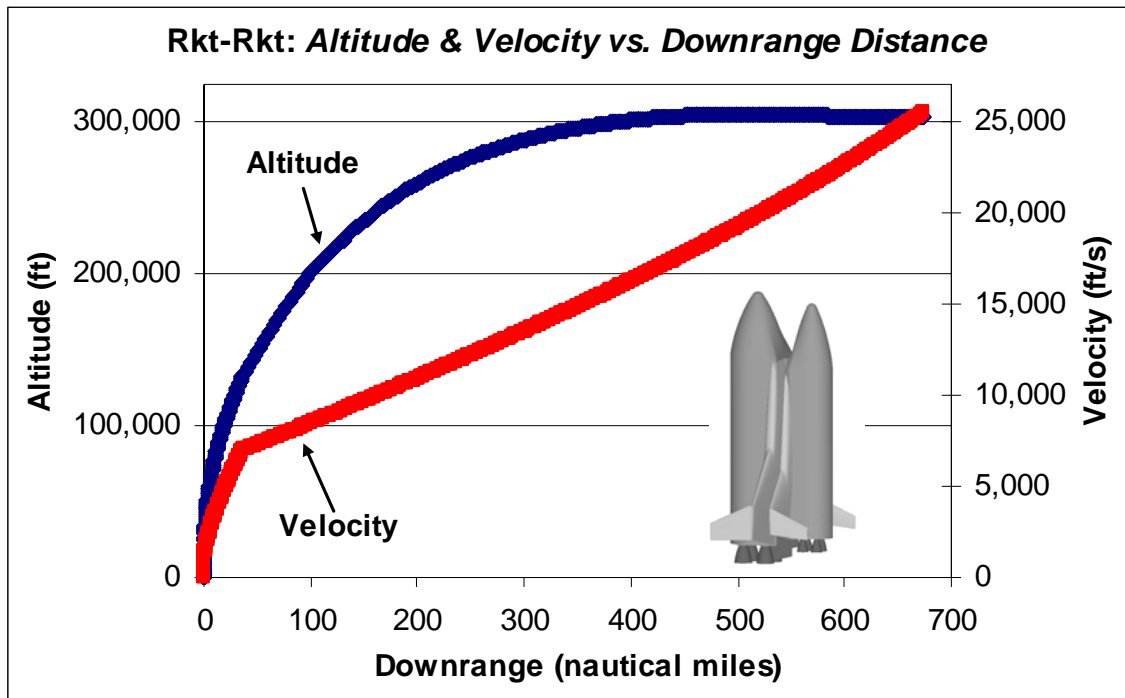   (change these values to refine VolRatio_VAoverFVR in Outputs {ratio of volume available over fuel volume required})
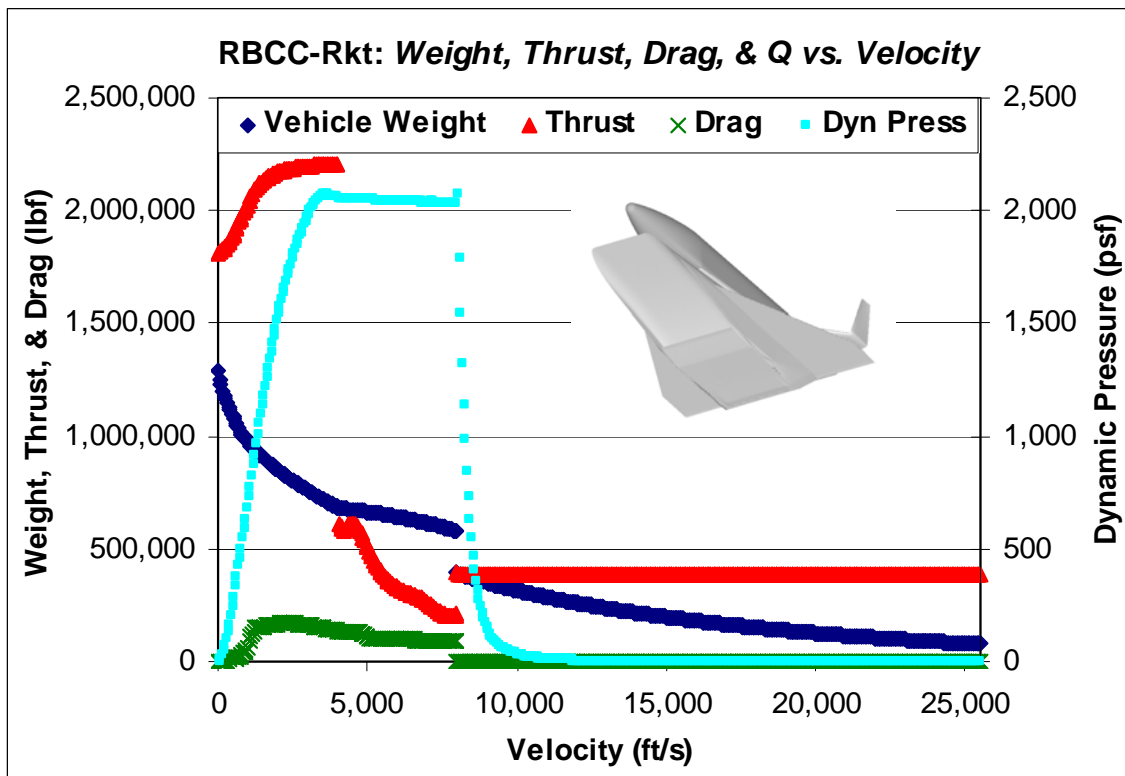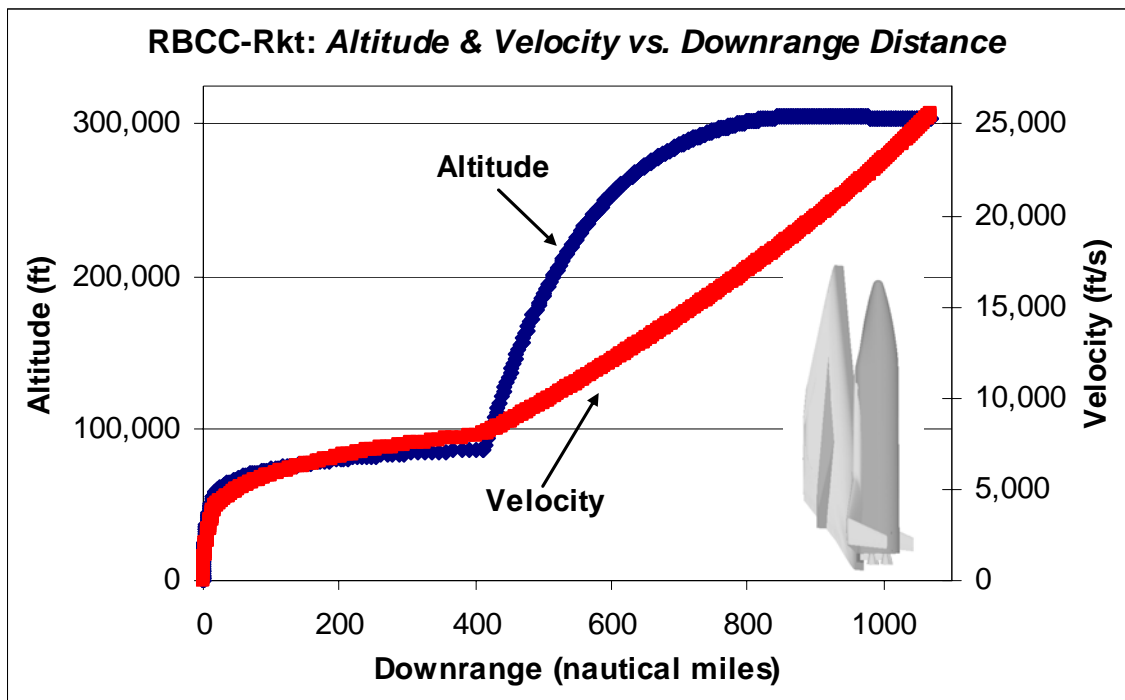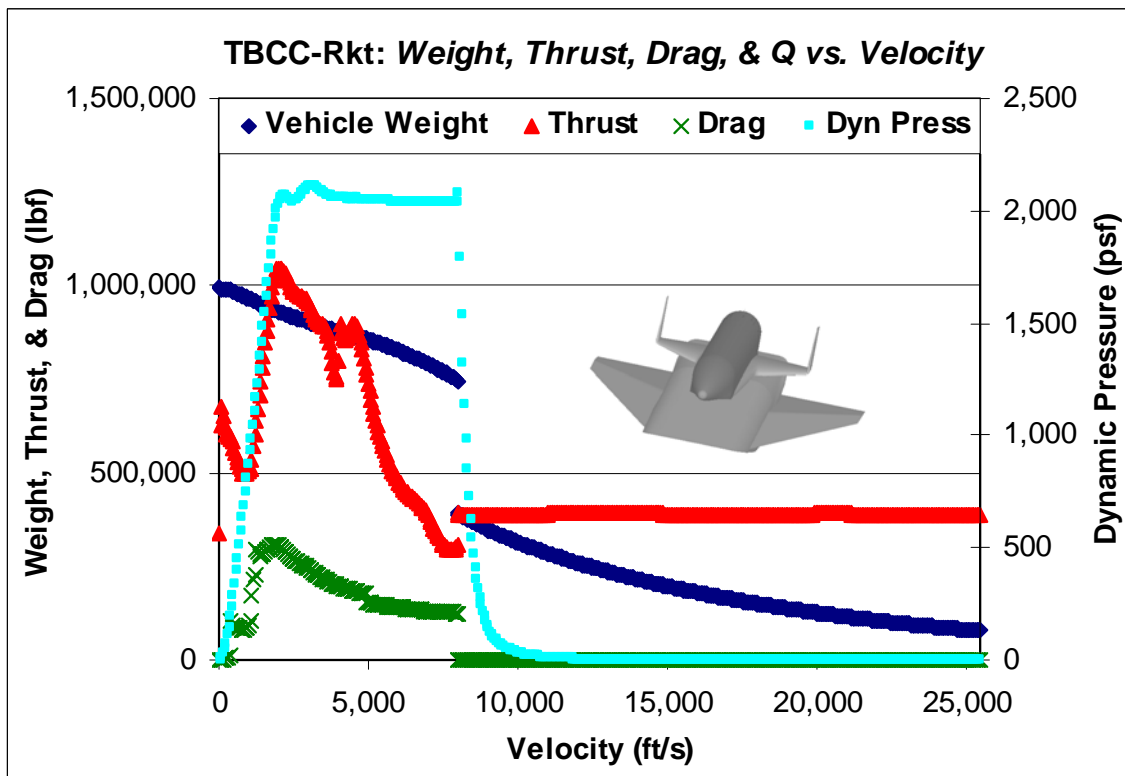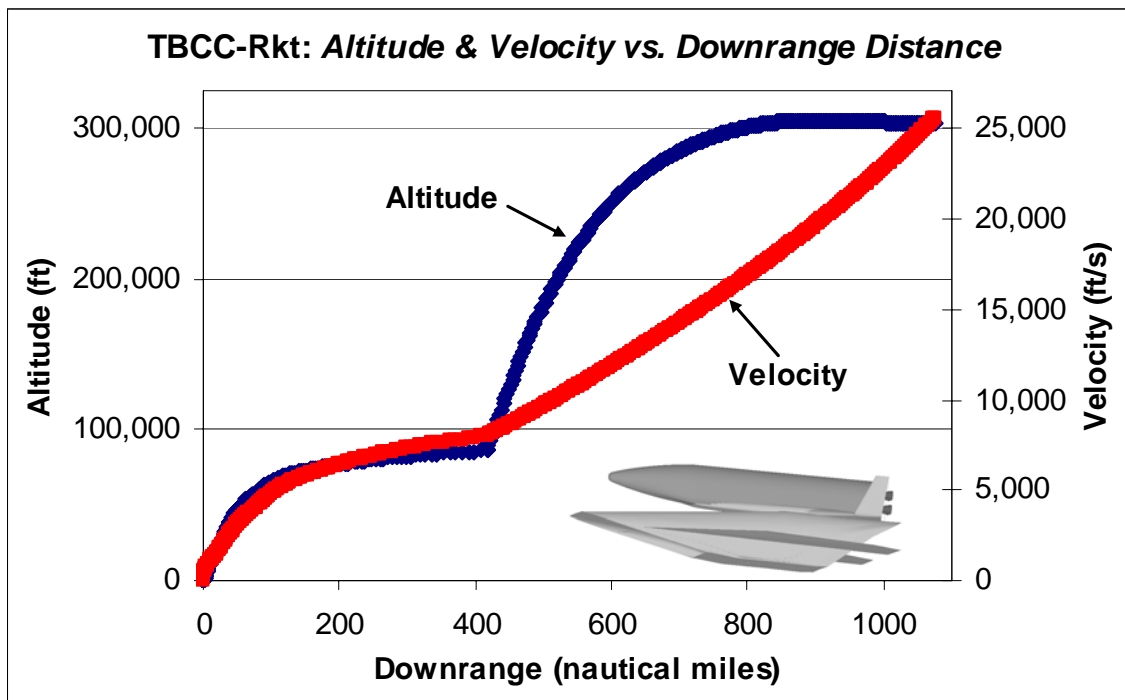   Reentry: False for 1st stage; True for 2nd stage

EngineCluster
    FuelNumber: 1 for H2; 6 for HC (JP-7)
    RocketParams_EEunits: 1 for H2 (SSME); 2 for HC (RD-180)
StructuralWeightsFromWt
    MassOfTakeOffPropulsion
        ThrustToWeightAtTakeoff: 0.7 for HTO; 1.4 for VTO; 1.0 for 2nd stage
        RocketEngine_ToverW_Inst: 73.5 for H2; 80.0 for HC
        Turbine: False
    FlybackPropulsion
        TurbineToverW: 4.0 for 1st stage above Mach 4; else 0.0
        Range (nm): vehicle dependent for 1st stage above Mach 4, get from Trajectory XYPlots Viewer; else 0.0
FixedWeights
    PayloadAndAccomodations (kg): 0.0 for 1st stage; 9070.2949219 for 2nd stage (20k lbm)
    PayloadVolume (m^3): 0.0 for 1st stage; 79.3199997 for 2nd stage (2800 ft^3)
PropellantUsage
    TrajSegment1 (rocket)
        VelISPMap: choose from drop-down list, or input your own
    TrajSegment2 (ram-scram)
        VelISPMap: N/A
    TrajSegment3 (rocket)
        VelISPMap: choose from drop-down list, or input your own
    V2 (ft/s): StagingVelocity
    V4 (ft/s): StagingVelocity for 1st stage; 25550 for 2nd stage (orbital velocity)
    PropTypeDetails
        Name: RP1 for HC; LH2 for H2
        MassRatio: 2.5 for HC; 5.9 for H2
Trajectory
    ThirdSegInitialHeight (ft): 86000 for DMSJ ending at Mach=8.0 and Q=2000 psf
    HeightFinal (ft): 303800 (50 nautical miles)
    ToverWSeg3: 1.0 (thrust/weight ratio for Segment 3)
    VelAltMapSeg1: DefaultHorizontalTakeoff for HTO, or RMLS_VerticalRocket for VTO
    Latitude: 28.5 for Cape Canaveral FL
ThrustToWeightAtTakeoff: 0.7 for HTO; 1.4 for VTO; 1.0 for 2nd stage

StagingVelocity: vehicle dependent

Appendix C. HySIDE Baseline Trajectory Plots

Rkt-Rkt: *Altitude & Velocity vs. Downrange Distance*

Rkt-Rkt: *Weight, Thrust, Drag, & Q vs. Velocity*

RBCC-Rkt: *Altitude & Velocity vs. Downrange Distance*

RBCC-Rkt: *Weight, Thrust, Drag, & Q vs. Velocity*

TBCC-Rkt: *Altitude & Velocity vs. Downrange Distance*

TBCC-Rkt: *Weight, Thrust, Drag, & Q vs. Velocity*

TJ-Rkt: *Altitude & Velocity vs. Downrange Distance*

TJ-Rkt: *Weight, Thrust, Drag, & Q vs. Velocity*
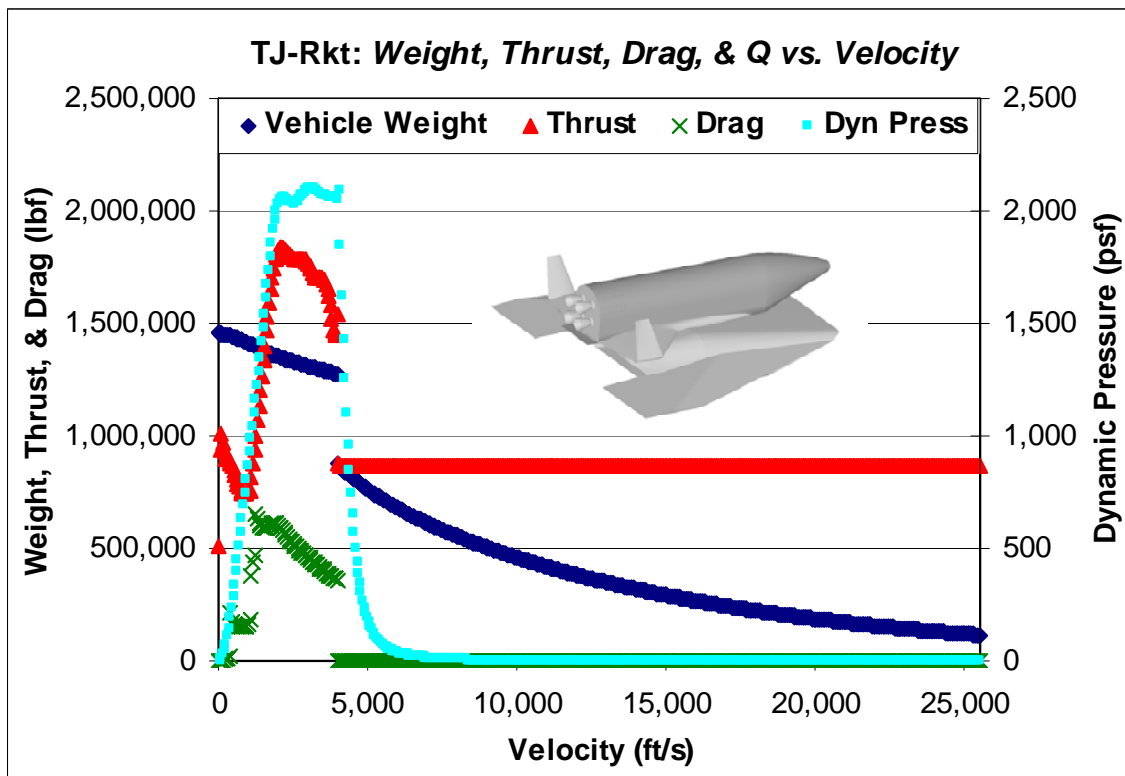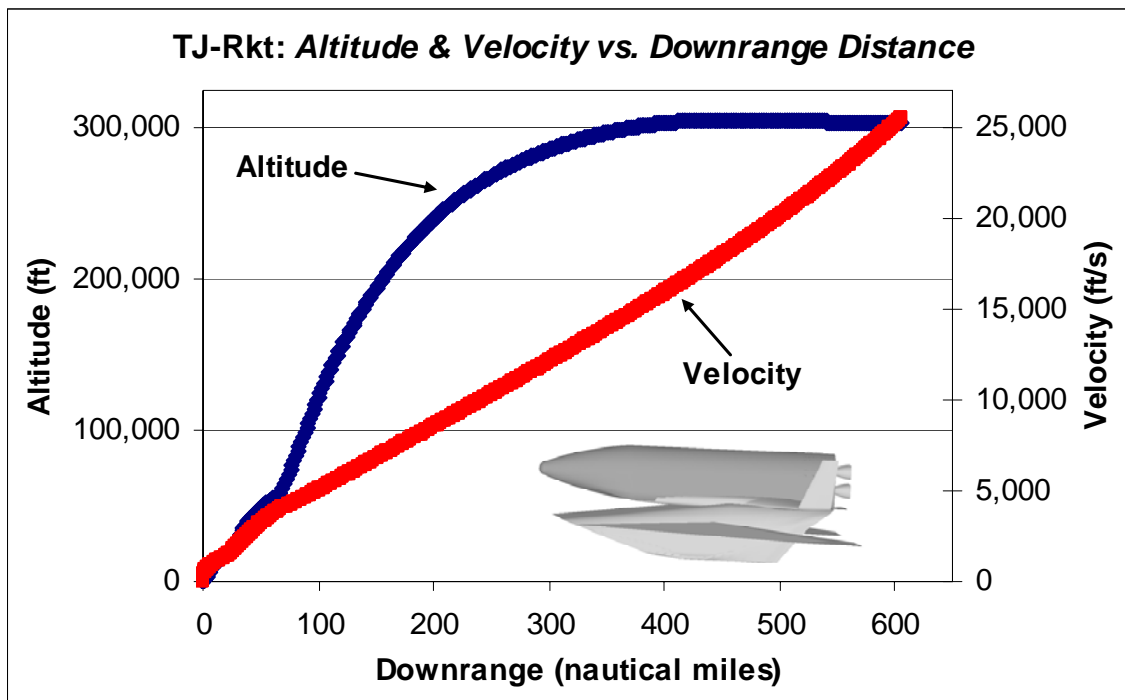
Bibliography

1. Andrews, Earl H. "Scramjet Development and Testing in the United States". AIAA 2001-1927, AIAA/NAL-NASDA-ISAS 10th International Space Planes and Hypersonic Systems and Technologies Conference, Kyoto Japan, April 2001.

2. Baurle, R. A. and D. R. Eklund. "Analysis of Dual-Mode Hydrocarbon Scramjet Operation at Mach 4 – 6.5". AIAA 2001-3299, 37th AIAA/ASME/SAE/ASEE Joint Propulsion Conference and Exhibit, Salt Lake City UT, July 2001.

3. Bilardo, V. J., F. M. Curran, J. L. Hunt, N. T. Lovell, G. Maggio, A. W. Wilhite, and L. E. McKinney. "The Benefits of Hypersonic Airbreathing Launch Systems for Access to Space". AIAA 2003-5265, 39th AIAA/ASME/SAE/ASEE Joint Propulsion Conference and Exhibit, Huntsville AL, July 2003.

4. Blake, William B. *Missile DATCOM User's Manual – 1997 Fortran 90 Revision*. AFRL-VA-WP-TR-1998-3009, Air Vehicles Directorate, Air Force Research Laboratory (AFMC), Wright-Patterson AFB OH, February 1998.

5. Boudreau, Albert H. and Glenn W. Liston. "Solutions for Hypersonic Airbreathing Launchers Lifting Military Payloads". AIAA 2002-5217, AIAA/AAAF 11th International Space Planes and Hypersonic Systems and Technologies Conference, Orleans France, September 2002.

6. Bradford, J. E., A. Charania, J. Wallace, and D. R. Eklund. "Quicksat: A Two-Stage to Orbit Reusable Launch Vehicle Utilizing Air-Breathing Propulsion for Responsive Space Access". AIAA 2004-5950, Space 2004 Conference and Exhibit, San Diego CA, September 2004.

7. Bradley, Marty, Kevin Bowcutt, James McComb, Paul Bartolotta, and Nancy McNelis. "Revolutionary Turbine Accelerator (RTA) Two-Stage-To-Orbit (TSTO) Vehicle Study". AIAA 2002-3902, 38th AIAA/ASME/SAE/ASEE Joint Propulsion Conference and Exhibit, Indianapolis IN, July 2002.

8. Brock, Marc A. *Performance Study of Two-Stage-To-Orbit Reusable Launch Vehicle Propulsion Alternatives*. MS Thesis, AFIT/GSS/ENY/04-M02. Graduate School of Engineering and Management, Air Force Institute of Technology (AU), Wright-Patterson AFB OH, March 2004.

9. Clough, Joshua A., and Mark J. Lewis. "Comparison of Turbine-Based Combined-Cycle Engine Flowpaths". AIAA 2003-6932, 12th AIAA International Space Planes and Hypersonic Systems and Technologies Conference, Norfolk VA, December 2003.

10. Crocker, Andrew M., Jeffery H. Cannon, and Dana G. Andrews. "A Comparison of Horizontal Takeoff RLVs for Next Generation Space Transportation". AIAA 2003-5037, 39th AIAA/ASME/SAE/ASEE Joint Propulsion Conference and Exhibit, Huntsville AL, July 2003.

11. Daines, Russel, and Corin Segal. "Combined Rocket and Airbreathing Propulsion Systems for Space-Launch Applications". *Journal of Propulsion and Power*, Vol. 14, No. 5, September-October 1998.

12. Department of the Air Force. *Mission Need Statement for Operationally Responsive Spacelift*. AFSPC 001-01, HQ AFSPC/DRS, United States Air Force, 20 December 2001.

13. Dissel, Adam F., Ajay P. Kothari, V. Raghavan, and Mark J. Lewis. "Comparison of HTHL and VTHL Air-Breathing and Rocket Systems for Access to Space". AIAA 2004-3988, 40th AIAA/ASME/SAE/ASEE Joint Propulsion Conference and Exhibit, Fort Lauderdale FL, July 2004.

14. Dornheim, Michael A. "NASA's X-43A Hyper-X Reaches Mach 10 in Flight Test". *Aviation Week & Space Technology*, http://www.aviationnow.com/avnow/, 23 November 2004.

15. Dornhiem, Michael A. "Quick, Cheap Launch". *Aviation Week and Space Technology*, Vol. 158, No. 14, 7 April 2003.

16. Earp, Ted. "Advanced Air-Breathing Propulsion". Presented to the Air Force Research Laboratory, Wright-Patterson AFB OH, 11 March 2003.

17. Eklund, Dean R. Aerospace Engineer, Aerospace Propulsion Division (AFRL/PRAT), Wright-Patterson AFB OH. Personal Correspondence, Phone: 937-255-0632, Email: dean.eklund@wpafb.af.mil. July 2004 – February 2005.

18. Escher, William J. D. "On the Airbreathing/Rocket Propulsion Relationship: For Advanced Spaceflight Systems, It's the Combination that Counts". AIAA 2003-5266, 39th AIAA/ASME/SAE/ASEE Joint Propulsion Conference and Exhibit, Huntsville AL, July 2003.

19. Hartong, Alicia R. and Brendan D. Rooney. "Near-Term RLV Options". AIAA 2004-5947, Space 2004 Conference and Exhibit, San Diego CA, September 2004.

20. Hatakeyama, S. Jason, Kieth L. McIver, Jon D. Embler, William G. Gillard, and Lee Jackson. "Operability Sensitivities of Airbreathing and Rocket Propulsion for a Two-Stage-To-Orbit Space Operations Vehicle (SOV)". AIAA 2002-3903, 38th AIAA/ASME/SAE/ASEE Joint Propulsion Conference and Exhibit, Indianapolis IN, July 2002.

21. Heiser, William H. and David T. Pratt. *Hypersonic Airbreathing Propulsion*. AIAA Educational Series. Washington DC: American Institute of Aeronautics and Astronautics, 1994.

22. Hill, Philip G. and Carl R. Peterson. *Mechanics and Thermodynamics of Propulsion* (2nd Edition). New York: Addison-Wesley Publishing Company, 1992.

23. Hueter, Uwe. "Rocket-Based Combined-Cycle Propulsion Technology for Access-to-Space Applications". AIAA 99-4925, 9th AIAA International Space Planes and Hypersonic Systems and Technologies Conference, Norfolk VA, November 1999.

24. Humble, Ronald W., Gary N. Henry, and Wiley J. Larson. *Space Propulsion Analysis and Design* (Revised). New York: McGraw-Hill Publishing Company, 1995.

25. *Hypersonic System Integrated Design Environment (HySIDE)*. Version 2.11, Created Using SIDE2000 Version 4.0. Computer Software. Astrox Corporation, College Park MD, 2004.

26. Kobayashi, H. and N. Tanatsugu. "Optimization Method on TSTO Spaceplane System Powered by Airbreather". AIAA 2001-3965, 37th AIAA/ASME/SAE/ASEE Joint Propulsion Conference and Exhibit, Salt Lake City UT, July 2001.

27. Kothari, Ajay P. President, Astrox Corporation, College Park MD. Personal Correspondence, Phone: 301-948-4646, Email: a.p.kothari@astrox.com. October 2004 – February 2005.

28. Lewis, Mark J., Iain D. Boyd, and Charles E. Cockrell, Jr. "Aerodynamics for Optimal Engine-Integrated Airbreathing Launcher Configurations". AIAA 2004-3983, 40th AIAA/ASME/SAE/ASEE Joint Propulsion Conference and Exhibit, Fort Lauderdale FL, July 2004.

29. Lewis, Mark J. "Significance of Fuel Selection for Hypersonic Vehicles". *Journal of Propulsion and Power*, Vol. 17, No. 6, November-December 2001.

30. Lewis, Mark J. "TSTO Airbreathing Propulsion Analysis with Lift and Drag". AIAA 2003-7020, 12th AIAA International Space Planes and Hypersonic Systems and Technologies Conference, Norfolk VA, December 2003.

31. Livingston, John W. "Comparative Analysis of Rocket and Air-breathing Launch Vehicles". AIAA 2004-5948, Space 2004 Conference and Exhibit, San Diego CA, September 2004.

32. Marshall, Andre W., Ashwani K. Gupta, Mark J. Lewis, and Thomas Lavelle. "Critical Issues in TBCC Modeling". AIAA 2004-3827, 40th AIAA/ASME/SAE/ASEE Joint Propulsion Conference and Exhibit, Fort Lauderdale FL, July 2004.

33. Moses, P. L., K. A. Bouchard, R. F. Vause, S. Z. Pinckney, S. M. Ferlemann, C. P. Leonard, L. W. Taylor III, J. S. Robinson, J. G. Martin, D. H. Petley, and J. L. Hunt. "An Airbreathing Launch Vehicle Design with Turbine-Based Low-Speed Propulsion and Dual Mode Scramjet High-Speed Propulsion". AIAA 99-4948, 9th International Space Planes and Hypersonic Systems and Technologies Conference, Norfolk VA, November 1999.

34. Munson, Bruce R., Donald F. Young, and Theodore H. Okiishi. *Fundamentals of Fluid Mechanics* (3rd Edition). New York: John Wiley & Sons, 1998.

35. Olds, John R. and Irene A. Budianto. "Constant Dynamic Pressure Simulation with POST". AIAA 98-0302, 36th Aerospace Sciences Meeting and Exhibit, Reno NV, January 1998.

36. Packard, James D. and Mark S. Miller. "Assessment of Engineering-Level Codes for Missile Aerodynamic Design and Analysis". AIAA 2000-4590, AIAA Atmospheric Flight Mechanics Conference and Exhibit, Denver CO, August 2000.

37. Powell, O. A., J. T. Edwards, R. B. Norris, K. E. Numbers, and J. A. Pearce. "Development of Hydrocarbon-Fueled Scramjet Engines: The Hypersonic Technology (HyTech) Program". *Journal of Propulsion and Power*, Vol. 17, No. 6, November-December 2001.

38. *Program to Optimize Simulated Trajectories (POST).* Computer Software. NASA Langley Research Center, Hampton VA, 1997.

39. Ramon, Chase, and Ming Tang. "The Quest for Single Stage Earth-to-Orbit: TAV, NASP, DC-X and X-33 Accomplishments, Deficiencies, and Why They Did Not Fly". AIAA 2002-5143, AIAA/AAAF 11th International Space Planes and Hypersonic Systems and Technologies Conference, Orleans France, September 2002.

40. Raymer, Daniel P. *Aircraft Design: A Conceptual Approach* (3rd Edition). AIAA Educational Series. Reston VA: American Institute of Aeronautics and Astronautics, 1999.

41. Scholz, Edwin, John Duffey, Steven Sasso, Gregory Peralta, and Lee Jackson. "Overview of SOV Concepts and Technology Needs". AIAA 2003-5120, 39th AIAA/ASME/SAE/ASEE Joint Propulsion Conference and Exhibit, Huntsville AL, July 2003.

42. Snyder, Lynn E. and Daric W. Escher. "High Mach Turbine Engines for Access to Space Launch Systems". AIAA 2003-5036, 39th AIAA/ASME/SAE/ASEE Joint Propulsion Conference and Exhibit, Huntsville AL, July 2003.

43. Spires, David N. *Beyond Horizons: A Half Century of Air Force Space Leadership* (Revised Edition). Washington DC: U.S. Government Printing Office, 1998.

44. Takashima, N. and A. P. Kothari. "Euler Calculations at Off-Design Conditions for an Inlet of an Inward Turning RBCC-SSTO Vehicle". Presented at the 1998 JANNAF Propulsion Meeting, Cleveland OH, July 1998.

45. United States Air Force Scientific Advisory Board. *Why and Whither Hypersonics Research in the U.S. Air Force*. SAB-TR-00-03, United States Air Force, December 2000.

46. World Wide Web. http://www.affordablespaceflight.com/nasa2.html

47. World Wide Web. http://www.daviddarling.info/encyclopedia/D/Dyna-Soar.html

48. World Wide Web. http://www.fas.org/irp/mystery/nasp.htm

49. World Wide Web. http://www.islandone.org/LEOBiblio/

50. World Wide Web. http://www.ksc.nasa.gov/shuttle/

51. World Wide Web. http://www.nasa.gov/missions/research/x43-main.html

Vita

  First Lieutenant Richard A. Caldwell graduated from Evant High School in Evant, Texas, in 1996. He entered undergraduate studies at Baylor University in Waco, Texas, where he graduated magna cum laude with a Bachelor of Science in Mechanical Engineering in 2001. Upon graduation from Baylor University, he was commissioned as an officer through the Air Force ROTC Detachment 810.

  Richard's first assignment was at the Space Test Program in Kirtland AFB, New Mexico, where he started out as a Spaceflight Test Engineer, and later transitioned into a DoD Spacecraft Mission Manager. In August 2003, he entered the Graduate School of Engineering and Management at the Air Force Institute of Technology. Upon graduation, he will be assigned to the Air Force Research Laboratory Air Vehicles Directorate in Wright-Patterson AFB, Ohio.

REPORT DOCUMENTATION PAGE

The public reporting burden for this collection of information is estimated to average 1 hour per response, including the time for reviewing instructions, searching existing data sources, gathering and maintaining the data needed, and completing and reviewing the collection of information. Send comments regarding this burden estimate or any other aspect of the collection of information, including suggestions for reducing this burden to Department of Defense, Washington Headquarters Services, Directorate for Information Operations and Reports (0704-0188), 1215 Jefferson Davis Highway, Suite 1204, Arlington, VA 22202-4302. Respondents should be aware that notwithstanding any other provision of law, no person shall be subject to an penalty for failing to comply with a collection of information if it does not display a currently valid OMB control number.
PLEASE DO NOT RETURN YOUR FORM TO THE ABOVE ADDRESS.

1. REPORT DATE (DD-MM-YYYY)	**2. REPORT TYPE**	**3. DATES COVERED** (From – To)
21 March 2005	Master's Thesis	August 2003 – March 2005

4. TITLE AND SUBTITLE		**5a. CONTRACT NUMBER**
Weight Analysis of Two-Stage-To-Orbit Reusable Launch Vehicles for Military Applications		**5b. GRANT NUMBER**
		5c. PROGRAM ELEMENT NUMBER
6. AUTHOR(S)		**5d. PROJECT NUMBER**
Caldwell, Richard A., First Lieutenant, USAF		**5e. TASK NUMBER**
		5f. WORK UNIT NUMBER

7. PERFORMING ORGANIZATION NAMES(S) AND ADDRESS(S)	**8. PERFORMING ORGANIZATION REPORT NUMBER**
Air Force Institute of Technology Graduate School of Engineering and Management (AFIT/EN) 2950 Hobson Way, Building 640 WPAFB OH 45433-8865	AFIT/GA/ENY/05-M02

9. SPONSORING/MONITORING AGENCY NAME(S) AND ADDRESS(ES)	**10. SPONSOR/MONITOR'S ACRONYM(S)**
AFRL/PRAT Attn: Dr. Dean Eklund 1950 5th Street Building 18D, Room D232 WPAFB OH 45433-7765 DSN: 785-0632	**11. SPONSOR/MONITOR'S REPORT NUMBER(S)**

12. DISTRIBUTION/AVAILABILITY STATEMENT

APPROVED FOR PUBLIC RELEASE; DISTRIBUTION UNLIMITED.

13. SUPPLEMENTARY NOTES

14. ABSTRACT

In response to Department of Defense (DoD) requirements for responsive and low-cost space access, this design study provides an objective empty weight analysis of potential reusable launch vehicle (RLV) configurations. Each two-stage-to-orbit (TSTO) RLV has a fixed payload requirement of 20,000 lbf to low Earth orbit. The propulsion systems considered in this study include pure rocket, pure turbine, rocket-based-combined-cycle (RBCC), and turbine-based-combined-cycle (TBCC). The hydrocarbon dual-mode scramjet (DMSJ) engines used in the RBCC and TBCC propulsion systems represent possible applications of the current research being performed in the U.S. Air Force HyTech program. Two sensitivity analyses were then performed on areas of interest directly affecting the propulsion systems in this study, including the effects of orbiter fuel selection, as well as the effects of increasing the turbine installed thrust to weight ratios for the RLVs utilizing afterburning turbine engines. The vertical-takeoff-horizontal-landing (VTHL) RLVs have an empty weight advantage over the horizontal-takeoff-horizontal-landing (HTHL) RLVs. The orbiter propellant switch has either negligible or no empty weight savings for the VTHL RLVs, while it leads to substantial empty weight savings for the HTHL RLVs. For the HTHL RLVs, increasing the turbine installed thrust to weight ratio causes a significant decrease in empty weight.

15. SUBJECT TERMS

Launch Vehicles, Hypersonic Vehicles, Rocket Propulsion, Jet Propulsion, Space Propulsion, Propulsion Systems

16. SECURITY CLASSIFICATION OF:			**17. LIMITATION OF ABSTRACT**	**18. NUMBER OF PAGES**	**19a. NAME OF RESPONSIBLE PERSON** Dr. Milton Franke
a. REPORT	**b. ABSTRACT**	**c. THIS PAGE**	UU	119	**19b. TELEPHONE NUMBER** (Include area code) (937) 255-6565, ext 4720 Email: milton.franke@afit.edu
U	U	U			